Egg-envelope formation and sperm activation by chicken ZP-domain proteins

By

Hiroki Okumura

A Dissertation Submitted to the Graduate School of Bioagricultural Sciences,

NAGOYA UNIVERSITY,

In Partial Fulfillment of the Requirements

For the Degree of Doctor of Philosophy in Agricultural Sciences

Laboratory of Morecular Bioregulation

Division of Applied Biochemistry

Department of Applied Molecular Biosciences

Graduate School of Bioagricultural Sciences

Nagoya University

March, 2006

報告番号	甲第 6935 号

CONTENTS

LIST OF ABBREVIATIONS

Ab:	antibody
BSA:	bovine serum albumin
CBB:	Coomassie brilliant blue
CD:	circular dichroism
CID:	collision induced dissociation
DIC:	differential interference contrast
DMBT1:	deleted in malignant brain tumors 1
DMEM:	Dulbecco's modified Eagle's Medium
ECL:	enhanced chemiluminescence
EDTA:	ethylenediaminetetraacetic acid
EGF:	epidermal growth factor
FBS:	fetal bovine serum
HA:	hemagglutinin
HEPES	2-[4-(2-hydroxyethyl)-1-piperazinyl]-ethanesulfonic acid
Ig:	immunoglobulin
IP:	immunoprecipitation
KDa:	kilodalton
LHS:	laying hen's serum
mAb:	monoclonal antibody
MALDI:	matrix-assisted laser-desorption ionization
MS:	mass spectrometry
PBS:	phosphate buffered saline
PNA:	peanut agglutinin
PMSF:	phenylmethylsulfonyl fluoride
PVDF:	poly(vinylidene difluoride)
RT-PCR:	reverse transcription-polymerase chain reaction

SDS-PAGE	sodium dodecyl sulfate-polyacrylamide gel electrophoresis
TGF:	transforming growth factor
TOF:	time-of-flight
Tris:	tris(hydroxymethyl)aminomethane
Trx.:	thioredoxin
ZP:	*Zona Pellucida*

CHAPTER 1

General Introduction

Fertilization is composed of multiple sequential steps to transfer the genome of one generation to the next generation [Primakoff and Myles, 2002], and the first step is the interaction of sperm to egg surface. The eggs in vertebrates are covered by the egg envelope, which is a non-collagenous multifunctional extracellular matrix and plays important roles in gamete recognition, sperm activation, polyspermy blocking, and provides a protection of the early embryo [Rankin and Dean, 2000] (Fig. 1-1). These biological functions of the egg envelope are closely associated with the functions of its individual components, the ZP glycoproteins, and probably with its matrix structures. The designation ZP stands for the mammalian egg envelope referred to as *Zona Pellucida*.

Although the vertebrates' egg envelopes share such common biological functions, there are large differences in the matrix histology. For example, mouse egg envelope, referred to as *Zona Pellucida* (ZP) is 7 μm thickness and consists of fine meshwork of thin filament, and surrounds a relatively small oocyte (~85 μm in diameter) [Greve and Wassarman, 1985]. In contrast, chicken has a thinner envelope (2-4 μm thickness), which consists of comparably rough meshwork of thick filament in spite of the huge oocyte (~40 mm in diameter) [Wyburn *et al.*, 1965; Bakst and Howarth, 1977] (see Fig. 1-1). Unlike eggs of eutherian mammals, the birds' oocytes markedly increased their size with the egg-yolk deposition during the follicular development and, especially during the final 8-9 days before ovulation, the oocyte diameter quickly increased from about 7 to 40 mm [Wyburn *et al.*, 1965] (see Fig. 1-4). The birds' egg envelope must therefore stretch and extend quickly through such a fast growing of the oocyte.

The egg-envelope matrix is composed of at least three ZP glycoproteins that share a common C-terminal domain (named ZP domain) consisting of ~260 amino acid residues with eight or ten conserved cysteine residues [Bork and Sander, 1992]. In early studies of mammalian egg envelope, these ZP glycoproteins were named ZP1, ZP2 and ZP3 according to their apparent mobility in electrophoresis [Bleil and Wassarman, 1980], or ZPA, ZPB and ZPC according to their protein sequence length [Harris *et al.*, 1994], although ZP1, 2 and 3 are not necessarily corresponding to ZPA, B and C, respectively. Afterwards, the fourth

mammalian ZP glycoprotein, ZP4/ZPB (human and rat) [Lefie`vre *et al*, 2004; Hoodbhoy *et al*., 2005], non-mammalian ZPAX (*Xenopus*) [Lindsay *et al*., 2001] and ZPD (*Xenopus* and chicken) [Lindsay *et al*., 2002; Okumura *et al*., 2004], which show lower sequence identities with the ZP1-3 or ZPA-C, have been identified, implying that the ZP-glycoprotein compositions of egg envelope are more complicated. More recently, these ZP glycoproteins have been classified into four subfamilies: ZPA, ZPB (ZPB1, ZPB2 and others), ZPC and ZPX (ZPX1 and ZPX2), according to their phylogenetic analyses [Spargo and Hope, 2003]. According to this nomenclature, mouse ZP1, ZP2 and ZP3 corresponds to ZPB1, ZPA and ZPC, respectively [Spargo and Hope, 2003]. I use this nomenclature based on phylogenetic relationship below. Examples of the ZP-glycoprotein compositions of mammalian (human, rat and mouse), avian (chicken and Japanese quail), amphibian (African clawed frog and Western clawed frog) and fish (medaka and zebrafish) egg envelopes are summarised in Fig. 1-2. These classifications of the ZP glycoproteins can be validated by subjecting the amino acid sequences of ZP domains in the ZP glycoproteins to a simple phylogenetic analysis using such as CLUSTAL W software [Thompson *et al*., 1994] (Fig. 1-3).

In addition to the ZP-glycoprotein composition, there is species diversity in the sites of ZP-glycoprotein synthesis. For example in medaka, ZP glycoproteins are synthesized in the liver [Sugiyama *et al*., 1998], in zebrafish and mouse, in the oocytes [Wang and Gong, 1999; Bleil and Wassarman, 1980], and in rabbit, one of the ZP glycoproteins (R55/ZPB1) is synthesized either in the granulosa cells of the ovary at early stages of folliculogenesis or in the oocytes [Lee and Dunbar, 1993]. In chicken, ZPB1 is synthesized in the laying hen's liver and secreted into the blood stream [Bausek *et al*., 2000], ZPB2 and ZPA are synthesized in the granulosa cells surrounding the prematured oocyte [Kohno, 2000], and ZPC and ZPX2 are synthesized in the granulosa cells at the latter stage of folliculogenesis [Takeuchi *et al*., 1999; Okumura *et al*., 2004; Iwata, 2002], and consequently, the composition of these egg-envelope ZP glycoproteins is changed through the folliculogenesis (Fig 1-4 and 1-5).

Three-dimensional structure of the egg envelope and its formation mechanism are

poorly understood, although ZP domains of these egg-envelope components have been believed to be essential for the matrix formation [Jovine *et al.*, 2002]. Almost all information about the egg-envelope structure has been derived from mouse one. Earlier biochemical and electron microscopic studies [Greve and Wassarman, 1985] and recent studies using ZP-knockout mice [Rankin *et al.*, 1996, 1999 and 2001] suggest that ZPC associates with ZPB1 and/or ZPA to form filament, ZPB1 and ZPA do not associate with each other, and ZPB1 cross-links the filaments by forming a disulfide-linked homodimer [Wassarman, 1988; Dean, 2004]. This mouse model of egg-envelope structure might not necessarily be applied to all mammals or vertebrates because of the diversity in their ZP-glycoprotein composition, structure, and synthesis as described above. Actually, a recent investigation on the fish egg-envelope ZP glycoproteins suggested some diversity in the matrix construction including disulfide-linked heterodimer formation [Darie *et al*, 2004], and differential C-terminal processing [Darie *et al*, 2005].

In addition to these egg-envelope components (ZP glycoproteins), several extracellular glycoproteins sharing the ZP domain have been identified (ZP-domain proteins), such as α- and β-tectorins [Goodyear and Richardson, 2002], Tamm-Horsfall protein [Säemann *et al.*, 2005], transforming growth factor (TGF)-β receptor type III [Blobe *et al.*, 2001] and DMBT1 (deleted in malignant brain tumors 1) [Mollenhauer *et al.*, 2001], and thought to be associated with human pathologies when these ZP-domain proteins are in disorder. [Jovine *et al.*, 2005]. Interestingly, all of these ZP-domain proteins are present in filaments or matrices like the egg-envelope ZP glycoproteins. They have been believed to associate via ZP domains [Jovine *et al.*, 2002], and a model for the molecular mechanism for ZP-ZP interaction is proposed [Jovine *et al.*, 2004].

The egg envelope plays some physiological roles through the egg-sperm interaction as described above. In particular, the sperm recognizes and binds to the egg envelope, and the binding between the sperm and the egg envelope initiates an exocytosis of the sperm acrosomal contents, including proteases and glycosidases to lyse the egg envelope, from the sperm head and activates sperm signal pathways [Howes and Jones, 2002]. This change in

the sperm is called acrosome reaction. During and after acrosome reaction, the activated sperm detaches from the egg envelope, penetrates through the envelope, binds to and fuses with the oocyte plasma membrane (see Fig. 1-1). Acrosome reaction is therefore essential for subsequent fertilization processes to inject the sperm nucleus into the egg cytosol. The initiation mechanism of acrosome reaction is thus inevitable to describe the whole story of vertebrate fertilization.

In almost all vertebrates, especially in birds and reptiles with large eggs, a physical strength is required for the egg envelope to hold and protect a large oocyte. At the same time, on fertilization, such a hard and solid envelope has to be proteolytically degraded and solubilized rapidly to make sperm penetrate into the egg envelope and interact with the egg. Our main goal is to reveal the matrix architecture including its formation mechanisms and the physiological functions in the egg-sperm interaction of the avian egg envelope. Comparison of these data with that of various vertebrates would be useful to understand that the profiles of egg envelope vary among the vertebrate species, although their ZP-glycoprotein components show certain levels of conservation of the ZP domain. For these purpose, I characterized the chicken egg-envelope ZP glycoproteins, examined the possibility of reconstruction of egg-envelope matrix *in vitro* and clarified the roles of each ZP glycoproteins in the matrix architecture of chicken egg envelope. Furthermore, I identified the ZP glycoprotein(s) inducing the sperm acrosome reaction using the *in vitro* assay system.

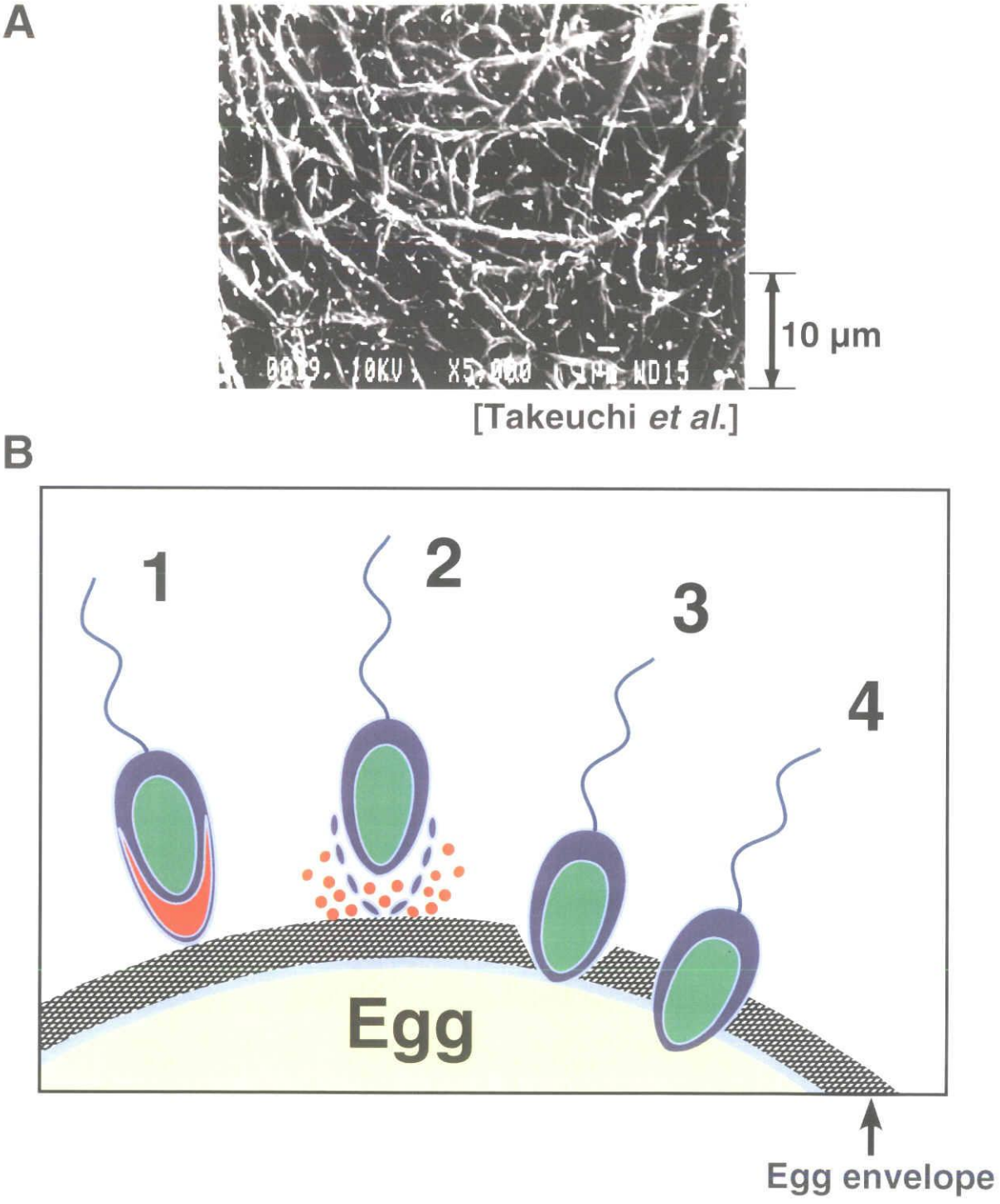

Fig. 1-1. A scanning-electron-microscopic image of chicken egg envelope (*A*) and a schematic drawing of sperm-egg-envelope reaction (*B*).

1, Sperm binding to the egg envelope; *2*, Induction of sperm acrosome reaction; *3*, Sperm penetration through the egg envelope; *4*, Fusion of egg- and sperm-plasmamembranes.

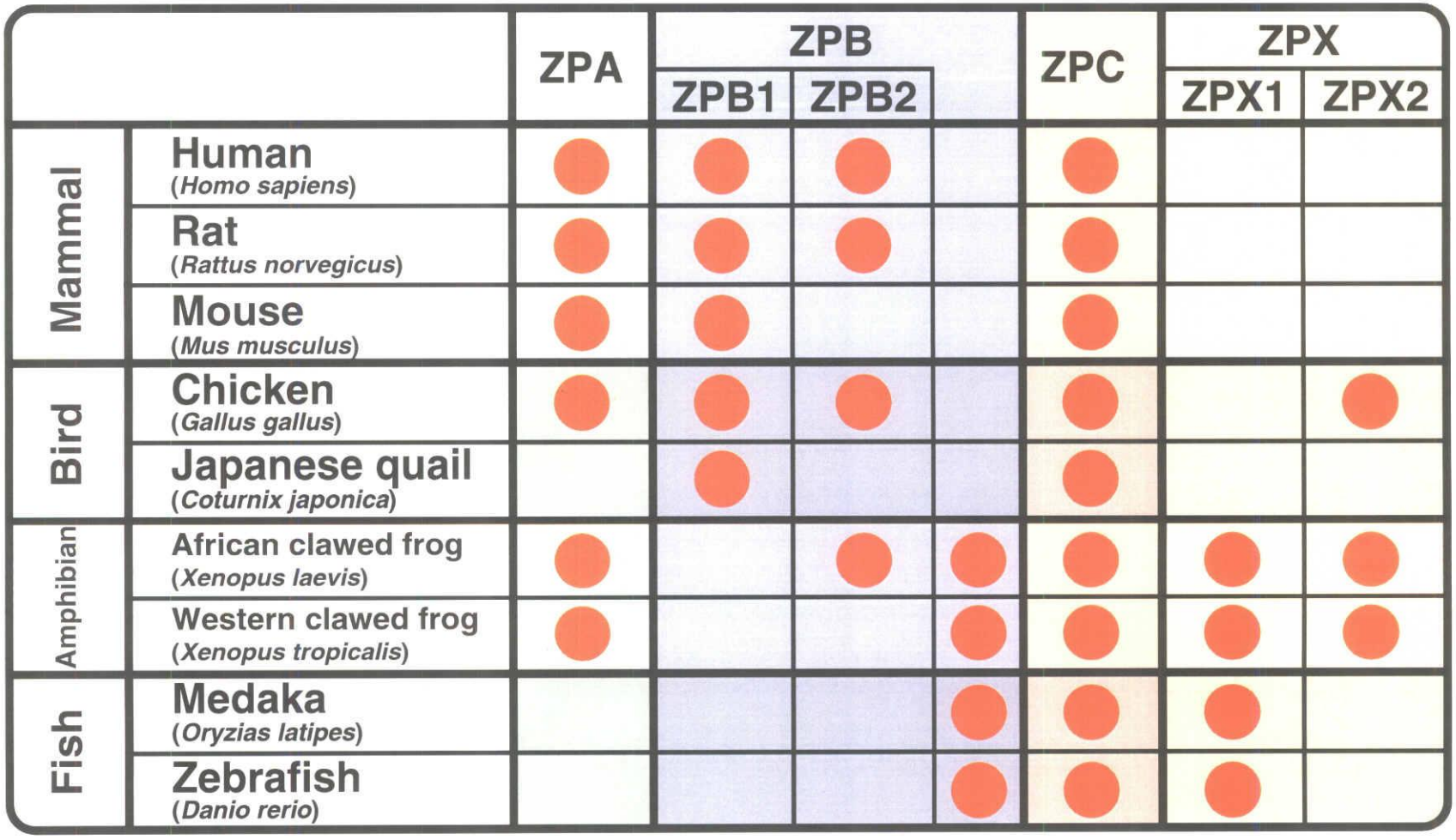

Fig. 1-2. Species diversity in ZP-glycoprotein composition of egg envelope (based on [Spargo and Hope, 2002]).

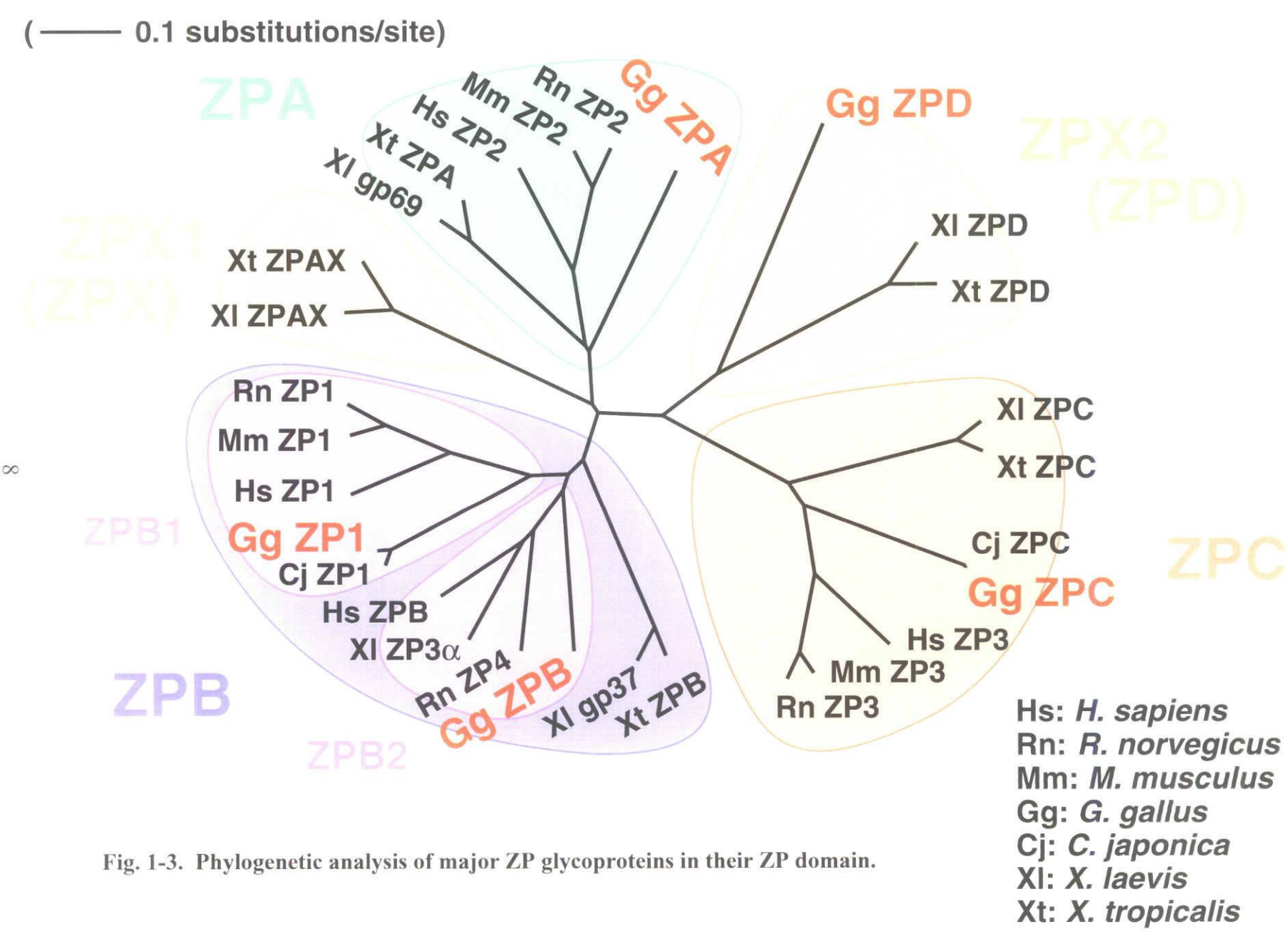

Fig. 1-3. Phylogenetic analysis of major ZP glycoproteins in their ZP domain.

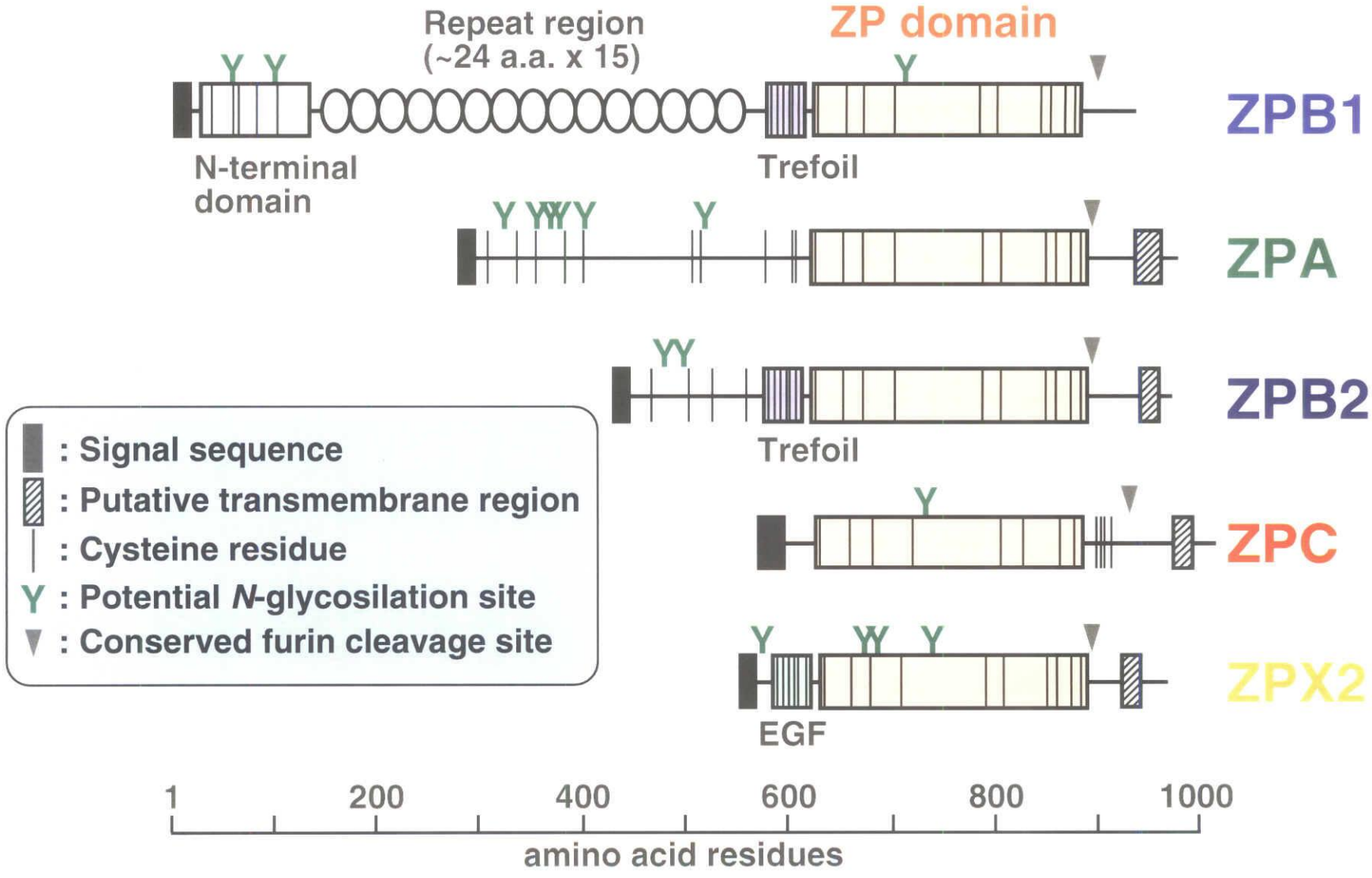

Fig. 1-4. Schematic representation of primary structures of chicken ZP glycoproteins including the signal peptides.

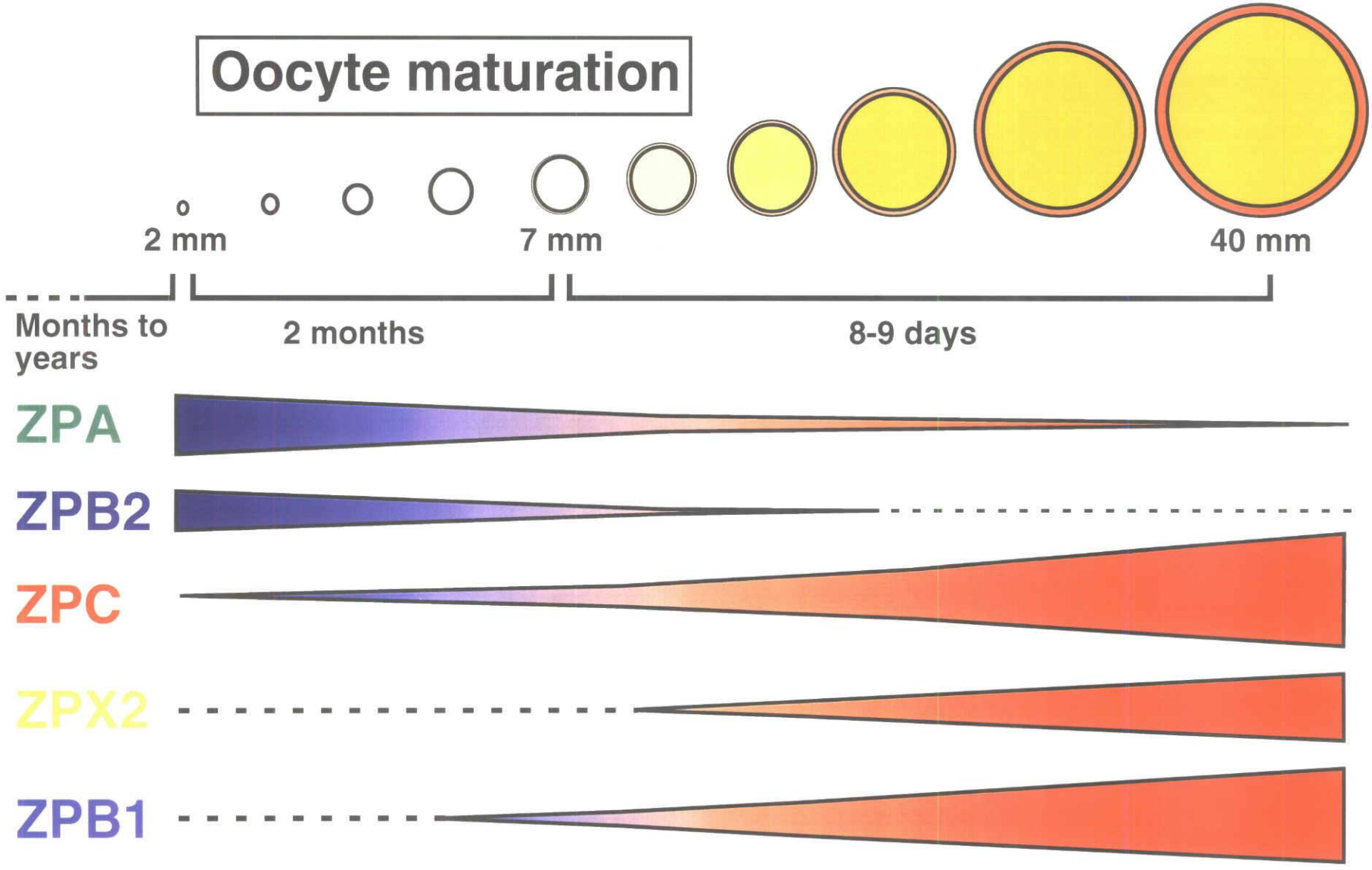

Fig. 1-5. Schematic drawing of changes of the ZP-glycoprotein compositions through the chicken oocyte maturation (based on [Iwata *et al.*, 2002]).

CHAPTER 2

Heterocomplex Formation of ZP-domain Proteins Leading to Egg-envelope Matrix Formation

Summary

The chicken egg envelope surrounding the oocyte just before the ovulation is composed of three ZP glycoproteins, ZPB1, ZPC and ZPX2, whereas the other two, ZPA and ZPB2 are expressed in the granulosa cells at the early stages of the folliculogenesis and would diffuse through the following rapid extension of the egg-envelope matrix. The ZPB1, ZPC and ZPX2 were confirmed to be the major constituents of chicken egg envelope surrounding the mature oocyte by MS on proteolytic digests of whole egg envelope.

I report here that through its ZP domain ZPB1 in laying hen's serum (LHS) prior to the incorporation to the egg envelope specifically associates with ZPC, which might lead to the construction of egg-envelope matrix, furthermore, ZPX2 forming homocomplexes loosely associates with both of ZPB1 and ZPC. ZPX2 was specifically released from the egg envelope by ultrasonication treatment without urea. The serum ZPB1 was eluted from a gel-filtration column as an about 200-kDa protein, while the detection pattern of the serum ZPB1 in the fractions was influenced in a dose dependent manner by egg-envelope derived ZPC incubated with the serum applied to the column. The serum ZPB1 specifically bound to ZPC, but not ZPX2, separated by SDS-PAGE and blotted on a membrane. HA-tagged ZPC expressed in COS-7 cells was processed and secreted as a mature-form into the culture medium. From the culture supernatant of ZPC-expressing transfectants cultured in the presence of ZPB1, both ZPB1 and ZPC were recovered as heterocomplexes by the immunoprecipitation using either anti-HA or anti-ZPB1 antibody. The heterocomplexes were precipitated by an ultracentrifugsation at 100,000 xg for 1 h. Interestingly, a monoclonal antibody, 8E1, which immunoprecipitated free ZPB1, did not immunoprecipitate the ZPB1-ZPC heterocomplexes. An 8E1 epitope was mapped on a C-terminal region of the ZP domain in a ZPB1 molecule by identifying an 8E1-positive peptide using mass spectroscopy. Furthermore, by laser scanning confocal microscopy ZPB1 and ZPC were observed to co-localize on the surface of ZPC-expressing transfectants cultured in the presence of ZPB1, whereas neither ZPB1 nor ZPC was detected on the surface of the

transfectants cultured in the absence of ZPB1.

Similarly, HA-tagged ZPX2 expressed in COS-7 cells was processed and secreted as a mature-form into the culture medium. From the culture supernatant of ZPX2-expressing transfectants cultured in the presence of ZPB1, ZPX2 was recovered as ZPB1-ZPX2 heterocomplexes by the immunoprecipitation using anti-ZPB1 antibody. By laser scanning confocal microscopy, ZPB1 and ZPX2 were observed to co-localize on the surface of ZPX2-expressing transfectants cultured in the presence of ZPB1, whereas ZPB1 was not accumulated on the surface of the mock transfectants. ZPX2 was accumulated either on the cell surface cultured in the presence or absence of ZPB1. Furthermore, from the culture supernatant mixture of the ZPX2- and ZPC-expressing transfectants, ZPC was recovered as ZPX2-ZPC heterocomplexes by the immunoprecipitation using anti-HA antibody.

Taken together, it is suggested that ZPB1 transported into ovarian follicles encounters and associates with ZPC secreted from granulosa cells resulting in the formation of heterocomplexes around an oocyte, and that such ZPB1-ZPC complexes accumulated on the oocyte surface act as a scaffold for subsequent matrix construction events including loose associations of ZPX2 homocomplexes with both of ZPB1 and ZPC.

Introduction

The egg envelopes surrounding chicken and mouse oocyte share two common components, ZPB1 and ZPC, and have individually specific component, ZPX2 and ZPA, respectively. Although ZPB1 is common in both mouse and chicken egg envelopes, only chicken ZPB1 has a unique repeat-structure between the N-terminal domain and trefoil domain. Furthermore, chicken ZPX2 has an EGF-like domain [Okumura *et al.*, 2004], which has not been found in mammalian eggs so far. As for biosynthesis of ZP proteins, mouse ZPA, ZPB1 and ZPC are all synthesized in the growing oocyte [Ringuette *et al.*, 1986; Liang *et al.*, 1990; Epifano *et al.*, 1995], whereas chicken ZPC and ZPX2 are in the granulosa cells surrounding the pre-ovulately growing oocyte [Okumura *et al.*, 2004; Takeuchi *et al.*, 1999]. Furthermore, chicken ZPB1 is synthesized in and secreted from laying hen's liver and transported through bloodstream to the ovary [Bausek *et al.*, 2000]. The matrix architecture of the egg envelope was suggested only in mouse but not in any other vertebrates including chicken as described in the General Introduction. In our earlier study, some anti-ZPB1 antibodies blocked the proteolytic degradation of not only ZPB1 but also ZPC during the egg-sperm interaction [Takeuchi *et al.*, 2001], and the repeat region of ZPB1 was preferentially hydrolyzed by the protease(s) from sperm acrosome [Iwata, 2002]. Interaction and association among the three components, ZPB1, ZPC and ZPX2 would play an important role not only in egg-envelope construction during the oocyte development but also in the matrix deconstruction on egg-sperm interaction at the initial stage of fertilization.

The main goals of this study were to examine the interactions between these ZP glycoproteins in the native egg envelope, to examine the possibility of reconstruction of egg-envelope matrix *in vitro*, and to clarify the roles of each ZP glycoproteins in the matrix architecture of chicken egg envelope. I confirmed that the egg envelope was composed of the three ZP glycoproteins; ZPB1, ZPC and ZPX2, biochemically separated them from the egg envelope, and found that ZPX2 was specifically detached from the envelope by a simple ultrasonic treatment. I examined whether hen's serum ZPB1 can bind specifically to the

other components, ZPC and/or ZPX2, of egg envelope *in vitro*, and whether the serum ZPB1 can form egg-envelope like complex through association with the other components in a cell culture system. Associations of ZPX2 with ZPC or the serum ZPB1 were also examined in the similar system. Consequently, ZPB1 was found to associate with ZPC, and ZPB1-ZPC complexes were shown to form a matrix-like structure around ZPC-secreting COS-7 cells, and ZPX2 was found to form homocomplexes and associate with both of ZPC or ZPB1 to form ZPX2-ZPC or ZPX2-ZPB1 complexes. A possible contribution of ZP domain of ZPB1 to the specific association with ZPC is also discussed.

Materials and Methods

Antibodies— Mouse monoclonal antibodies against chicken ZPB1 (5G9 and 8E1) were as described in [Takeuchi *et al.*, 2001], mouse polyclonal antisera against recombinant proteins of chicken ZPX2 was as described in [Okumura *et al.*, 2004], and mouse polyclonal antisera against recombinant proteins of chicken ZPB1 (its N-terminal domain or repeat region) and ZPC were prepared in this study. Mice (6-wk-old female ddY; Japan SLC, Inc., Hamamatsu, Japan) were immunized by intraperitoneal injection of the purified fusion proteins described below (20-40 μg/mouse) emulsified with Freund's complete adjuvant (Difco Laboratories, Detroit, MI), then 2 wk after the first injection, boosted twice by the injection with each fusion protein (10-20 μg/mouse) emulsified with Freund's incomplete adjuvant (Difco Laboratories) every 3 wk. Seven days after the last injection, blood was collected from individual mouse. The serum was separated and stored at –20°C before use. Rabbit polyclonal antibody against hemagglutinin (HA) epitope tag was purchased from Covance Research Products (Denver, PA). Note that for the primary antibodies specific for ZPB1 (anti-ZPB1), the anti-repeat region antiserum was used in immunoblotting and immunofluorostaining unless otherwise noted.

Preparation of chicken serum— Blood was collected from carotid artery of laying White Leghorn hens, coagulated overnight at 4 °C and centrifuged at 2,000 x g for 10 min to remove a clot. After further centrifugation at 13,000 x g for 10 min, the supernatant was collected as the laying hen's serum (LHS) and stored at –20 °C before use. When subject to following experiments, thawed LHS was filtered through a 0.2-μm-pore-size cellulose acetate filter (DISMIC-13CP; ADVANTEC, Tokyo, Japan) to sterile.

Collection and solubilization of the chicken egg envelope— The egg envelope was isolated from the largest pre-ovulatory mature follicles of laying White leghorn hens as described previously [Takeuchi *et al.*, 1999]. Briefly, the granulosa cell layer composed of the

perivitelline layer (egg envelope), the monolayer of granulosa cells and the basal lamina (basement membrane) was mechanically separated from the oocyte with forceps. The granulosa cells and the basement membrane were removed from the egg envelope by shaking it gently in distilled water with forceps. After checking for isolation under a stereoscopic microscope, the egg envelope was stored at -20°C until use.

The isolated egg envelope was suspended in 500 μl of cold phosphate-buffered saline (PBS) and subjected to sonication (output, 3; duty cycle, 30%) using Sonifier 250 (Branson Ultrasonics Corporation, Danbury, CT). The egg-envelope suspension was centrifuged at 13,000 x g for 20 min to separate the supernatant (fraction X) and the precipitate. After being washed with cold PBS twice, the precipitate was sonicated in 7 ml of the solubilization buffer: 50 mM sodium acetate buffer, pH 5.0, containing 0.2 M NaCl, 50 mM glycine, and 8 M urea (ultrapure grade; ICN Biomedicals, Irvine, CA), and kept on ice for 60 min for further solubilization. This solution was then centrifuged at 10,000 x g for 15 min to remove insoluble materials, and the supernatant was filtered through a 0.45 μm cellulose acetate filter. The filtrate (fraction Y) was immediately used for gel filtration. To solubilize all envelope proteins for electrophoretic analysis, the egg envelope was sonicated in the presence of 8 M urea and, after centrifugation, the supernatant was subjected to electrophoresis.

Purification of ZP glycoproteins using a gel filtration— The fraction Y was applied on a column of Sephacryl S-400 SF (Amersham Biosciences, Piscataway, NJ) (gel bed: 2.6 x 88 cm) previously equilibrated with the elution buffer: 50 mM sodium acetate buffer, pH 5.0, containing 6 M urea, 0.2 M NaCl, and 50 mM glycine. The column was eluted at a rate of 18 ml/h, and 5.9-ml fractions were collected. The absorbance at 280 nm of each fraction was measured by a spectrophotometer U-2001 (Hitachi, Tokyo, Japan). Peak fractions were analyzed by SDS-PAGE followed by CBB staining. Pooled fractions were dialyzed extensively against distilled water [Bleil and Wassarman, 1980], lyophilized, and dissolved in PBS before use.

Protein determination— Protein concentration was estimated by using the BCA protein assay kit (Pierce, Rockford, IL), except that densitometric analyses of the CBB-stained PAGE gel by an ATTO lane & spot analyzer 6.0 (ATTO corporation, Tokyo, Japan) was used for the ZPX2 preparation because of its slight turbidity. Bovine serum albumin was used as the standard.

Amino acid sequencing analysis— The fraction X and its tryptic digest were subjected to SDS-PAGE and the proteins in the gel were electroblotted onto PVDF membrane. The bands of ZPX2 and its flagment on the membrane stained with CBB were excised and applied to a peptide sequencer, Procise HT (Applied Biosystems, Foster City, CA).

Incubation of LHS with ZPC— ZPC protein prepared from chicken egg envelope described above was used. Each one milliliter of 10% LHS in PBS, 10% LHS in PBS containing 0.163 μg, 1.31 μg, 10.5 μg or 41.8 μg of ZPC, PBS containing 41.8 μg of ZPC was incubated in a 6-well culture plate (Sumitomo Bakelite, Tokyo, Japan) at 37 °C for 48 h in a humidified atmosphere with 5% CO_2. These reactants were immediately subjected to gel-filtration chromatography below.

Gel-filtration chromatography— Each one micro liter of sample was applied on a column of Sephacryl S-300 (Amersham Biosciences) (gel bed: 1.6 cm x 53 cm) previously equilibrated with PBS. The column was eluted at a rate of 15 ml/h, and 2-ml fractions were collected. The absorbance at 280 nm of each fraction was measured as described above.

Enzyme-linked immunosorbent assays (ELISA)— Multi-well plates (Nunc-Immuno™ Plate, 96-well Maxisorp; Nalge Nunc International, Rochester, NY) were coated with 100 μl/well of samples overnight at 4 °C. The wells were washed with PBS containing 0.05% Tween-20 (PBS-Tween) 3 times, and blocked with 100 μl/well of 1% BSA in PBS-Tween

(1%BSA/PBS-Tween) at 37 °C for 30 min. After single washing with PBS-Tween, the wells were incubated at 37 °C for 1.5 h with 100 μl/well of the several primary antibodies described above diluted with 1%BSA/PBS-Tween. The wells were then washed with PBS-Tween 3 times, incubate at 37 °C for 1 h with 100 μl/well of horseradish peroxidase-labeled anti-mouse (Cappel, Costa Mesa, CA) diluted with 1% BSA/PBS-Tween, washed with PBS-Tween 3 times, and then incubated with 100 μl/well of a substrate solution (0.4 mg/ml of *o*-phenylenediamine and 0.003% H_2O_2 in 0.05 M citrate/0.1 M Na_2PO_4, pH 5.0) at room temperature (25 °C) for 10 to 40 min in darkness, then 25 μl/well of 2.5 M H_2SO_4 was added to stop reaction. The 492-nm absorption-values were measured by using a microplate reader (SpectraMax® 250; Molecular Devices, Sunnyvale, CA).

Protease digestion of egg envelope— The egg envelope (1.04 mg by wet weight) was solubilized with 15 μl of 0.1% SDS, 5 mM 2-mercaptoethanol, 50 mM Tris-HCl (pH 8.0), and heated at 95°C for 20 min for protein denaturation. Then, 4.7 units of trypsin (Trypsin Gold, Mass Spectrometry Grade; Promega, Madison, WI) or 0.1 μg of Endoproteinase Lys-C (Sigma-Aldrich, Inc., St. Louis, MO) in 5 μl of 50 mM Tris-HCl (pH 8.0) was added to the solubilized and denatured egg envelope, and the mixture was incubated at 37°C for 2 to 18 h.

Mass spectrometry and data analysis— The proteolytic digests (0.5 μl) were spotted onto the MALDI sample target plate with a matrix consisting of a saturated solution of α-cyano-4-hydroxycinnamic acid (Sigma-Aldrich, Inc.) prepared in 50% acetonitrile/0.1% trifluoroacetic acid. Mass spectrometry (MS) and MS/MS analyses were performed in the positive ion reflector mode by using a MALDI-TOF-TOF mass spectrometer (4700 Proteomics Analyzer; Applied Biosystems). Peptide mass spectra were obtained in the mass range between 850 and 4000 Da with *ca.* Mass accuracy of the instrument was externally calibrated to the 4700 Proteomics Analyzer Calibration Mixture (Applied Biosystems). Amino acid sequences of the major MS peaks were deduced from the MS/MS data using the DeNovo Explorer™ and Data Explorer™ softwares (Applied Biosystems). The obtained

peptide sequences were assigned to known proteins by using a BLAST search (National Center for Biotechnology Information, Bethesda, MD), while theoretical masses of the peptides were calculated with the PeptideMass software (http://us.expasy.org/tools/peptide-mass.html).

Production of recombinant chicken ZP proteins and their fragments— The cDNA of chicken ZPB1 were amplified by reverse transcription-PCR (RT-PCR). The first strand cDNA was synthesized from the Poly(A)$^+$RNA isolated from laying White Leghorn hen's liver using Superscript^{TM} II RNase H$^-$ Reverse Transcriptase (Invitrogen, Carlsbad, CA) and random hexamer primers. The PCR was performed using the first strand cDNA as a template with gene specific primers synthesized based on the cDNA sequence of chicken ZPB1, GenBank^{TM} accession number AJ289697 [Bausek *et al.*, 2000]. Amplified cDNA was cloned into pTargeT vector (Promega) according to the manufacturer's instructions, and the DNA sequence was verified using the ABI PRISM 310 DNA sequencer (Applied Biosystems).

ZPB1 cDNA fragments coding for N-terminal domain (nucleotides 81-593) and approximately three fourth of repeat region (nucleotides 594-1475) were amplified by PCR using the ZPB1 cDNA as a template with a sense primer, 5′ -CCATGGCTCTGCTGCAGTACCATTACGAC- 3′, and an antisense primer, 5′ -TGTGCCATGGAGTGACTCTG- 3′ (*Nco*I sites introduced and existed in the primers, respectively; were underlined), and with a sense primer, 5′ -GGATCCGCACACACTCAATCCATCCTG- 3′, and an antisense primer, 5′ -GGATCCGACAAACCCTGCTTGTGT- 3′ (*Bam*HI sites introduced in the primers were underlined), respectively. Resultant DNA fragments, *N* and *repeat* digested with *Nco*I and *Bam*HI, respectively, were inserted via the same restriction sites into the pET-32a(+) vector (Novagen, Darmstadt, Germany) (*N/pET32a(+)* and *repeat/pET32a(+)*, respectively). The N-terminal domain/thioredoxin (N/Trx.) and the repeat region/thioredoxin (repeat/Trx.) fusion proteins were expressed in *E.coli* Origami™B(DE3)pLysS (Novagen) and purified by

a stepwise elution with varied imidazole concentrations according to the manufacturer's instructions (Novagen). The solutions of the fusion proteins were dialyzed against phosphate-buffered saline (PBS) and stored at –20 °C until use for immunization.

Similarly, DNA fragment coding mature ZPC (nucleotides 282-1047 of the ZPC cDNA) without the N-terminal signal sequence and the C-terminal putative transmembrane region was amplified by PCR using the full length cDNA [Takeuchi *et al.*, 1999] as a template, cloned, and inserted into pET 32a(+) vector (Novagen). The thioredoxin fusion protein was produced and processed as above.

Electrophoresis, immunoblotting and ligand blotting— Sodium dodecyl sulfate-polyacrylamide gel electrophoresis (SDS-PAGE) and Tricine SDS-PAGE were performed according to the method of Laemmli, and Schägger and Von Jagow, respectively. Protein samples were boiled for 3 min in SDS-PAGE sample buffer in the presence or absence of 2-mercaptoethanol. To detect protein bands, gels were stained with Coomassie brilliant blue R-250 (CBB). For immunoblotting, proteins were electroblotted onto a poly(vinylidene difluoride) (PVDF) membrane (Immobilon; Millipore, Bedford, MA). After blocking with 2.5% gelatin, the membrane was incubated with primary antibody and then with horseradish peroxidase-labeled anti-mouse IgG or anti-rabbit IgG antibody (Cappel) as described [Aoki and Matsuda, 2000]. The signal was detected by the ECL® (enhanced chemiluminescence) Western Blotting Detection Reagents (Amersham Biosciences). For a ligand blotting analysis, electroblotting, blocking, incubation with antibodies and detection were performed in the same manner as above, except that after blocking the membrane was incubated with ZPB1 solution (1% LHS in the incubation buffer of 150 mM NaCl, 5 mM EDTA, 50 mM Tris-HCl pH 8.0, 0.05% Triton X-100 and 0.25% gelatin) or 1% fetal bovine serum (FBS) in the incubation buffer, at 4 °C for 24 h.

Transient expression of ZPC, ZPC-HA and ZPX2-HA in COS-7 cells— The full-length cDNA of the ZPC [Takeuchi *et al.*, 1999] was transfered into an expression plasmid, pTargeT

(Promega), by restriction enzyme digestion and insertion, and the resultant plasmid named *pZPC* was used for cell transfection described below.

Expression plasmid of HA-tagged chicken ZPC (ZPC-HA) was constructed by PCR-based strategy using overlapping PCR method [Ho *et al.*, 1989]. One primer set, *C-HA-S*, 5′ -TACGACGTGCCCGACTACGCGCGCTTCCGTCGTGATGCC- 3′ and *C-HA-AS*, 5′ -GTAGTCGGGCACGTCGTACGGGTAGCGGCTCTGCCATCTCTC- 3′ including parts of the *HA* sequence (underlined nucleotides), which 18 nucleotides from each 5′ terminal were complement, and another primer set, gene-specific primers *LFSI*, 5′ -TGGAAGCAGGCGGGATGCAA- 3′ and *LFAS*, 5′ -TGCACTCACACCGCAGCTGAG- 3′ were used for PCR. The first PCR was performed at an annealing temperature of 50 °C for 25 cycles using the ZPC cDNA [Takeuchi *et al.*, 1999] as a template with two primer sets, one, *LFSI* and *C-HA-AS*, and another, *C-HA-S* and *LFAS*. The PCR products were annealed to form hybrid in those complementary sequences and primer extension reaction was performed. The resultant mutant product was amplified by the second PCR at annealing temperature of 55 °C for 25 cycles with the primer pair, *LFSI* and *LFAS*. Amplification and primer extension reaction were all carried out with Pyrobest® DNA Polymerase (Takara Bio Inc., Otsu, Japan). The final PCR product was cloned into pTargeT vector (Promega) and sequenced as above (*ZPC-HA/pTargeT*, namely *pZPC-HA*). HA-tag (-Tyr-Pro-Tyr-Asp-Val-Pro-Asp-Tyr-Ala-) was placed upstream of conserved furin cleavage site, between amino acids Arg^{367} and Arg^{368}.

Expression plasmid of HA-tagged chicken ZPX2 (ZPX2-HA) was constructed similarly. The primer set including parts of HA-sequences, *D-HA-S*, 5′ -TACGACGTGCCCGACTACGCGCTCTGGAGGAGCAAGCGG- 3′ and *D-HA-AS*, 5′ -GTAGTCGGGCACGTCGTACGGGTAAGTGGGACATTGCTTGGC- 3′, and another primer set, gene-specific primers *A-F-S*, 5′ -TGGGCAAGTGTGGAGTGGTCT- 3′ and *A-F-AS2*, 5′ -GCCACATTTATTTGGAACCGGC- 3′ were used. The final PCR product was cloned into pTargeT vector (Promega) and sequenced (*ZPX2-HA/pTargeT*, namely *pZPX2-HA*). HA-tag was placed upstream of conserved furin cleavage site, between amino

acids Thr^{341} and Leu^{342}.

African green monkey kidney epithelial cells, COS-7 were obtained from American Type Culture Collection and cultured in DMEM (Sigma-Aldrich, St. Louis, MO) supplemented with 10% FBS or 10% LHS, 100 units/ml penicillin, 0.1 mg/ml streptomycin at 37 °C in a humidified atmosphere with 5% CO_2. The plasmid DNA (*pZPC*, *pZPC-HA*, *pZPX2-HA* or *empty pTargeT*, 4 μg/well) was introduced into the cells according to Chen and Okayama's calcium phosphate method as described [Aoki and Matsuda, 2000]. The cells were washed 3 times with ice-cold PBS and cultured in 1 ml/well of fresh medium containing 10% FBS or 10% LHS for additional 48 h. The cells were washed 3 times with ice-cold PBS, lysed on ice with 100 μl/well of lysis buffer (1% Triton X-100, 5 mM EDTA, 10% glycerol, 150 mM NaCl and 50 mM HEPES, pH 7.5) supplemented with 100 μg/ml leupeptin and 1 mM phenylmethylsulfonyl fluoride (PMSF). Cell lysates were then centrifuged at 13,000 x g for 10 min, and resultant Triton X-100 insoluble precipitates and soluble supernatants were subjected to subsequent analyses. The culture supernatants collected were centrifuged at 1,200 x g for 15 min to remove detached cells, and immediately subjected to immunoprecipitation experiments.

For the experiments on the binding efficiency of two mAbs, the culture supernatant of transfected COS-7 cells was pooled, mixed with 1/10 volume of LHS or FBS as a control, and incubated at 37 °C for 60 min followed by further incubation at 4 °C for 22h. Each solution of the culture supernatant/LHS mixture was divided into two and then they were subjected to the immunoprecipitation using two distinct monoclonal anti-ZPB1 antibodies, 5G9 and 8E1, respectively.

For an experiment analyzing specific interactions between ZPC and ZPX2, two of three distinct culture supernatants from the three transfectants (transfected with *pZPC*, *pZPX2-HA* and *empty pTargeT*) cultured in the FBS-supplemented medium were mixed and incubated at 37 °C for 1 h followed by further incubation at 4 °C for 24 h. Eight hundred microliter of the mixture was subjected to an immunoprecipitation.

Immunoprecipitation— Protein G Magnetic Beads (25 μl of 50% slurry, New England Biolabs, Beverly, MA) was prepared according to the manufacturer's instructions and rotated for 24-48 h at 4 °C in 80 μl of binding buffer (0.1 M sodium phosphate, pH 8.0) with each antibody described above to couple IgG to the beads, pulled by magnetic field and washed 3 times with 500 μl of the binding buffer. Eight hundred microliter of the culture supernatant of COS-7 described above was pre-cleared with 25 μl of the beads (50% slurry) by rotating for 24-48 h at 4 °C. The beads were pulled by magnetic field, and the supernatants were incubated with the antibody-bound beads for 24-48 h at 4 °C. The immunoprecipitate was washed twice as described above and dissolved in 25 μl of SDS-PAGE sample buffer in the absence of 2-mercaptoethanol (non-reducing conditions) and subjected to electrophoresis.

Identification of the ZPB1 peptide fragment recognized by 8E1 and mass spectroscopic analysis of the antigenic peptide— The egg envelope (3.6 mg by wet weight) was solubilized in 0.1% SDS without 2-mercaptoethanol and digested with trypsin for 6 h as described above. The digest was reduced with 2-mercaptoethanol followed by acrylamide treatment for blocking [Brune, 1992] and subjected to Tricine SDS-PAGE (16.5% T, 6% C) under reducing conditions. The peptide bands were detected by CBB staining or immunoblotting using the anti-ZPB1 antibody (8E1) described above. The 8E1-positive band was excised and cut into small pieces for the following in-gel digestion. After being destained with a 50% acetonitrile/25 mM NH_4HCO_3 mixture, the gel pieces were washed with 100 μl of acetonitrile, dried by vacuum centrifugation, and then rehydrated in buffer containing 25 mM NH_4HCO_3 and 1.1 units of trypsin (Trypsin Gold, MS Grade; Promega). Following the digestion at 37 °C for 17 h, the peptides were extracted from the gel stepwise with 0.1% trifluoroacetic acid, 0.1% trifluoroacetic acid/50% acetonitrile mixture, and 100% acetonitrile. The pooled extract was concentrated by vacuum centrifugation. The extracted peptides were subjected to MALDI mass spectrometry as described above.

Immunofluorostaining and confocal laser microscopy— COS-7 cells were plated onto

poly-L-lysine-coated coverslips in the 6-well culture plate, transiently transfected and cultured under the same conditions as described above. The cells on coverslips were washed with PBS and fixed with 3% paraformaldehyde in PBS for 30 min on ice. The cells for permeabilization were washed again with PBS and incubated with 0.1 % Triton X-100 in PBS for 30 min on ice. The permeabilized and non-permeabilized cells were washed again with PBS and blocked with 2% BSA in PBS (2% BSA/PBS) for 30 min at room temperature. The cells were incubated with 2% BSA/PBS containing the mouse anti-ZPC, the rabbit anti-HA, or the mouse anti-ZPB1 overnight at 4 °C, washed with PBS, and finally incubated with 2% BSA/PBS containing Alexa Fluor® 488 goat anti-mouse IgG (Molecular Probes, Eugene, OR; 6.7 μg/ml) and Alexa Fluor® 568 goat anti-rabbit IgG (Molecular Probes; 6.7 μg/ml) for 30 min at room temperature in darkness. After washing with PBS, the cells on coverslips were mounted onto glass slides containing a drop of 90% glycerol in PBS. Imaging was performed on a Zeiss Axioplan2 microscope equipped with a LSM5 PASCAL laser scanning confocal optics (Carl Zeiss, Thornwood, NY) in the multi track mode. For imaging Alexa Fluor® 488, an excitation filter of 488 nm and a 505-530 nm band-pass emission filter was used; and for Alexa Fluor® 568, an excitation filter of 543 nm and a 560 nm long-pass filter were used. Differential interference contrast (DIC) microscopy images were taken on the same system. Three-dimensional image reconstruction and orthogonal sectioning were carried out using the Zeiss LSM Image Browser Version 3.5 software (Carl Zeiss).

Ultracentrifugation— One milliliter of sample was centrifuged at 100,000 x g for 60 min using Micro Ultracentrifuge himac CS 100 (Hitachi High-Technologies) with a rotor RP100AT-268 (Hitachi High-Technologies). After collecting supernatant, 500 μl of PBS was added into the centrifugation tube, and centrifuged similarly to wash the precipitate. The precipitate was dissolved in 25 μl of SDS-PAGE sample buffer in the absence of 2-mercaptoethanol (non-reducing conditions) and subjected to electrophoresis.

Results

ZPB1, ZPC and ZPX2 are components of matured chicken egg envelope— I confirmed whether ZPB1, ZPC and ZPX2 proteins were components of the egg envelope by electrophoretic methods (Fig. 2-1). SDS-PAGE of total envelope proteins under reducing conditions followed by CBB staining (*lane 1* of *A*) showed two major bands, ZPB1/gp97 and ZPC/gp42, which is consistent with our previous report [Takeuchi *et al.*, 2001]. No additional ZPX2-like band was identified under these conditions. Under non-reducing conditions, however, total four major protein bands were detected (*lane 1* of *B*). To identify these bands, immunoblotting with antibodies against ZPB1, ZPC, and ZPX2 were performed. The upper two bands under non-reducing conditions (97 kDa and 180 kDa) were stained with anti-ZPB1 antibody (data not shown) [Takeuchi *et al.*, 2001]. Because ZPB1 forms homodimer covalently linked with disulfide bonds [Takeuchi *et al.*, 2001], the two bands cross-reacted with anti-ZPB1 antibody were judged to be ZPB1 dimer and ZPB1 monomer. Under non-reducing conditions, ZPC migrated much faster (compare the *lanes 2* of *A* and *B*) so that the ZPC band was observed as a 35-kDa band at the bottom of the gel (*lane 1* of *B*). Immunoblotting with anti-ZPX2 antibody revealed that the cross-reactive materials of 42 kDa and 38 kDa exist under reducing and non-reducing conditions, respectively, and that the protein cross-reactive with anti-ZPX2 antibody co-migrated with ZPC under reducing conditions (*lanes 3* of *A* and *B*). These two bands were separated under non-reducing conditions mainly due to the drastic shift of the ZPC band described above. These data indicates that ZPX2 is included in the egg envelope as its main constituent. The N-terminal amino acid sequence for the ZPX2 band could not be determined even when a larger amount of protein was subjected for the analysis. Therefore, ZPX2 was digested with trypsin, resulting in the production of a 37-kDa fragment. The N-terminal amino acid sequence was determined to be SSDAXVPNP, which corresponds to the sequence Ser^{43}-Pro^{51} in the deduced amino acid sequence of ZPX2.

Furthermore, whole egg envelope was degraded by tryptic or Lys-C limited

hydrolysis, and resultant peptide fragments were subjected to MS analyses (Fig. 2-2). *Panels A* and *B* shows typical mass spectra of the tryptic and Lys-C digests. Nine major MS-peaks were detected in the tryptic digest (2 h-digestion), while only two major ones in the Lys-C digest (18-h digestion). Almost the same mass spectra with lower mass intensities were obtained by the proteolytic hydrolysis for longer or shorter periods. As shown in *C*, all these MS-peaks except two were identified to be peptide fragments from ZPB1, ZPC or ZPX2 by MS/MS sequencing, while the mass data of the exceptional two *peaks* (*h* and *k*) agreed well with theoretical masses of ZPB1 and ZPC fragments. Thus, all tryptic and Lys-C peptides could be assigned to ZPB1, ZPC or ZPX2.

Isolation of the ZP glycoproteins from the mature egg envelope— In order to examine the associations between these ZP glycoproteins in the native mature egg envelope, and to prepare the ZP glycoproteins for later experiments on the sperm-egg-envelope interaction, the ZP glycoproteins were isolated from the mature egg envelope (Fig. 2-3). As mentioned later in the Discussion section, I found that, distinct from other ZP glycoproteins, ZPX2 was quantitatively released from the egg envelope by sonication in the absence of urea. ZPX2 prepared by this method (fraction X) was almost homogeneous as judged by SDS-PAGE followed by CBB staining (*lane 2* of *B*). After the removal of ZPX2 from the egg envelope, ZPB1 and ZPC were solubilized successfully by sonication at pH 5.0 in the presence of 8M urea (under non-reducing conditions), and could be separated each other by gel filtration (*A*). As shown in *B* (*lanes 3-5*), the SDS-PAGE under non-reducing condition indicated that *fractions I*, *II*, and *III* contained dimeric and monomeric forms of ZPB1, monomeric ZPB1, and ZPC, respectively. However, the *fraction I*, as well the *fraction II*, showed a single band of monomeric ZPB1 on the SDS-PAGE under reducing condition (data not shown), indicating the presence of intermolecular disulfide bond (s) in the dimer form. The identification of all ZP glycoproteins was confirmed by immunoblotting with their specific antibodies (data not shown). Then, these four *fractions* (*I*, *II*, *III* and *X*) were used as dimeric/monomeric ZPB1, monomeric ZPB1, ZPC and ZPX2 in the following experiments.

The yields of *fraction I* (dimeric/monomeric ZPB1), *fraction II* (monomeric ZPB1), *fraction III* (ZPC), and *fraction X* (ZPX2) were 1.70, 0.92, 1.67, and 0.88 mg, respectively, from 89.3 mg (wet weight) of the egg envelope.

Characterization of a soluble form ZPB1 in laying hen's serum— Chicken ZPB1 has been reported being synthesized in laying hen's liver and transported to the ovary through blood stream [Bausek *et al.*, 2000]. By immunoblotting and immunoprecipitation analyses, ZPB1 was detected actually in laying hen's serum (LHS), but not in non-laying hen's or cock's ones (data not shown). To characterize the molecular nature of serum ZPB1, LHS was subjected to gel-filtration chromatography and the distribution of ZPB1 was analyzed by immunoblotting. As shown in Figure 2-4, each fraction eluted from the gel-filtration column was subjected to SDS-PAGE under a non-reducing condition followed by CBB staining (*upper panel*) or immunoblotting with anti-ZPB1 monoclonal antibody (8E1) (*lower panel*). The LHS and the egg envelope were also subjected as controls. The ZPB1 protein band with molecular mass of 97 kDa was detected in the fractions 31-34 by immunoblotting, but not CBB staining. Another ZPB1 band of about 180 kDa corresponding to the dimeric form through disulfide bridge(s) [Takeuchi *et al.*, 2001] was neither observed by immunoblotting nor CBB staining, though it was in the egg-envelope preparation. Major protein components of LHS, such as vitellogenin (*VTG*), immunoglobulin Y (*IgY*) and serum albumin (*SA*) [Yamamura *et al.*, 1995], were eluted with their peak fractions of no. 28, 33 and 37, respectively. The ZPB1 (97 kDa) and immunoglobulin Y (*IgY*, ~200 kDa) were eluted in nearly the same fractions (*fractions no. 31-34*), implying apparent molecular size of the ZPB1 in LHS was approximately 200 kDa. This apparent molecular mass of 200 kDa is much larger than that of ZPB1 monomer (97 kDa) estimated from the mobility in SDS-PAGE (Fig. 2-4).

Dose dependent interaction between serum ZPB1 and ZPC prepared from the egg envelope— To examine whether ZPB1 in the LHS interact with ZPC separated from the

egg envelope, LHS was fractionated by gel-filtration chromatography after incubations with several amounts of the ZPC preparation from the egg envelope (Fig. 2-5). Mixtures of the LHS (100 μl, containing ≈10 μg of ZPB1) with 0, 0.163, 1.31, 10.5 and 41.8 μg of ZPC protein prepared from egg envelope and 41.8 μg of the ZPC were incubated for 48 h at 37 °C and subjected to gel-filtration chromatography. The eluted fractions were subjected to the UV-detection (*A*) and the ELISA with the domain-specific antibodies for ZPB1 (*B* to *E*) and the anti-ZPC (*F*). In the UV-detection, two major peaks corresponding to IgG (180 kDa) and serum albumin (66 kDa) were detected (*broken gray lines* and *solid gray lines*, respectively). In the ELISA, ZPB1 was detected as several peaks that our ZPB1-specific antibodies present with distinct intensities of ELISA values. By using the anti-ZPB1 (N-terminal domain) (*B*), single weak peaks were detected near the void volume, and the intensities of the peaks did not change as the amount of the ZPC increased. By using the anti-ZPB1 (repeat region) (*C*), two peaks were detected in high-molecular-size fractions and near the 180-kDa ones, and the intensities of the two peaks decreased as the amount of the ZPC increased to 10.5 μg (*panels 1* to *4* of *C*). The intensities were recovered when the ZPC amount increased to 41.8 μg (*panels 4* to *5* of *C*), and that of the high-molecular-size peak was obviously higher than the 180-kDa one. By using the 5G9 (*D*), two weak peaks were detected near the void volume and the 66-kDa fractions, and the intensity of the latter decreased as the amount of the ZPC increased to 1.31 μg (*panels 1* to *3* of *D*). As the ZPC amount increase 1.31 to 41.8 μg, two peaks in the high-molecular-size fractions and near the 180-kDa ones were appeared, and the intensities of those peaks increased (*panels 3* to 5 of *D*). By using the 8E1 (*E*), a major peak was detected near the 66-kDa fractions (*panels 1* to *3* of *E*). As the ZPC amount increase from 1.31 to 41.8 μg, the intensities of the 66-kDa peaks diminished (*panels 3* to *4* of *E*), and two peaks were appeared similarly to the 5G9 (*panels 4* to *5* of *E*). Additional peaks were also appeared around fractions no. 36 to 38 (*panels 3* to *5* of *E*). By using the anti-ZPC (*F*), ZPC was detected around a fraction no. 36 (*panel 6* of *F*). The intensity of ZPC peak increased suddenly as the amount of ZPC increased from 10.5 to 41.8 μg, and two peaks were appeared in the high-molecular-size fractions and near the

180-kDa ones (*panels 1* to *5* of *F*). By using the anti-ZPB1s (N-terminal domain and repeat region), anti-repeat and 5G9, no peaks were detected when ZPC was incubated and fractionated without the LHS (*panels 6* of *B*, *C* and *D*), but by using the 8E1, there were two peaks near the high-molecular-size fractions and around fractions no. 37 and 38 (*panel 6* of *E*). When the LHS (100 μl, containing ≈10 μg of ZPB1) was fractionated without the incubation, results were similar to the *panels 1* (data not shown). These results suggested that the serum ZPB1 and the egg-envelope derived ZPC interacted with each other in a dose dependent manner, and that the binding affinities of the ZPB1 and ZPC with the specific antibodies or the ELISA plates were influenced through the ZPB1-ZPC interaction.

Specific binding of serum ZPB1 to egg-envelope ZPC as analyzed by ligand blotting— The ZPB1 in LHS was expected to bind to the other ZP glycoproteins when it joins the formation of egg-envelope matrix in the ovary. To identify egg-envelope components interacting with ZPB1, a type of ligand blotting analysis was performed (Fig. 2-6). Egg-envelope proteins were solubilized with the SDS sample buffer under non-reducing conditions and subjected to SDS-PAGE followed by electroblotting onto a PVDF membrane. The membrane was incubated in the presence or absence of ZPB1 as a ligand, and the bound ZPB1 was detected immunologically with anti-ZPB1 antibody. A 35-kDa band corresponding to ZPC, but not 40-kDa ZPX2, was clearly detected with anti-ZPB1 antibody only on the membrane incubated with LHS, indicating the specific binding of ZPB1 to ZPC. Except for this 35-kDa band, there were no significant differences in the anti-ZPB1 immune-staining pattern between the two membranes incubated with and without LHS containing ZPB1.

Expression, processing and secretion of HA-tagged ZPC by transfected COS-7 cells— For the *in vitro* analyses of ZPB1-ZPC interaction, an epitope (HA)-tagged ZPC was expressed transiently in a mammalian cell line, COS-7. To confirm whether the recombinant ZPC-HA was processed correctly and secreted into the culture medium, the cell

lysate and the culture supernatant were subjected to immunoblotting and immunoprecipitation analyses, respectively (Fig. 2-7). A 42-kDa band, which is expected to be pro-form of ZPC-HA, was clearly detected in the cell lysate either by anti-ZPC or anti-HA antibody. In contrast with cell lysate, a 35-kDa band corresponding to the mature form of ZPC (see Fig. 2-6, *lane 1*) was detected in the culture supernatant by the specific antibodies. No mature form was detected in the cell lysates. These results suggested that HA-tagged ZPC expressed as a pro-form with its carboxy-terminal hydrophobic region in transfected COS-7 cells was processed, at least in part, to an expected mature form and secreted to the culture medium.

Specific binding of serum ZPB1 to ZPC secreted by the transfected COS-7 cells— The culture supernatants of the COS-7 cells, which had been transfected and then cultured in the presence of serum ZPB1, were subjected to reciprocal co-immunoprecipitation analysis using anti-ZPB1 monoclonal antibody (5G9) and anti-HA antibody (Fig. 2-8). The probable mature ZPC-HA secreted into the medium (*open arrowheads*) was co-precipitated with ZPB1 (*closed arrowheads*) by immunoprecipitation using the anti-ZPB1 (*A*) and, conversely, ZPB1 was co-precipitated with the ZPC-HA by immunoprecipitation using the anti-HA (*B*), indicating the presence of ZPB1-ZPC complexes in the culture supernatant of ZPC-expressing cells cultured in the ZPB1-containing medium. A 180-kDa band corresponding to dimeric ZPB1 (*striped arrowhead* of *B*) was also detected particularly in the immunoprecipitate by the anti-HA, which was expected to be richer in ZPB1-ZPC complexes as compared with the immunoprecipitates by anti-ZPB1 because an excess of free ZPB1 was present in the culture medium. This 180-kDa band was confirmed to migrate to the same position of 97-kDa monomeric ZPB1 on SDS-PAGE under reducing conditions (data not shown) as the dimeric ZPB1 of egg envelope did [Takeuchi *et al.*, 2001]. These results indicated that ZPB1 interacted specifically with ZPC-HA secreted into the medium and formed ZPB1-ZPC heterocomplexes.

To determine whether the ZPB1 and ZPC formed the high-molecular-weight

complexes, the culture supernatants were fractionated by ultracentrifugation (Fig. 2-9). The ZPB1-ZPC complexes composed of dimeric ZPB1 (*di-ZPB1*; *striped arrowhead*), monomeric ZPB1 (*mono-ZPB1*; *closed arrowhead*) and probable mature ZPC-HA (*open arrowhead*) were precipitated by ultracentrifugation of the culture supernatant from the ZPC-HA-expressing cells cultured in the ZPB1-containing medium. Accordingly, it was suggested the molecular size of the ZPB1-ZPC heterocomplexes was high enough to be precipitated by ultracentrifugation.

Contribution of ZPB1 C-terminal region to the association with ZPC— To compare the binding efficiency of the two anti-ZPB1 monoclonal antibodies (5G9 and 8E1) [Takeuchi *et al.*, 2001] to the ZPB1-ZPC heterocomplexes more quantitatively, the culture supernatants were pooled from the ZPC-HA-expressing COS-7 cells, mixed with ZPB1-containing serum, and incubated to induce the complex formation. The ZPC-HA-ZPB1 mixture was subjected to the immunoprecipitation by each monoclonal antibody, 5G9 or 8E1 (Fig. 2-10). Interestingly, one monoclonal antibody, 5G9, effectively immunoprecipitated the ZPB1-ZPC heterocomplex, whereas another one, 8E1, did not. The monoclonal antibody 8E1 of course immunoprecipitated free ZPB1 particularly from the culture supernatant of the mock transfectants.

No binding of 8E1 to ZPB1 associated with ZPC suggested that ZPC bound to the region nearby an 8E1-binding site (epitope) in ZPB1. To map the 8E1 epitope, 8E1-positive ZPB1 fragments were screened among the tryptic peptides of whole egg envelope by Tricine-SDS-PAGE followed by immunoblotting (Fig. 2-11*A*). A 5.5 kDa-band was clearly stained with 8E1. The MS analyses on the in-gel digest of this band revealed that this 8E1-positive fragment contained two ZPB1-derived sequences (*peaks a* and *b* in Fig. 2-11*B*), and that the two sequences were identical except for one residue at position 897 (Val or Leu probably due to ZPB1 isoforms). The proprotein of ZPB1 has a consensus sequence, RARR (from 900 to 903) for the furin cleavage. Accordingly, the 5.5-kDa-fragment was found to contain a decapeptide (Pro^{891}-Arg^{900}) corresponding to the putative C-terminus of mature

ZPB1 (Fig. 2-11*B*, *C*), suggesting that the 5.5 kDa fragment was Phe^{852}-Arg^{900} with theoretical molecular mass of 5258.82 and 5272.84 (containing the *peak a* and *b* sequences, respectively). The *peaks c*, *d* and *f* were derived from ZPC, while the *peak e* was from ZPX2 (data not shown). Thus, the 8E1 epitope was mapped in a C-terminal peptide within ZP-domain of a ZPB1 molecule.

Co-localization of ZPB1 and ZPC around the ZPC-transfected COS-7 cells cultured in the ZPB1-containing medium— To determine whether ZPB1 is accumulated with ZPC on the surface of ZPC-expressing cell, the transfected COS-7 cells were cultured in the presence of serum ZPB1. After being cultured for two days, the cells were fixed with and without the permeabilization treatment. The fixed cells were stained with anti-ZPB1 and anti-HA antibodies followed by incubation with fluorescence-conjugated secondary antibodies, and observed under a confocal laser scanning microscopy (Fig. 2-12). Both ZPB1 (*green*) and ZPC-HA (*red*) were detected on the surface of the ZPC-HA-expressing cells treated without permeabilization. A strong ZPC-HA signal was observed in the cytoplasm of permeabilized cells. Three-dimensional graphic images constructed from the multiple confocal images demonstrated that not only ZPC but also ZPB1 were accumulated on the almost whole part of the cell surface, and that localization of the two proteins was identical, indicating that ZPB1-ZPC complexes were formed and accumulated on the cell surface. As expected, ZPB1 accumulation was not at all observed in the case of mock transfectants.

Absence of ZPC on the surface of transfected COS-7 cells cultured in the absence of ZPB1— As shown in Fig. 2-12, ZPC was required for ZPB1 in the medium to be accumulated on the cell surface. Then, another experiment was conducted to elucidate whether ZPC-HA alone accumulated on the surface of transfected cells. The transfected COS-7 cells were cultured for two days in the absence of serum ZPB1, fixed and stained with anti-ZPC antibody as well as anti-HA antibody. As shown in Figure 2-12, when serum ZPB1 was not present in the medium, no ZPC accumulation on the surface of

non-permeabilized cells was observed by using anti-ZPC in addition to anti-HA. The intracellular signal of ZPC-HA was detected in the permeabilized cells, and the stained image with anti-ZPC (*green*) was identical to that with anti-HA (*red*).

Expression, processing and secretion of HA-tagged ZPX2 by transfected COS-7 cells— Next, I examined interactions of ZPX2 with ZPB1 or ZPC using the cell-culture system. As a tool for the *in vitro* analyses for interaction of ZPX2 with ZPB1 or ZPC, an epitope (HA)-tagged ZPX2-expressing system was established using a mammalian cell line, COS-7. To confirm whether the recombinant ZPX2 was processed correctly and secreted as a soluble mature-form into the culture medium, the cell lysate and the culture supernatant were subjected to immunoblotting analysis (Fig. 2-14). COS-7 cells were transfected with an expression plasmid for ZPX2-HA (*pZPX2-HA*) or a control plasmid (*mock*) and cultured for 1-2 days. Approximately 47-kDa and 40-kDa bands, expected to be pro-form and mature form of ZPX2-HA, respectively, was clearly detected in the cell lysate (both Triton-insoluble and soluble fractions). Native ZPX2 from egg envelope was detected as a 38-kDa band (see *right panel* and Fig. 2-6). In contrast with cell lysate, only a 40-kDa band of the mature form was detected in the culture supernatant. These results suggested that HA-tagged ZPX2 could be expressed as a pro-form with its carboxy-terminal hydrophobic region in transfected COS-7 cells, processed to an expected mature form, and secreted as a soluble protein to the culture medium. It is noteworthy that the mature form of the ZPX2-HA was also detected in the cell lysates of the transfectants, whereas the mature form of the ZPC-HA was detected only in the culture supernatant (see Fig. 2-7). These features on the expression and the secretion of the HA-tagged ZPC and ZPX2 expressed by the transfectants were agreed well with that of normal ZPC and ZPX2 (data not shown).

Specific association of ZPX2 secreted into culture supernatant of transfected COS-7 cells with ZPB1 in laying hen's serum— To determine whether ZPX2 expressed in and secreted from ZPX2-expressing cells interact with ZPB1 in laying hen's serum, the culture

supernatants of the COS-7 cells, which had been transfected and then cultured in the presence or absence of serum ZPB1 were subjected to co-immunoprecipitation analysis using anti-ZPB1 polyclonal antibody (N-terminal domain) (Fig. 2-15). The probable mature ZPX2-HA secreted into the medium (*closed gray arrowhead*) was co-precipitated with ZPB1 (*closed black arrowhead*) by immunoprecipitation using the anti-ZPB1, indicating the presence of ZPB1-ZPX2 complexes in the culture supernatant of ZPX2-expressing cells cultured in the ZPB1-containing medium. These results indicated that ZPX2-HA secreted into the medium interacted specifically with ZPB1 and formed ZPB1-ZPX2 heterocomplexes.

Co-localized deposition of ZPB1 and ZPX2 around the ZPX2-transfected COS-7 cells cultured in the ZPB1-containing medium— The ZPB1-containing serum was added to the culture medium for the COS-7 cells transfected with the ZPX2-HA expression plasmid (*pZPX2-HA*), and localization of ZPB1 and ZPX2-HA around the cells was analyzed by immunofluorescence microscopy (Fig. 2-16). After being cultured for two days, the cells were fixed with paraformaldehyde (without permeabilization treatment), stained with anti-ZPB1 and anti-HA antibodies followed by incubation with fluorescence-conjugated secondary antibody, and observed under a confocal laser scanning microscopy. Both ZPB1 (*green*) and ZPX2-HA (*red*) were detected around the ZPX2-HA-expressing cells cultured in the presence of serum ZPB1, and localization of the two proteins was identical. ZPX2 could accumulate on the cell surface by itself regardless of the presence of serum ZPB1 in the medium. As expected, ZPB1 accumulation was not at all observed in the case of mock transfectants. It is noteworthy that ZPX2-HA was accumulated on the surface of the transfectants either in the presence or absence of ZPB1 in the medium, whereas the cell surface accumulations of neither normal ZPC nor ZPC-HA were detected in the absence of ZPB1 (see Figs. 2-10 and 11).

Specific association of ZPX2 with ZPC both secreted into culture supernatants of

transfected COS-7 cells— To determine whether ZPX2 and ZPC both expressed in and secreted from expressing cells interact with each other, the culture supernatants from the distinct COS-7 cells transfected with the ZPX2-HA expression plasmid (*pZPX2-HA*) or ZPC expression plasmid (*pZPC*) were mixed each other, incubated and subjected to reciprocal co-immunoprecipitation analyses using anti-HA and anti-ZPC antibodies (Fig. 2-17). The probable mature ZPC secreted into the medium (*open arrowhead*) was co-precipitated with probable mature ZPX2-HA (*closed gray arrowhead*) by immunoprecipitation using the anti-HA, indicating that ZPX2 associated with ZPC both secreted into culture medium to form ZPX2-ZPC complexes. However, the ZPX2-ZPC complex was not immunoprecipitated effectively using the anti-ZPC, although the anti-ZPC could immunoprecipitate free ZPC secreted into the medium effectively, suggesting that the accessibility of the anti-ZPC to ZPC was decreased through association of ZPC with ZPX2.

Discussion

In chicken, cDNAs of the five ZP glycoproteins, ZPA (not submitted to data base) [Kohno, 2000], ZPB1 (GenBank® accession no. AJ289697) [Bausek *et al.*, 2000], ZPB2 (GenBank® accession no. AB025428) [Tsuda, 1999], ZPC (GenBank® accession no. D89097) [Takeuchi *et al.*, 1999] and ZPX2 (GenBank® accession no. AB114441) [Okumura *et al.*, 2004] are cloned. Furthermore, it is suggested that the ZP-glycoprotein compositions in the egg envelope are changed through the follicular development by immunoblotting analyses for whole follicles or egg envelopes prepared from several immature and mature follicles, and that the egg envelope surrounding the mature oocyte just before the ovulation was composed of ZPB1, ZPC and ZPX2 [Iwata, 2002]. However, the SDS-PAGE of ZP glycoproteins has usually been performed under reducing conditions in our previous studies. We therefore have not been able to separate the band of ZPX2-protein from that of ZPC in the SDS-PAGE gel and demonstrate the presence of ZPX2 in the mature egg envelope clearly. In the present study, the ZP glycoproteins in the mature egg envelope were further confirmed by immunoblotting and MS analyses (Figs. 2-1 and 2). As shown in Figure 2-1*A*, ZPX2 co-migrates with ZPC in SDS-PAGE under reducing conditions and is not identified as a separate band. Furthermore, in the present study, the N-terminal amino acid sequence of ZPX2 could not be determined probably due to α-amino group blocking, indicating that ZPX2 hidden behind the ZPC band had escaped the detection by the amino acid sequencing analysis for ZPC in our previous study [Takeuchi *et al.*, 1999]. ZPC and ZPX2 are separated under non-reducing conditions (Fig. 2-1*B*). This difference in electrophoretic patterns is caused mainly by a drastic increase in mobility of ZPC in the absence of a reducing reagent. Although I do not know exactly why this mobility shift occurs, ZPC may have a compact structure supported by intramolecular disulfide bonds. Actually, the CD spectrum of ZPC purified here showed a strong negative peak at 210 nm, suggesting its β-sheet-rich structure (data not shown).

Although ZPX2 is a component of the hard egg envelope, ZPX2 is easily released

and separated from the egg-envelope matrix by the ultrasonication treatment in the absence of urea (Fig. 2-3*B*). This unexpected property of ZPX2 rendered us difficult to evaluate this protein as a main component of the egg envelope. In our initial experiments, some amounts of ZPX2 were lost during unnecessarily harsh wash of the collected envelope so that the yield of ZPX2 varied from preparation to preparation. I then found that this protein was quantitatively and specifically released under the conditions described here (gentle wash and sonication without urea). According to this procedure, the yield of isolated ZPX2 has been constant and comparable to that of other ZP proteins in every preparation. Therefore, I now believe that ZPX2 is a major component of the mature egg envelope. Because no other distinct bands and spots were detected in SDS-PAGE (Fig. 2-1), it is unlikely that yet unidentified protein exists as a major component of the mature envelope. This conclusion is supported by the fact that all of the proteolytic peptides from whole egg envelope were assigned to ZPB1, ZPC or ZPX2 (Fig. 2-2). However, a possibility could not completely be ruled out that egg envelope contains such unidentified protein(s) as those with resistance against proteolytic digestion. In fact the ZPX2-derived peptide was only one of the 11 identified peptides, suggesting that proteolytic digestibility of ZP proteins largely differ.

Among the ZP family members chicken ZPB1 is unique in its domain structure. In addition to a common ZP domain, an N-terminal domain with 5 (an odd number) cysteine residues, a trefoil domain, and a "repeat" region consisting of 15 repeat sequences, each of which has about 24 amino acid residues rich in Gln and Arg. Based on this characteristic domain structure predicted simply by the deduced amino acid sequence, a non-globular but a linear conformation was speculated for a ZPB1 molecule. However, only limited biochemical or physicochemical information of the ZPB1 molecule has been obtained so far [Basusek *et al.*, 2000 and 2004; Takeuchi *et al.*, 2001]. ZPB1 in the hen's serum was eluted from the gel-filtration column as an about 200-kDa protein, i.e., similarly to serum immunoglobulin but much faster than serum albumin (see Fig. 2-4). This apparent molecular mass of 200 kDa agrees well with a ZPB1 dimer estimated by SDS-PAGE (see Fig. 2-1*B*, *lane 1*), suggesting the presence of soluble homodimer in the serum. However,

further studies are needed to clarify whether ZPB1 exist in blood as a monomer or a homodimer without any covalent cross-linkages. A possibility of heterocomplex formation with some serum proteins also could not be ruled out.

As described above, ZPB1 was solubilized from isolated egg envelope with SDS or a urea solution without reducing agents, and was eluted as monomer and dimer into two separate fractions from a gel-filtration column in the presence of urea (Fig. 2-3). By contrast to the egg-envelope ZPB1, the ZPB1 secreted from liver cells was soluble itself in blood even in the absence of such denaturing agents or strong detergents. The ZPX2 was released from the envelope without urea and other ZP glycoproteins were not as described above, strongly suggesting that ZPX2 was loosely associated with strong matrix structure composed of dimeric and monomeric ZPB1 and ZPC. Accordingly, it was indicated that non-covalent association of ZPB1 with the other ZP components, especially ZPC, would important for the matrix formation. Interestingly, it was suggested that the serum ZPB1 and the egg-envelope derived ZPC interacted with each other in a dose dependent manner, and that the binding affinities of these proteins with the specific antibodies or the ELISA plates were influenced through the ZPB1-ZPC interaction (see Fig. 2-5). Furthermore, the ZPB1 specifically bound to ZPC but neither ZPX2 nor ZPB1 itself blotted on the membrane (Fig. 2-6), and it accumulated around the cells only when the cells secreted ZPC (Fig. 2-12). These findings are consistent in part with the results of a recent work on Japanese quail egg envelope [Ohtsuki *et al.*, 2004] that ZPB1 in the egg-envelope lysate was coprecipitated with ZPC secreted by cultured granulosa cells. In this immunoprecipitation experiment, however, the whole egg-envelope lysate was used as a ZPB1 origin, and only ZPB1 dimer was shown being coprecipitated. Therefore, this previous experiment [Ohtsuki *et al.*, 2004] could not rule out a possibility that ZPC interacted with ZPC-ZPB1 complexes or some unknown component(s), which had associated with ZPB1, already present in the egg-envelope lysate. In the present study using serum ZPB1, both ZPB1 monomer and dimer were coprecipitated with ZPC in a proportion similar to those of the egg envelope (see Fig. 2-8*B*). This result in addition to the fact that serum ZPB1 is monomer [Bausek *et al.*, 2000] suggest that serum

monomeric ZPB1 interacts with ZPC secreted from granulosa cells and then ZPB1 dimerization by intermolecular disulfide bonding is induced during the formation of ZPB1-ZPC heterocomplexes and further polymerization.

The disulfide-linked dimer of ZPB1 present in part in the isolated egg envelope is believed to play important roles in the construction of fibrous matrix of egg envelope. Presumably, at least some conformational changes in ZPB1 molecules are required for a free sulfhydryl-group to be exposed for a sulfhydryl or disulfide group of another ZPB1. The monoclonal anti-ZPB1, 8E1, could precipitate free ZPB1 but not ZPB1-ZPC complexes in the culture medium (see Fig. 2-10). A simple explanation for this result is that the C-terminal region of ZP domain in a ZPB1 molecule was masked with the associated ZPC resulting in the prevention of the antibody, 8E1, from binding. Such ZP-domain dependent interaction between ZPB1 and ZPC might be reasonable, because the ZP-domain proteins including the egg-envelope ZP glycoproteins are suggested to associate via ZP domains [Jovine *et al.*, 2002]. Alternative speculation is that a certain level of conformational changes in the C-terminal region of a ZPB1 molecule, including the 8E1 epitope, was induced through ZPB1-ZPC interaction or complex formation. Further studies are needed to determine how ZPB1-ZPC polymerization and inter-ZPB1 disulfide cross-linking are induced during the egg-envelope construction in the laying hen's ovary. It would be of special interest to examine a possible C-terminal processing of serum ZPB1 after its transport to oocyte surface, because such a processing has recently been reported on fish ZP glycoproteins [Darie *et al.*, 2005], which is also synthesized in liver.

After the separation from ZPC, ZPB1 could remain soluble even after removal of urea by dialysis at least in a low concentration (microgram per ml level) solution (see Fig. 2-3). In addition to this previous observation, the binding specificity of ZPB1 to ZPC as demonstrated by using two distinct monoclonal antibodies in the present study suggests that the association between ZPB1 and ZPC is not simply due to hydrophobic aggregation but some specific association including hydrogen and electrostatic bonds. I have suggested above that the chicken egg envelope is constructed with ZPB1 and ZPC, and ZPX2 associate

loosely with the ZPB1-ZPC complex, because ZPX2 is released from the complex easily by a mechanical treatment such as sonication (Fig. 2-3) or vigorous washing [Takeuchi *et al.*, 1999 and 2001; Bausek *et al.*, 2000]. This suggestion on the egg-envelope construction by ZP proteins would be consistent with the results of the present study that ZPB1 associated with ZPC, not ZPX2, and only the two components, ZPB1 and ZPC, could form a type of matrix on the surface of cultured cells (see Figs. 2-8 and 11).

HA-tagged ZPC was successfully expressed, processed and secreted in part by the transfected COS-7 cells (see Fig. 2-7). Mature native ZPC in the egg-envelope was detected as a 35-kDa signal in non-reducing SDS-PAGE (Fig. 2-1 and 6) and the calculated molecular mass of C-terminal hydrophobic peptide derived from the processing of proZPC at the conserved furin cleavage site was approximately 7 kDa. The sum of masses for mature ZPC and the C-terminal peptide agrees well with that of probable proZPC (42 kDa) (see Fig. 2-7). Such a transient expression of ZPC has been reported also on CHO cells by using Japanese quail ZPC [Sasanami *et al.*, 2003a-c]. The intracellular accumulation of proproteins and the extra-cellular secretion of processed and probably matured proteins are common in both of the two cell-lines originated from different organs, kidney and ovary. COS-7 cells are known to endogenously express a processing enzyme, furin, and can process some ectopically expressed pro-hormones resulting in the secretion of bioactive hormones [Warren and Shields, 1984; Galanopoulou *et al.*, 1993; Yanagita *et al.*, 1992; Hayashi *et al.*, 1994]. Taken these together, the 35-kDa ZPC-HA secreted into culture medium by COS-7 cells is expected to be matured and correctly folded ZPC with HA-tag at its C-terminus.

The confocal laser scanning microscopic analyses clearly demonstrated that ZPB1 was deposited and accumulated together with the secreted ZPC on the cell surface (Fig. 2-12). No accumulation of ZPB1 on the mock transfectants was as scheduled, but it should be noticed that the ZPC signal was also under detectable level on the surface of *pZPC-HA* transfectants cultured in the absence of ZPB1 (see Fig. 2-13), which actually expressed and secreted ZPC-HA (see Fig. 2-7). These results indicate that ZPC proprotein with the transmembrane region does not stably exist on the cell surface and the mature ZPC was

released from the cells immediately after the removal of its putative transmembrane region by furin cleavage. Thus, it would be unlikely that ZPB1 was accumulated around the cell by binding to ZPC which had been localized or pre-deposited alone on the cell surface. The ZPB1 would rather associate with the secreted ZPC nearby the cell and/or the cell surface proZPC just before furin-cleavage, which leads to the accumulation of ZPB1-ZPC matrix-like complexes around the cell.

Although biochemical and physicochemical differences between the ZPB1-ZPC complexes present in the medium and those accumulated on the cell surface are still unclear, I speculate that a part of the ZPB1-ZPC complexes was diffused into the medium as a small complexes or particles before larger particles or matrices were formed on the cell surface. In fact, in preliminary experiments, I have found that the ZPB1-ZPC complexes were precipitated by a simple ultracentrifugation at 100,000 x g for 60 min (Fig. 2-9), indicating that ZPB1-ZPC complexes in the culture medium were present as small particles. In hen's ovary the secreted ZPC would be accumulated in a narrow space between a granurosa cell layer and an oocyte, and therefore, such small particles will also participate in the construction of the egg-envelope matrix.

The third egg-envelope ZP glycoprotein, ZPX2 would be associated with the ZPB1-ZPC matrix in the egg envelope as described above. The ZPX2 secreted by the transfected COS-7 cells bound to the ZPB1 added to its culture medium to form ZPB1-ZPX2 heterocomplexes (see Figs. 2-15 and 16), although the serum ZPB1 bound to the ZPX2 blotted on a membrane was under detectable level (see Fig. 2-6), indicating that ZPX2 bound to serum ZPB1 with lower affinity. The confocal laser scanning microscopic analyses clearly demonstrated that ZPB1 was deposited and accumulated together with the secreted ZPX2 on the cell surface (Fig. 2-16). No accumulation of ZPB1 on the mock transfectants was as scheduled. Interestingly, the secreted ZPX2 was accumulated on the surface of the cell either in the presence or absence of ZPB1 (Fig. 2-16), in contrast with ZPC accumulated on the cell surface only when ZPB1 was in the medium and did not accumulate by itself (Figs. 2-12 and 13). Actually, the mature ZPX2 was detected in the lysate of ZPX2 expressing

cells (see Fig. 2-14) but not detected in that of ZPC expressing cells (Fig. 2-7). Taken these together, it is suggested that ZPX2 forms homocomplexes and binds to ZPB1 weakly, while ZPC does not form homocomplexes but form solid ZPB1-ZPC heterocomplexes as described above.

Either ZPC or ZPX2 was secreted into the culture medium of each expressing cell as a mature form (see Figs. 2-7 and 14), although in the hen's ovary, it is unknown whether ZPC and ZPX2 are coexpressed in homogeneous granulosa cells or there are two types of granulosa cells expressing ZPC or ZPX2, respectively. In this study, the culture supernatants of ZPX2-HA expressing cells and ZPC expressing ones were mixed and incubated each other, and the specific association of ZPX2 with ZPC was demonstrated by immunoprecipitation analyses (see Fig. 2-17). Free ZPX2-HA and ZPC were immunoprecipitated effectively using the anti-HA and anti-ZPC antibodies, respectively. However, anti-ZPC antibody could not immunoprecipitate the ZPX2-HA-ZPC complexes, whereas anti-HA antibody could immunoprecipitated ones effectively (Fig. 2-17). Considering that ZPX2 secreted from the expressing cells would form homocomplexes by itself (see Figs. 2-14 and 16) and ZPC could not form homocomplexes (see Figs. 2-7 and 13), it is suggested that the ZPX2 secreted into the medium would form small particles or homocomplexes, and surrounds ZPC molecule(s) to form the ZPX2-ZPC complexes.

Recent studies on disulfide bridges of ZP glycoproteins mapped by mass spectrometry [Boja *et al.*, 2003; Darie *et al.*, 2004; Zhao *et al.*, 2004; Hoodbhoy *et al.*, 2005], suggest that there are two types of ZP domain having partially distinct positions of conserved cysteine residues and disulfide bridges, ZP3-type and ZP1/ZP2-type. It is predicted by the alignment between amino acid sequences of ZP domains in mouse and chicken ZP glycoproteins (data not shown) that ZP domains of chicken ZPB1 and ZPX2 were ZP1/ZP2-type and ones of chicken ZPC were ZP3-type, although intermolecular disulfide bonds of chicken ZP glycoproteins have not been analyzed yet. From these suggestions and revealed associations between ZP glycoproteins of fish [Darie *et al.*, 2004] and mouse [Greve and Wassarman, 1985; Rankin *et al.*, 1996, 1999 and 2001] egg envelopes, it is hypothesized

that proteins having the ZP1/ZP2-type ZP domain form homocomplexes or heterocomplexes with other ones having the ZP1/ZP2-type ZP domain, or heterocomplexes with ones having the ZP3-type ZP domain [Jovine *et al.*, 2005]. This hypothesis would be further supported by the present studies on the avian egg-envelope structure.

I am studying on the matrix architecture of an avian egg envelope including its formation mechanism(s) from the ZP-glycoprotein components. The results in the present studies speculate that ZPB1 transported to the ovary through the blood stream and ZPC secreted from the granulosa cell into a narrow space between an oocyte and a granulosa cell layer interact preferentially with each other to form the ZPB1-ZPC heterocomplexes or matrices, and ZPX2 secreted from the granulosa cell forms homocomplexes by itself and be bound to both of ZPB1 and ZPC in the ZPB1-ZPC matrix. The mechanism of the preferential formation of the ZPB1-ZPC heterocomplexes is unclear. The predicted structure of the avian (chicken) egg envelope is largely different from that of the mammalian (mouse) one [Greve and Wassarman, 1985; Rankin *et al.*, 1996, 1999 and 2001], and the egg-envelope ZP-glycoprotein compositions vary from species to species, implying that the egg-envelope structures and its formation mechanisms would be strongly related to the oocyte maturation processes and the fertilization pathways of the vertebrates. The investigations on the egg-envelope structures and its formation mechanisms would give new insights into understanding the evolution of vertebrate reproduction, in addition the molecular mechanism for construction of non-collagenous extracellular matrices by ZP-domain proteins.

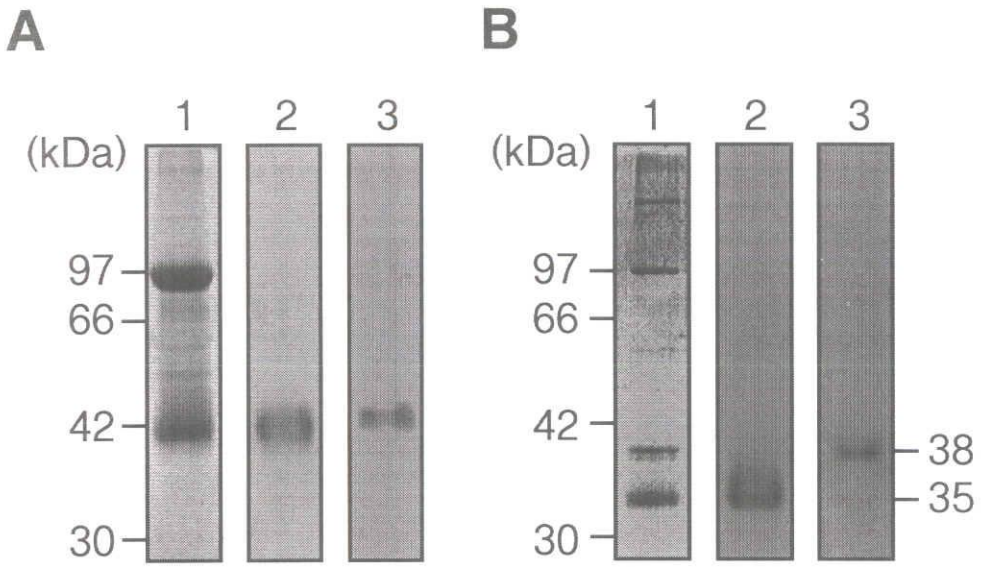

Fig. 2-1. Electrophoresis of egg-envelope proteins. SDS-PAGE under reducing conditions (*A*) and non-reducing conditions (*B*). Proteins separated on 10% gels were stained with CBB (*lanes 1*) or subjected to immunostaining with anti-ZPC antibody (*lanes 2*) and anti-ZPX2 antibody (l*anes 3*). The migration positions of the protein markers are shown in the *far left panels*.

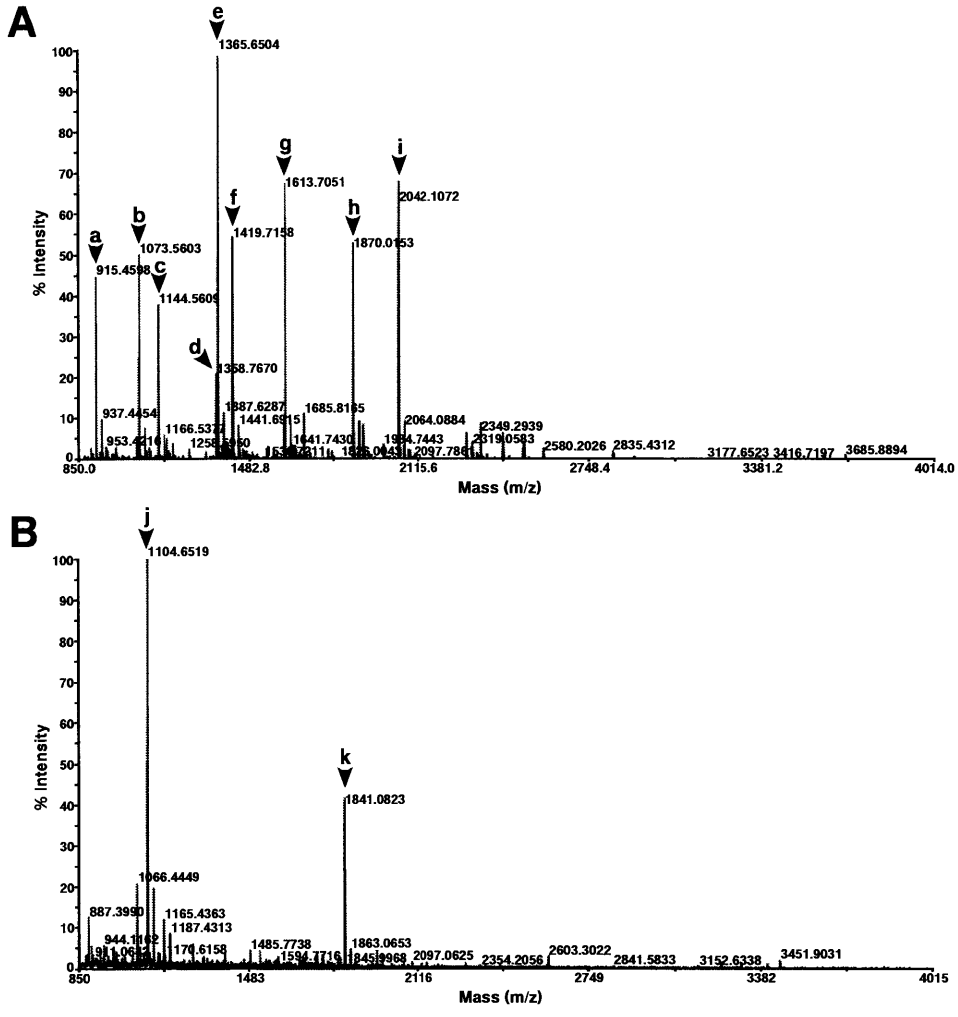

C

	Peak	Actual mass (Da)	Protein	Position	Sequence	Theoretical mass (Da)
Trypsin	a	915.4598	ZPC	357-363	RLNPMER	915.4829
	b	1073.5603	ZPB1	711-719	DSVYILHAR	1073.5738
	c	1144.5609	ZPC	329-338	NTWVPVEGSR	1144.5745
	d	1358.7670	ZPB1	775-785	VLRDPIYVEVR	1358.7790
	e*	1365.6504	ZPC	30-40	YTPWDISWAAR	1365.6586
	f	1419.7158	ZPB1	638-650	GLSAQPYNLDSVR	1419.7226
	g	1613.7051	ZPC	41-55	GDPSAWSWGAEAHSR	1613.7091
	h**	1870.0153	ZPC	135-151	TLINYDPSPASNPVIIR	1870.0068
	i	2042.1072	ZPB1	688-705	LVYENQLISTIDVQPGPR	2042.0916
Lys-C	j	1104.6519	ZPX2	106-114	IPRELVHLK	1104.6887
	k**	1841.0823	ZPB1	775-789	VLRDPIYVEVRLLQK	1841.1007

Fig. 2-2. Identification of peptides derived from tryptic and Lys-C digests of egg-envelope constituents by mass spectrometry

Fig. 2-2. Identification of peptides derived from tryptic and Lys-C digests of egg-envelope constituents by mass spectrometry. The tryptic digest (2-h incubation) (*A*) and the Lys-C digest (18-h incubation) (*B*) were analyzed by using a MALDI-TOF-TOF mass spectrometer. The major peaks (*arrowheads a* to *k*) were further subjected to MS/MS analysis to obtain sequence data. The mass and sequence data for the major 11 peptides are summarized in *C*.

* The N-terminal end fragment of ZPC mature protein.

**As for these 2 peptides no sequence data could be obtained by MS/MS analysis.

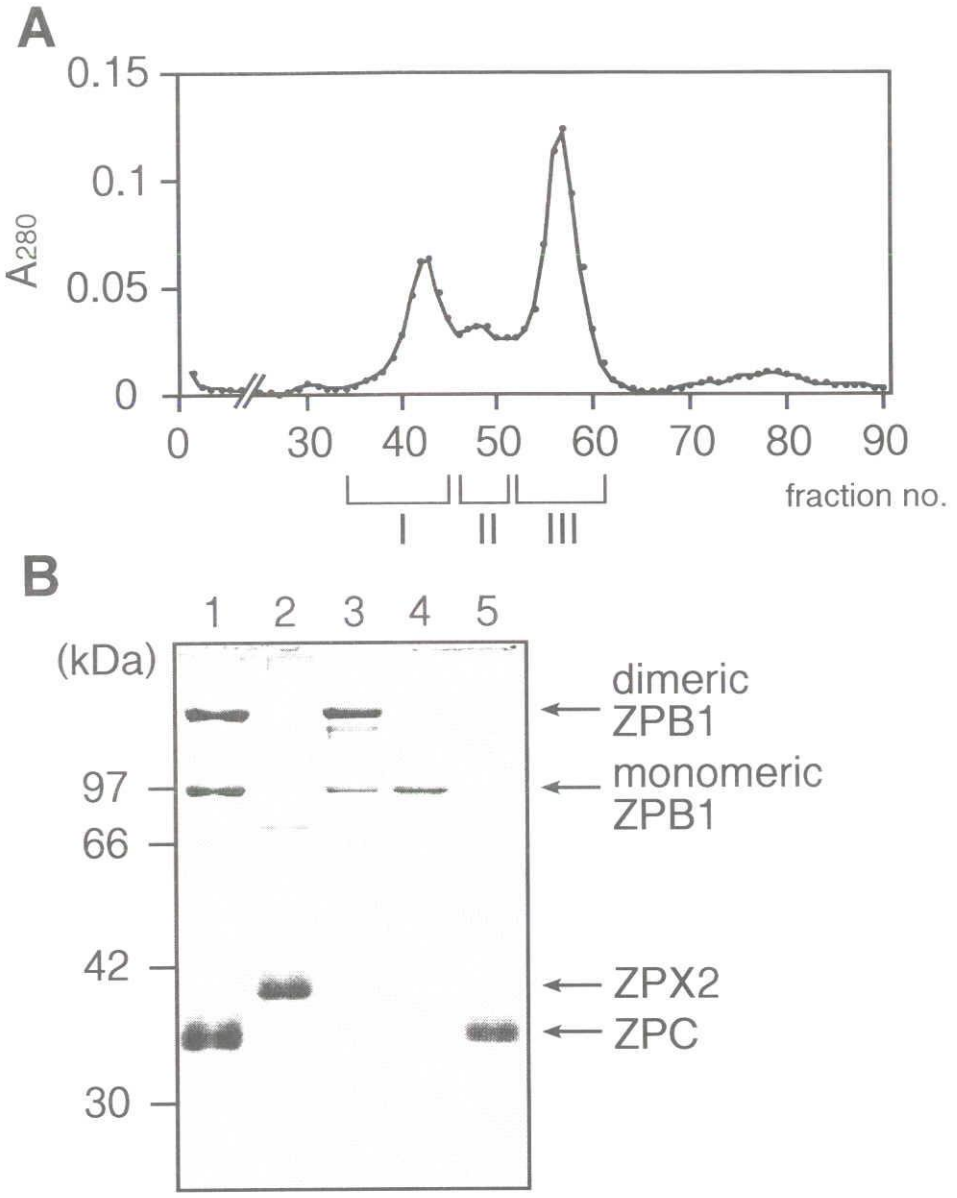

Fig. 2-3. Preparation of ZP glycoproteins from the egg envelope. Fraction X was obtained as the supernatant fraction of the egg envelope sonicated in the absence of urea. The precipitated material was then sonicated in the acetate buffer containing 8 M urea and centrifuged. The supernatant (fraction Y) was subjected to gel filtration. *A*, Gel filtration. Fractions were pooled as indicated by the horizontal bars. Chromatographic conditions are described in Experimental. *B*, SDS-PAGE of the fractions thus obtained. Proteins were separated on 10% gel under non-reducing condition and stained with CBB. The migration positions of the protein markers are shown on the left of the *panel*. A typical PAGE pattern of egg envelope and the protein bands identified by immunoblotting with antibodies against each ZP glycoprotein are indicated on the right.

Lanes: *1*, fraction Y; *2*, fraction X; *3*, fraction I; *4*, fraction II; *5*, fraction III.

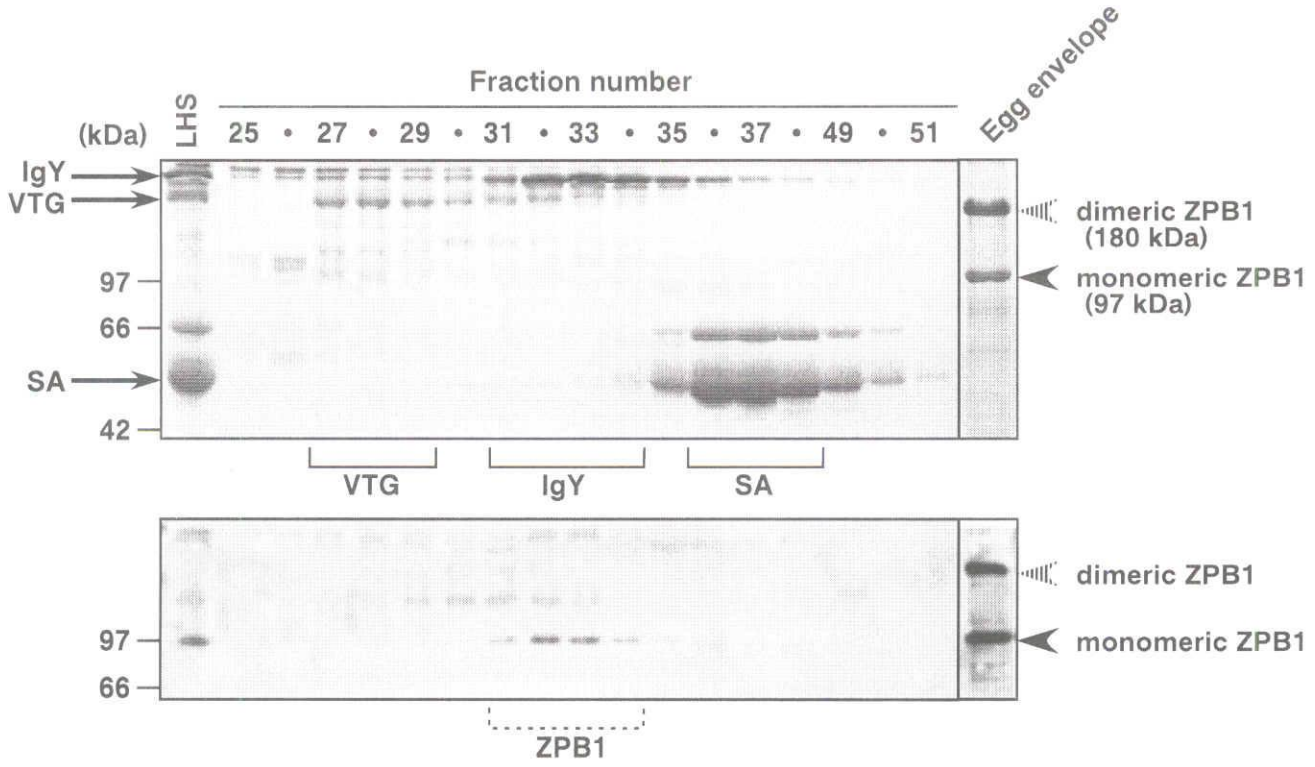

Fig. 2-4. Gel-filtration analysis of hen's serum ZPB1. The eluted protein fractions (4 µl each) were sub - jected to SDS-PAGE under non-reducing conditions followed by CBB staining (*upper panel*). Another gel was used for immunoblotting with anti-ZPB1 monoclonal antibody, 8E1 (*lower panel*). Protein bands and fractions of immunogrobulin Y (*IgY*), vitellogenin (*VTG*) and serum albumin (*SA*) detected by CBB staining are indicated on the left and the bottom of *upper panel*, respectively, and the fractions of ZPB1 detected by immunoblotting are indicated on the bottom of *lower panel*. The monomeric (*closed arrowheads*) and dimeric (*striped arrowheads*) ZPB1 bands of egg-envelope (*EE*) are indicated on the right.

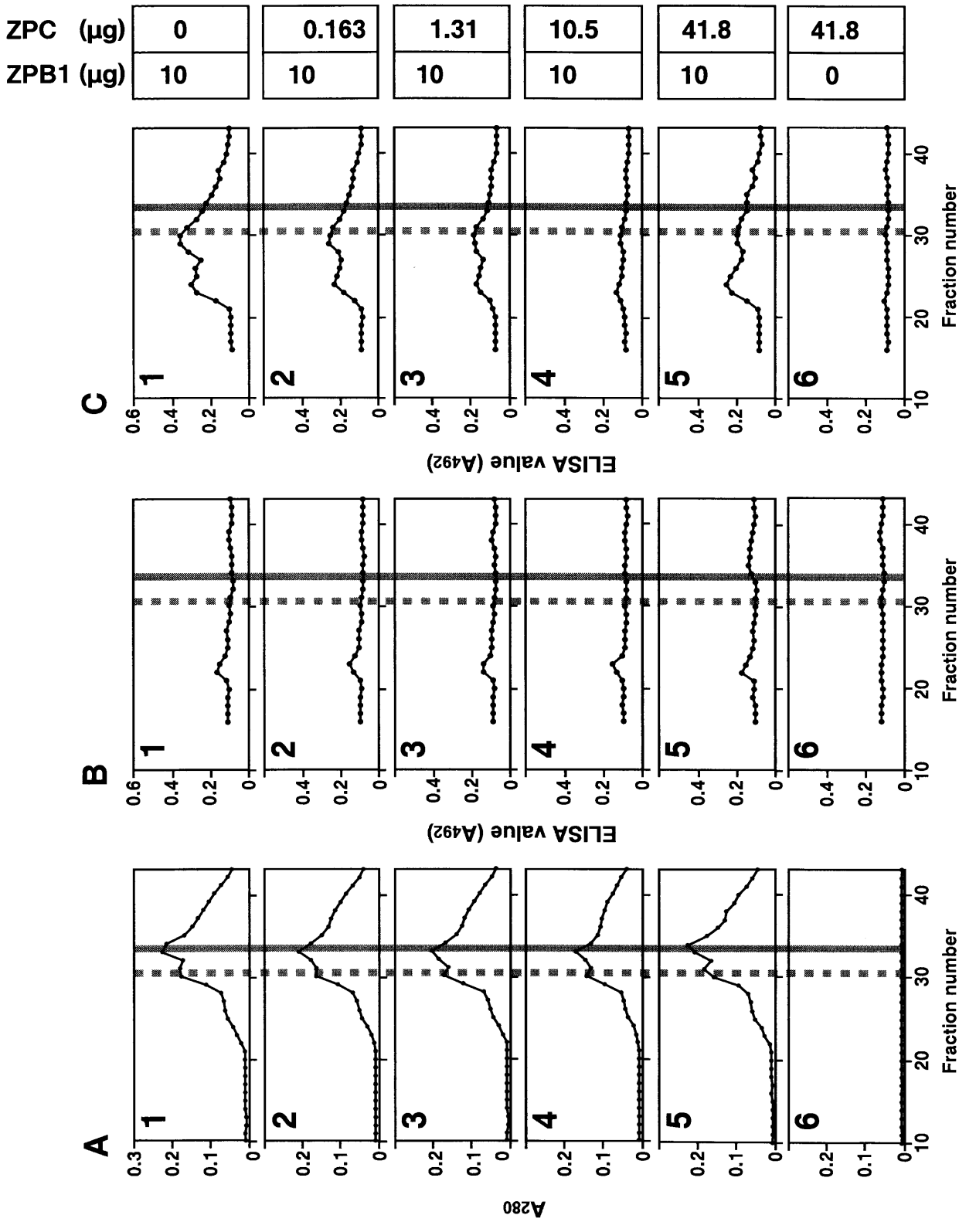

Fig. 2-5. Heterocomplex formation of serum ZPB1 with ZPC at various ratios of ZPC/ZPB1

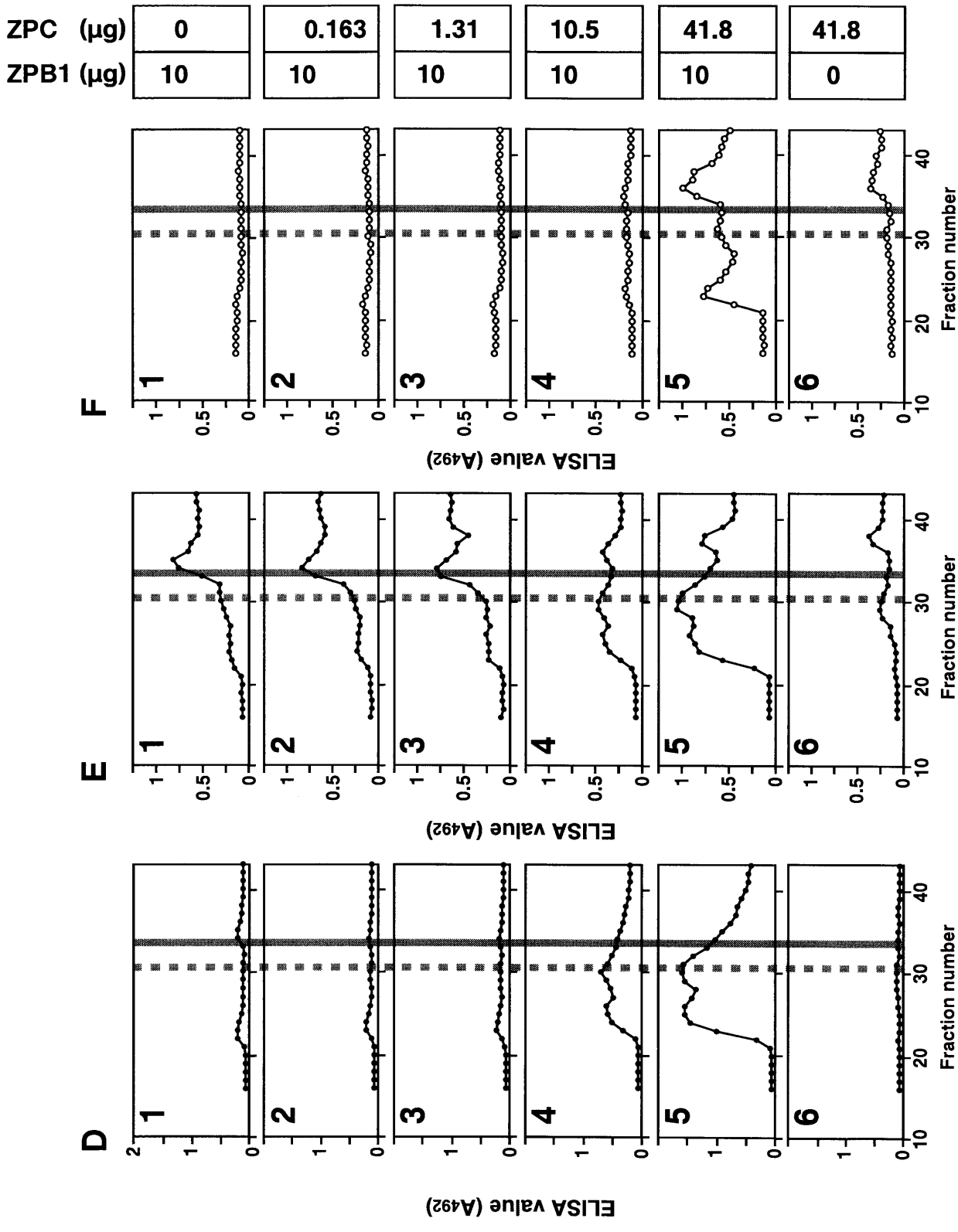

Fig. 2-5. Heterocomplex formation of serum ZPB1 with ZPC at various ratios of ZPC/ZPB1

Fig. 2-5. Heterocomplex formation of serum ZPB1 with ZPC at various ratios of ZPC/ZPB1. LHS (100 μl, containing 10 μg of ZPB1) and ZPC protein prepared from the egg envelope were incubated and subjected to gel-filtration chromatography. The eluted fractions were subjected to the UV-detection (*A*) and the ELISA with the domain-specific antibodies for ZPB1; polyclonal anti-ZPB1s (N-terminal domain and repeat region) (*B* and *C*, respectively) , monoclonal anti-ZPB1s (5G9 and 8E1) (*D* and *E*, respectively), and the anti-ZPC (*F*). The amounts of ZPB1 and ZPC in the LHS-ZPC mixture were indicated on the right of *C* and *F*. Fractions which IgG (180 kDa) and serum albumin (66 kDa) were eluted were indicated by *broken gray lines* and *solid gray lines*, respectively.

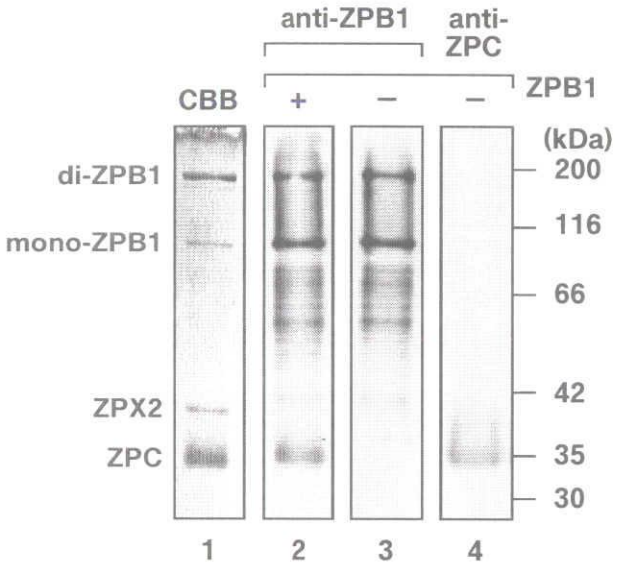

Fig. 2-6. A ligand-blotting analysis showing the specific binding of serum ZPB1 to electrophoretically separated egg-envelope ZPC. Aliquots of egg envelope (670 μg for *lane 1*, and 11 μg each for *lanes 2-4* by wet weight) were solubilized by the SDS sample buffer and separated by SDS-PAGE under non-reducing conditions. One lane of the gel was stained with CBB (*lane 1*) and the other lanes (*lanes 2-4*) were used for electroblotting. After being incubated with (+; *lane 2*) or without (–; *lanes 3* and *4*) ZPB1-containing serum, the blotted membranes were immuno-stained with anti-ZPB1 (*lanes 2* and *3*) and anti-ZPC (*lane 4*) antibodies, respectively. The migration positions of the protein markers are shown on the right. The bands of monomeric- (*mono-ZPB1*) and dimeric-ZPB1 (*di-ZPB1*), ZPC and ZPX2 are indicated on the left.

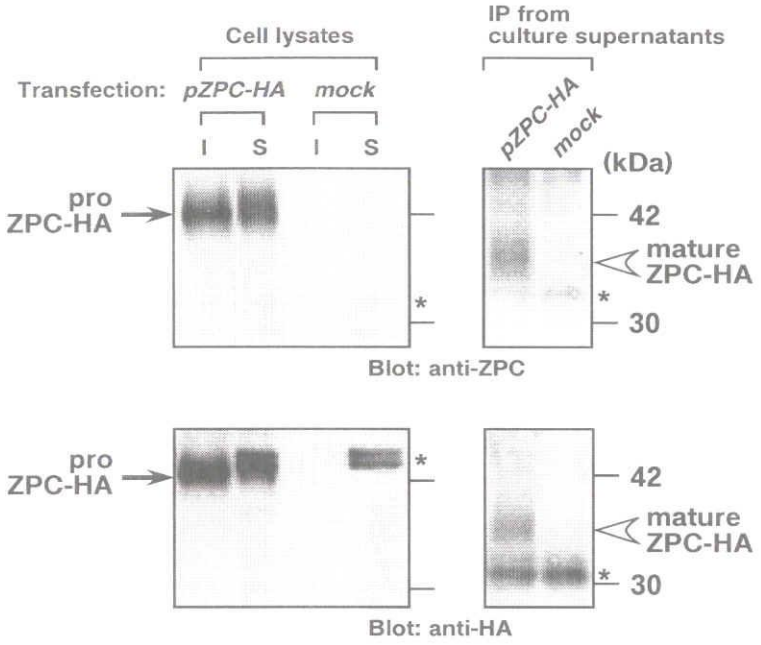

Fig. 2-7. Expression, processing and secretion of HA-tagged ZPC by transfected COS-7 cells. COS-7 cells were transfected with an expression plasmid for the epitope-tagged ZPC (*pZPC-HA*) or an empty vector (*mock*) and cultured. The culture supernatants were collected, while the cells were lysed with the Triton X-100 containing lysis buffer and harvested. The cell lysates were separated into two fractions, soluble supernatant and insoluble pellet. The Triton X-100-insoluble (*I*, 1/5 of the total cell lysates) and -soluble (*S*, 1/6 of the total cell lysates) fractions were subjected to SDS-PAGE under non-reducing conditions (*left-two panels*), followed by immunoblotting with anti-ZPC (*top*) or anti-HA (*bottom*) antibodies. The secreted ZPC-HA was immunoprecipitated from the culture supernatants (800 μl, 4/5 of the culture supernatant) using anti-ZPC, and subjected to the SDS-PAGE/immunoblotting analysis (*right-two panels*). The migration positions of protein markers are shown on the right. Protein bands estimated to be proZPC-HA (*arrows*) and mature ZPC-HA (*open arrowheads*) are also indicated on the left and the right, respectively. Asterisks (*) represent non-specific staining.

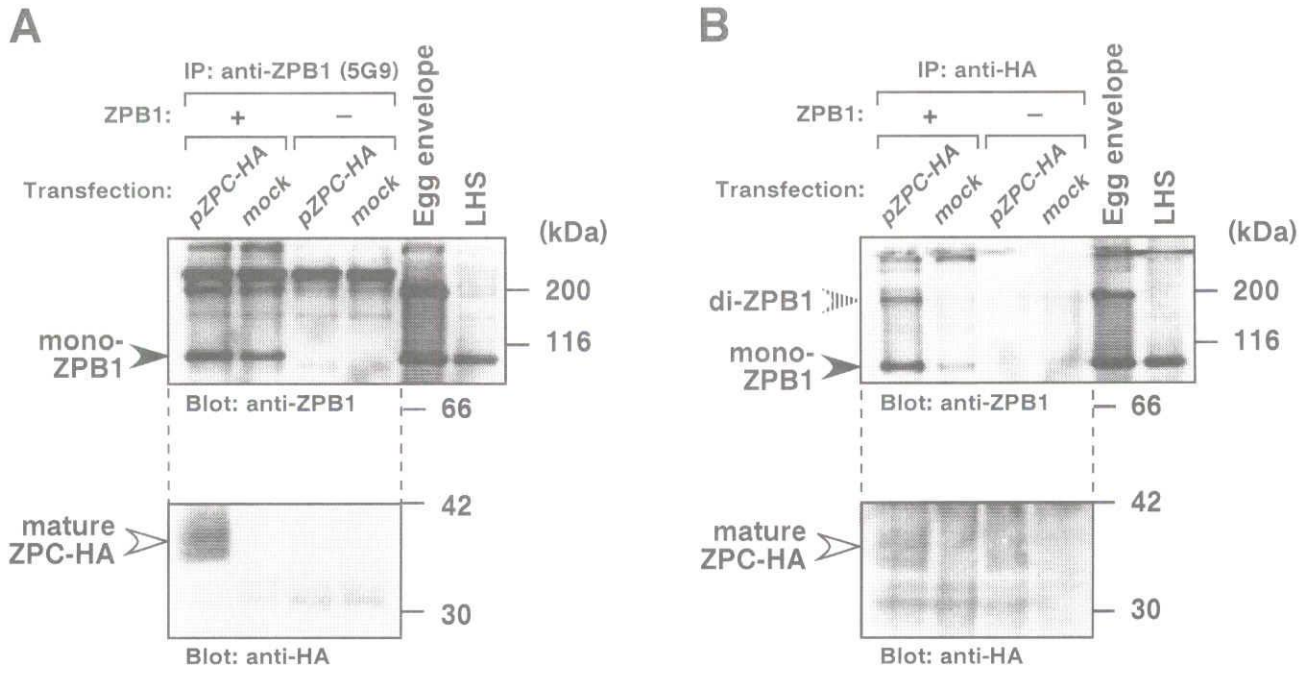

Fig. 2-8. Immunoprecipitation of ZPB1-ZPC heterocomplexes from the culture supernatant of the transfect - ed COS-7 cells cultured in the presence of ZPB1. COS-7 cells transfected with an expression plasmid for ZPC-HA (*pZPC-HA*) or a control plasmid (*mock*) were cultured in the presence (+) or absence (–) of ZPB1. The culture supernatants were collected and subjected to the immunoprecipitation (IP) using anti-ZPB1 monoclonal antibody, 5G9 (*A*), and anti-HA (*B*). The immunoprecipitates (1/5 and 1/2 of the precipitates in *upper* and *lower panels*, respectively), were subjected to SDS-PAGE under non-reducing conditions followed by immunoblotting with anti-ZPB1 (*upper panels*) and anti-HA (*lower panels*) antibodies. The migration positions of the protein markers are shown on the right. Protein bands corresponding to dimeric ZPB1 (*di-ZPB1*; *striped arrowhead*), monomeric ZPB1 (*mono-ZPB1*; *closed arrowheads*) and mature ZPC-HA (*open arrowheads*) are indicated on the left.

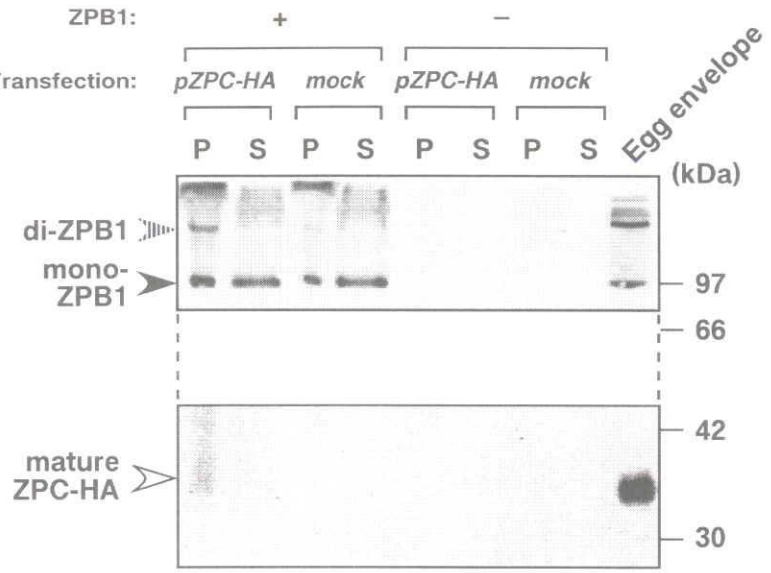

Fig. 2-9. Precipitation of ZPB1/ZPC-HA heterocomplexes by ultra-centrifugation. COS-7 cells transfected with expression plasmid for ZPC-HA (*pZPC-HA*) or a control plasmid (*mock*) were cultured in the presence (+) or absence (–) of ZPB1. the culture supernatants were collected and subjected to ultracentrifugation at 100,000 x g for 60 min. The precipitates (*P*, 1/5 of the precipitates) and the supernatants (*S*, 1/250 of the supernatants) were subjected to SDS-PAGE under non-reducing conditions followed by immunoblotting with anti-ZPB1 (*upper panel*) and anti-ZPC (*lower panel*). The migration positions of the protein markers are shown on the right of *panels*. Protein bands corresponding to dimeric ZPB1 (*di-ZPB1*; *striped arrowhead*), monomeric ZPB1 (*mono-ZPB1*; *closed arrowhead*) and mature ZPC-HA (*open arrowhead*) are indicated on the left.

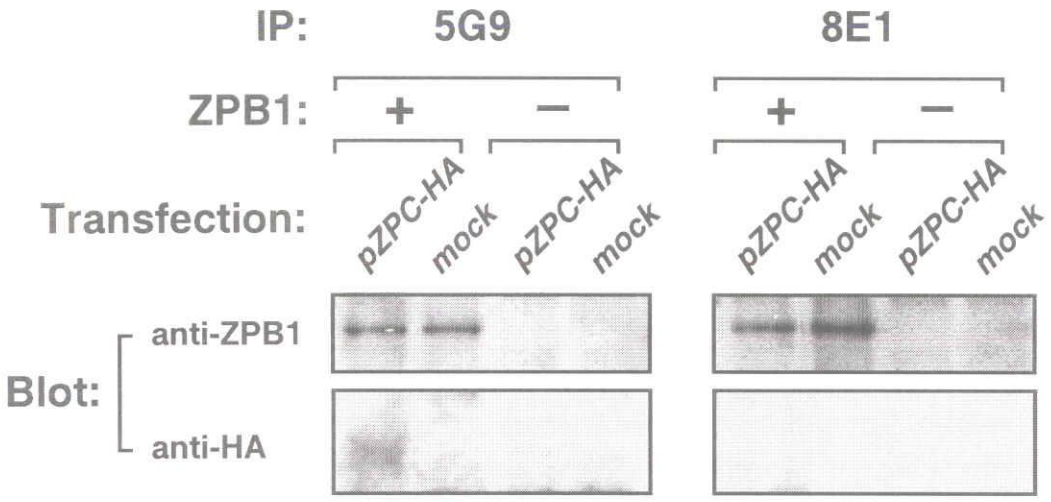

Fig. 2-10. Differential accessibility of two distinct monoclonal antibodies to ZPB1 of the ZPB1-ZPC heterocomplexes. The culture supernatants of COS-7 cells transfected with an expression plasmid for ZPC-HA (*pZPC-HA*) or a control plasmid (*mock*) were collected, mixed and incubated with (+) or without (–) ZPB1, and subjected to immunoprecipitation using the anti-ZPB1 monoclonal antibodies, 5G9 and 8E1. The immunoprecipitates were subjected to SDS-PAGE under non-reducing conditions followed by immunoblotting with anti-ZPB1 (*upper panels*) and anti-HA (*lower panels*) antibodies.

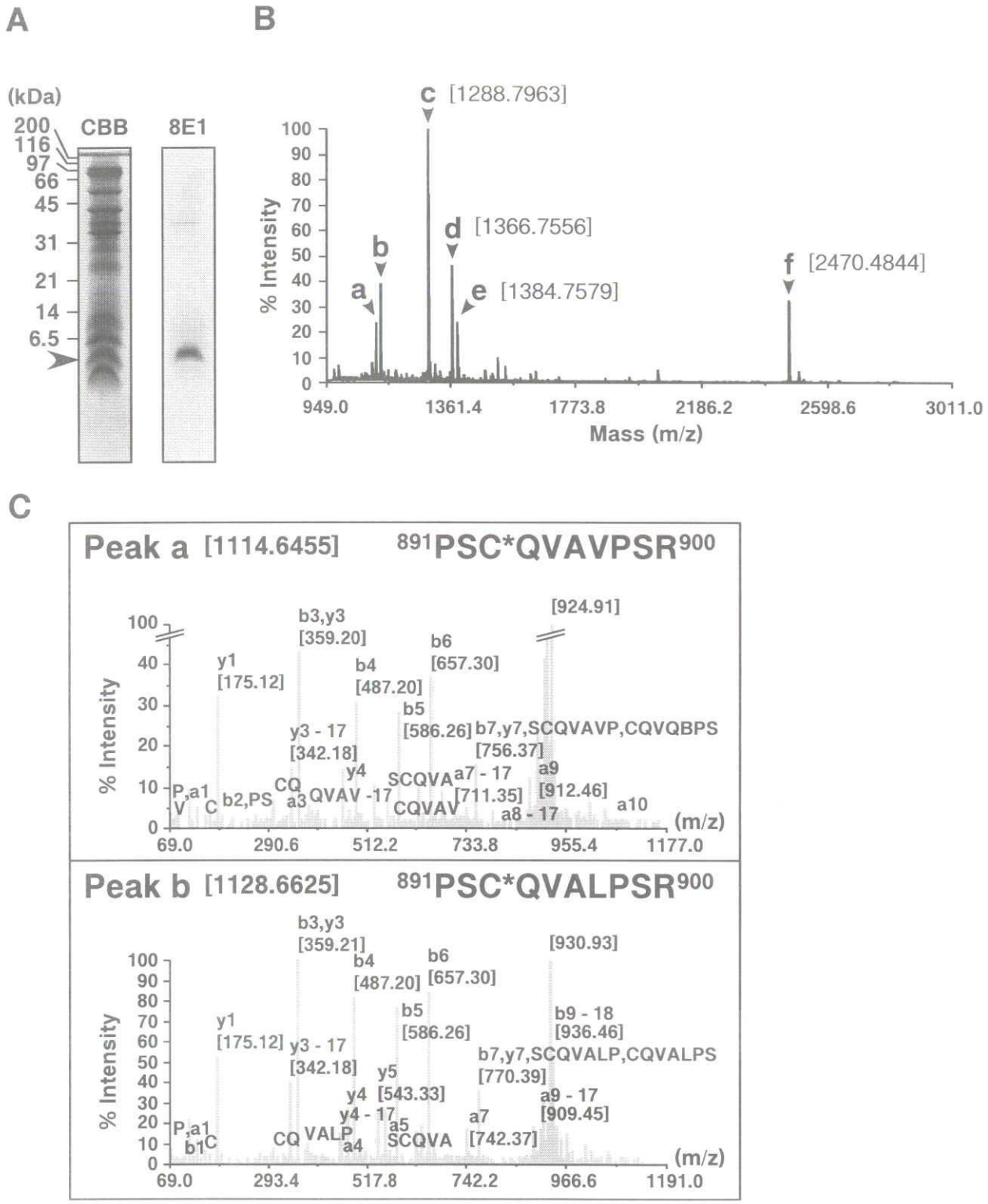

Fig. 2-11. Epitope mapping for an anti-ZPB1 monoclonal antibody, 8E1, by using mass spectrometry analysis

Fig. 2-11. Epitope mapping for an anti-ZPB1 monoclonal antibody, 8E1, by using mass spectrometry analysis. *A*, The tryptic digest of egg envelope (0.81 mg by wet weight) was reduced with the SDS sample buffer containing 1% 2-mercaptoethanol, and resultant free sulfhydryl groups were blocked with acrylamide. Peptide fragments were separated by Tricine SDS-PAGE under reducing conditions. Polypeptide bands were detected by CBB (*left lane*) or immunoblotting with 8E1 (*right lane*). The band in the CBB-stained gel corresponding to the 8E1 positive one on the immunostained membrane (*arrowhead*) was excised. The migration positions of the protein markers are shown on the left. *B*, Polypeptides in the excised band were further digested in gel with trypsin and analysed by using a MALDI-TOF/TOF mass spectrometer. The six major peaks (*arrowheads a* to *f*) were detected. *C*, Each peak shown in *panel B* was subjected to further MS/MS analysis to obtain sequence data, and typical CID spectra and sequence data of the *peaks a* and *b* are shown. The second Val of *peak a* was substituted by a Leu in *peak b*. All Cys were modified with acrylamide (*C**). Molecular mass of each peak was shown in bracket.

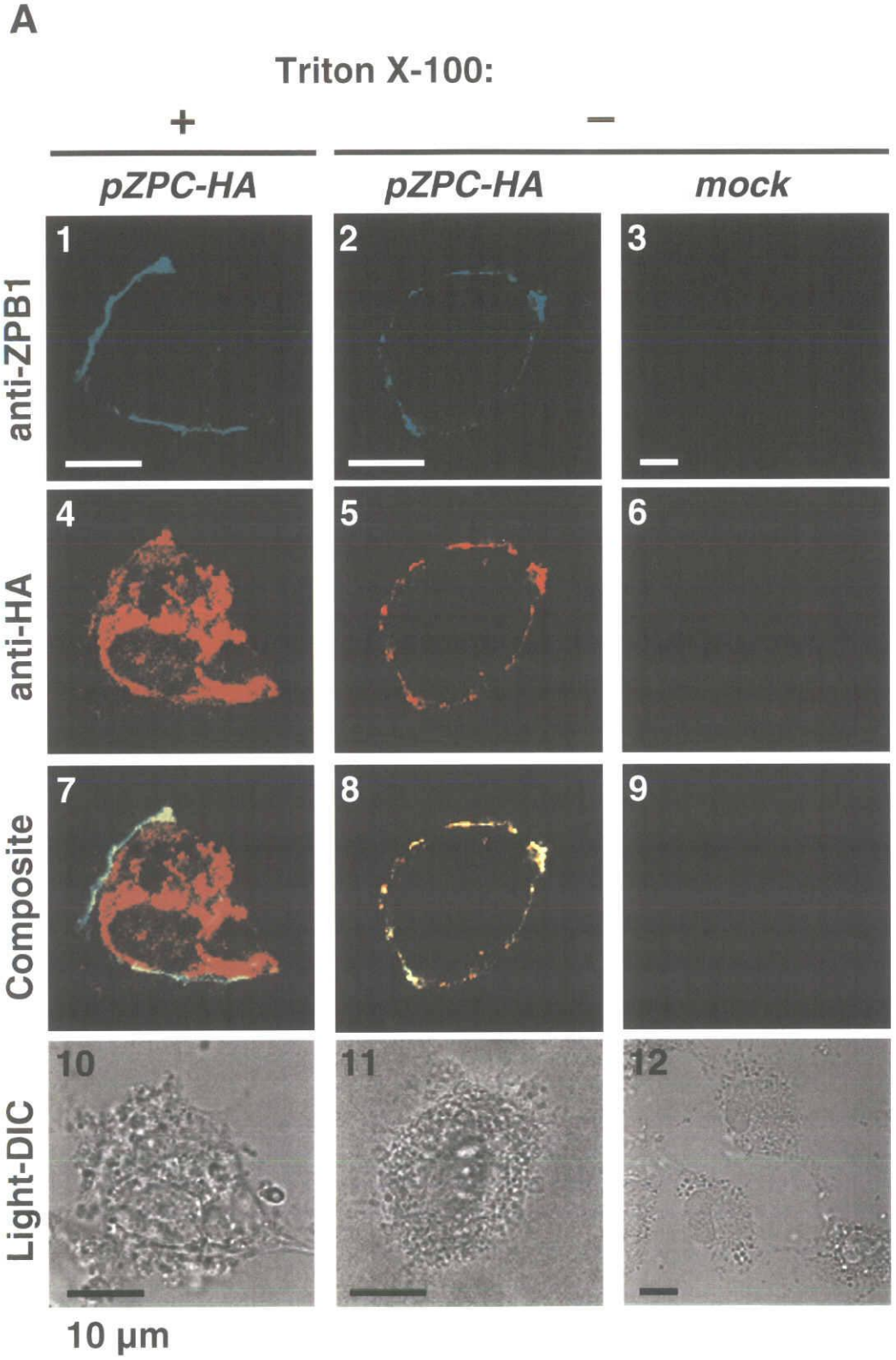

Fig. 2-12. Co-localized deposition of ZPB1 with ZPC around the ZPC-transfected COS-7 cells cultured in the presence of ZPB1

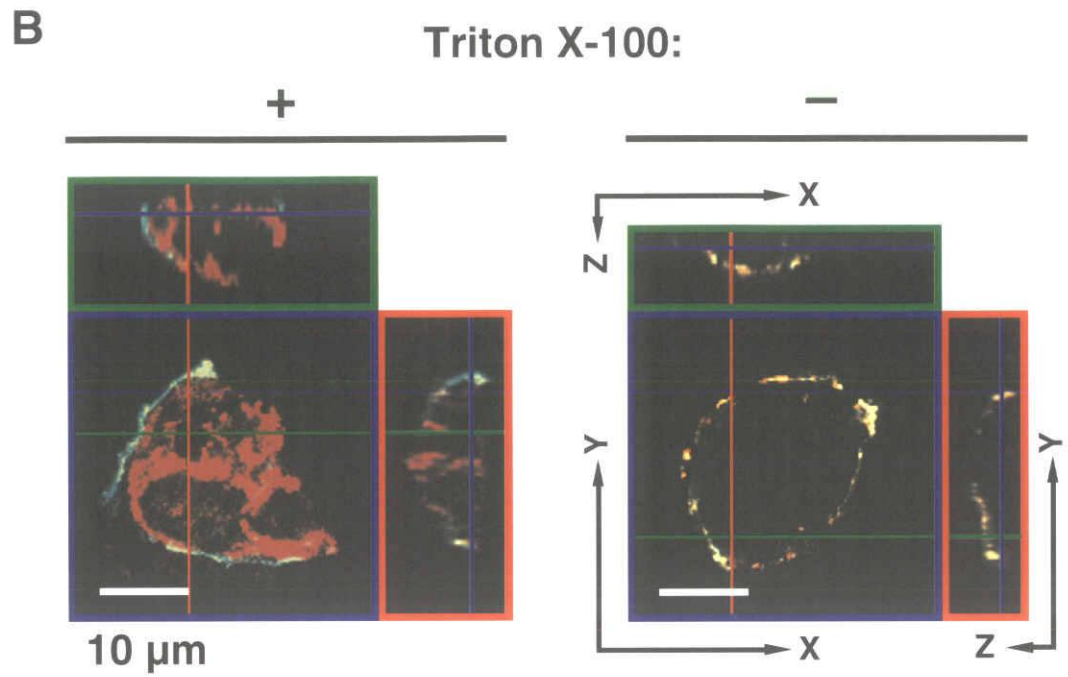

Fig. 2-12. Co-localized deposition of ZPB1 with ZPC around the ZPC-transfected COS-7 cells cultured in the presence of ZPB1. *A*, COS-7 cells transfected with an expression plasmid for ZPC-HA (*pZPC-HA*; *panels 1*, *2*, *4*, *5*, *7*, *8*, *10* and *11*) or a control plasmid (*mock*; *panels 3*, *6*, *9* and *12*) were cultured in the presence of ZPB1. The cells were fixed with (+; *1*, *4*, *7* and *10*) or without (–; *2*, *3*, *5*, *6*, *8*, *9*, *11* and *12*) the permeabilization treatment, treated with a combination of anti-ZPB1 (*green*; Alexa Fluor® 488) and anti-HA (*red*; Alexa Fluor® 568), and then observed under a laser-scanning confocal microscope equipped with an excitation filter of 488 nm (*panels 1*, *2* and *3*) or 543 nm (*panels 4*, *5* and *6*). Superimposed images constructed from the two color images are shown (*Composite*; *panels 7*, *8* and *9*). Light images of differential interference contrast microscopy (*Light-DIC*) of the cells are also shown (*panels 10*, *11* and *12*). *Bar*: 10 µm. *B*, COS-7 cells transfected with an expression plasmid for ZPC-HA were cultured in the presence of ZPB1. The cells were fixed with (+) or without (–) the permeabilization treatment, stained and observed as above. A series of 13-18 horizontal (XY) contiguous sections, 0.74-0.78 µm apart were collected at each depth along the vertical (Z-) axis of each cell from its bottom to top (see *right panel*). Based on these data the images of vertical sections (XZ and YZ) were constructed digitally using the Zeiss LSM Image Browser Version 3.5 software. Typical XY sections were shown in *blue frames*. The constructed XZ and YZ sections at a position shown by *green* and *red lines* on the XY sections (in *blue frames*) were indicated in the *green* and *red frames*, respectively. Depth of the XY sections was indicated as *blue line* both in the XZ and YZ sections. *Bar*: 10 µm.

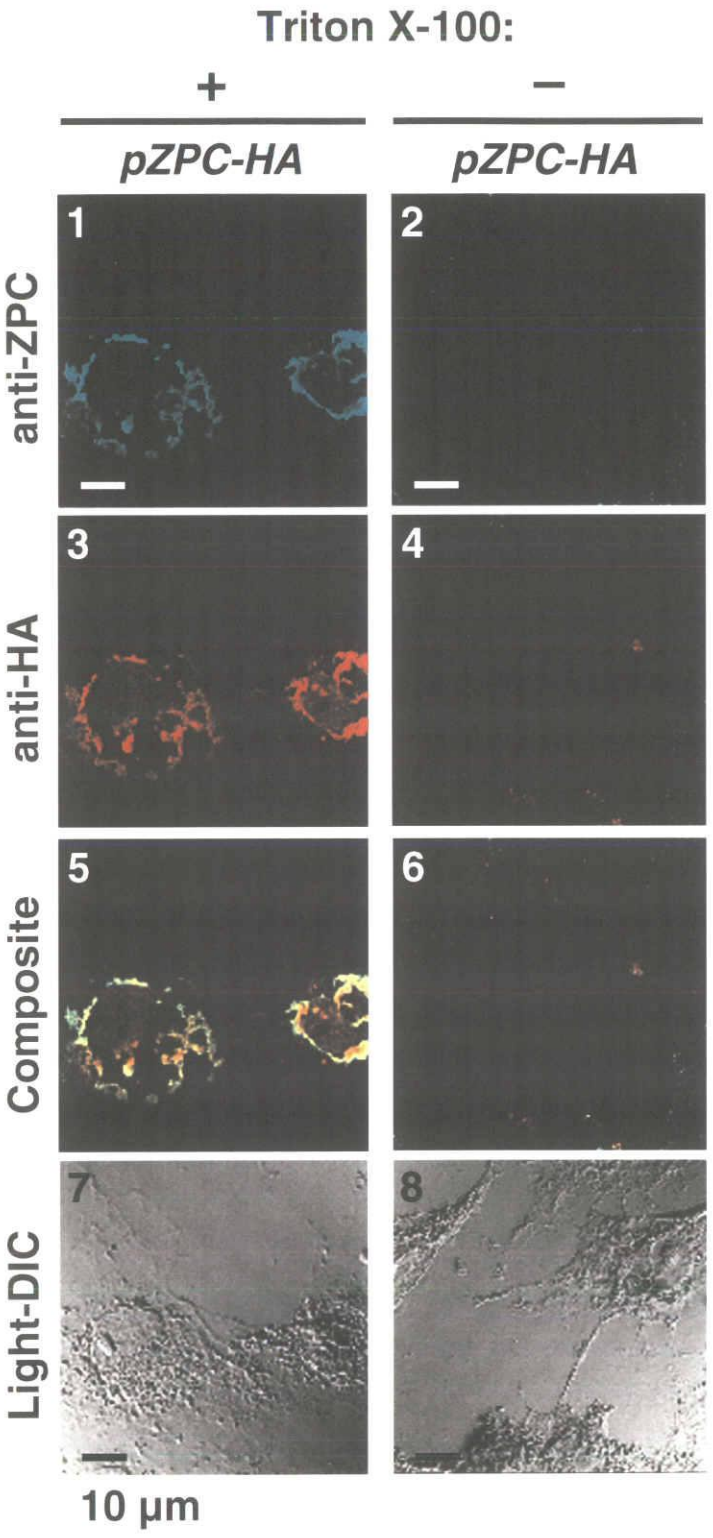

Fig. 2-13. Contribution of ZPB1 for ZPC accumulation on the surface of ZPC-expressing COS-7 cells

Fig. 2-13. Contribution of ZPB1 for ZPC accumulation on the surface of ZPC-expressing COS-7 cells. COS-7 cells transfected with expression plasmid for ZPC-HA (*pZPC-HA*) were cultured in the absence of ZPB1. The cells were fixed with (+; *panels 1*, *3*, *5* and *7*) or without (–; *panels 2*, *4*, *6* and *8*) the permeabilization treatment, treated with a combination of anti-ZPC (*green*; Alexa Fluor® 488) and anti-HA (*red*; Alexa Fluor® 568), and then observed under a laser-scanning confocal microscope equipped with an excitation filter of 488 nm (*panels 1* and *2*) or 543 nm (*panels 3* and *4*). Superimposed images constructed from the two color images are shown (*Composite*; *panels 5* and *6*). Light images of differential interference contrast microscopy (*Light-DIC*) of the cells are also shown (*panels 7* and *8*). *Bar*: 10 μm.

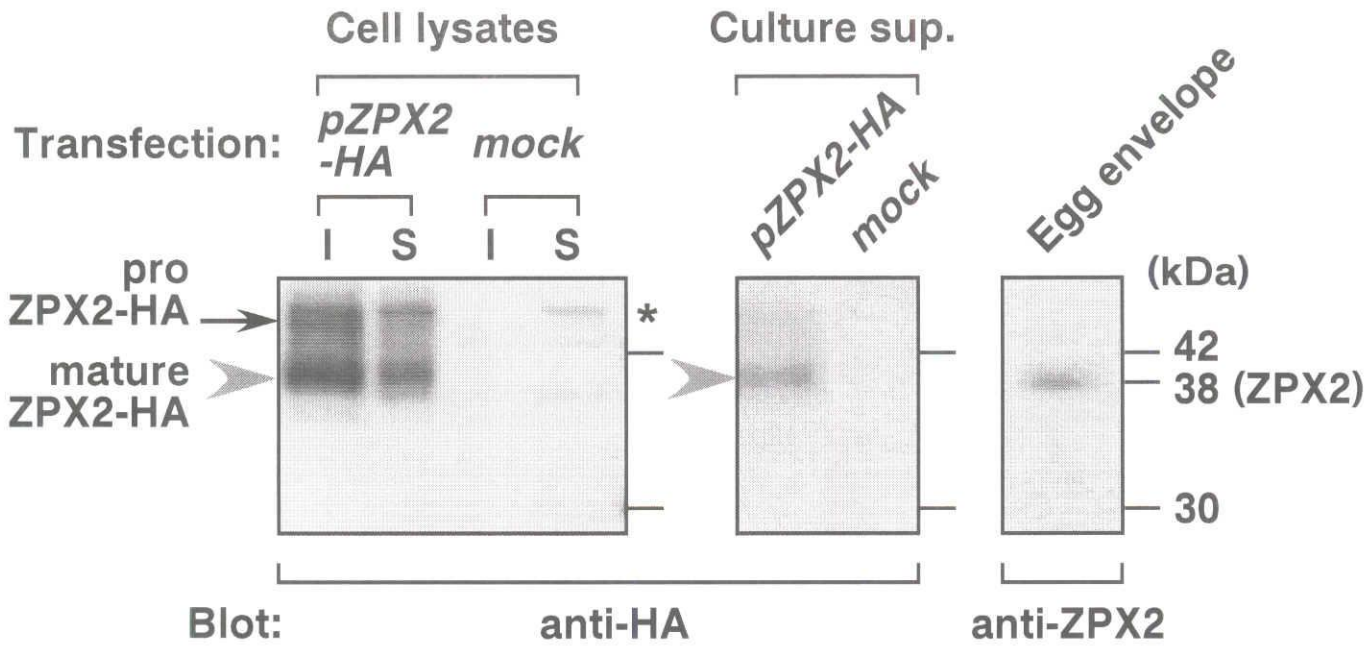

Fig. 2-14. Expression, processing and secretion of HA-tagged ZPX2 by transfected COS-7 cells. COS-7 cells were transfected with an expression plasmid for the epitope-tagged ZPX2 (*pZPX2-HA*) or an empty vector (*mock*) and cultured. The culture supernatants were collected, while the cells were lysed with the Triton X-100 containing lysis buffer and harvest - ed. The cell lysates were separated into two fractions, soluble supernatant and insoluble pellet. The Triton X-100-insoluble (*I*, 1/6 of the total cell lysates) and -soluble (*S*, 1/6 of the total cell lysates) fractions (*left panel*), and the culture supernatants (16 µl, 2/125 of the culture supernatant, *middle panel*) were subjected to SDS-PAGE under non-reducing conditions, followed by immunoblotting with anti-HA antibody. The lysates and culture supernatants were prepared from individual cultures. Egg envelope (11 µg by wet weight) was also analyzed for comparison (immunoblotted with anti-ZPX2 antibody, *right panel*). The migration positions of protein markers are shown on the right. Protein bands estimated to be proZPX2-HA (*arrows*) and mature ZPX2-HA (*closed gray arrowheads*) are also indicated on the left. Asterisk (*) represents non-specific staining.

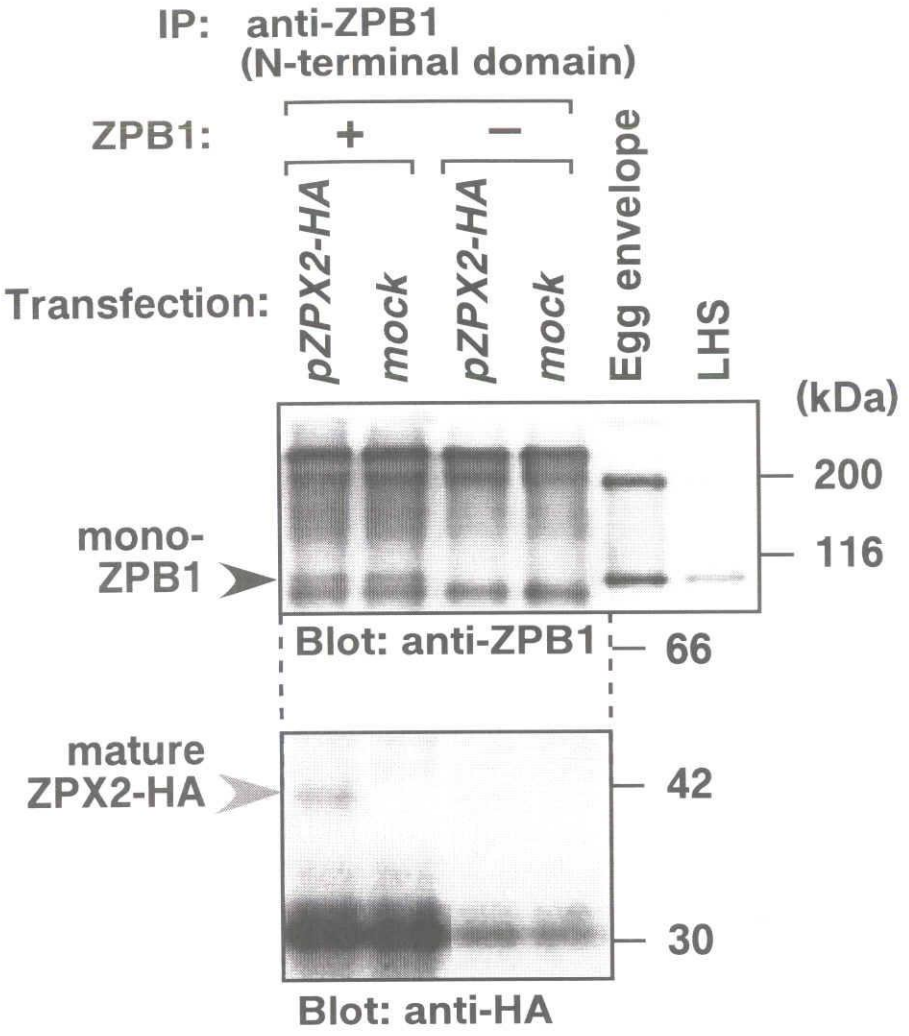

Fig. 2-15. Immunoprecipitation of ZPB1-ZPX2 heterocomplexes from the culture supernatant of the transfected COS-7 cells cultured in the presence of ZPB1. COS-7 cells transfected with an expression plasmid for ZPX2-HA (*pZPX2-HA*) or a control plasmid (*mock*) were cultured in the presence (+) or absence (–) of ZPB1. The culture supernatants were collected and subjected to the immunoprecipitation (IP) using anti-ZPB1 (N-terminal domain) polyclonal antibody. The immunoprecipitates (1/8 and 1/2 of the precipitates in *upper* and *lower panels*, respectively), were subjected to SDS-PAGE under non-reducing conditions followed by immunoblotting with anti-ZPB1 (*upper panels*) and anti-HA (*lower panels*) antibodies. The laying hen's serum (*LHS*) and egg envelope were also analyzed for comparison. The migration positions of the protein markers are shown on the right. Protein bands corresponding to monomeric ZPB1 (*mono-ZPB1*; *closed black arrowheads*) and mature ZPX2-HA (*closed gray arrowheads*) are indicated on the left.

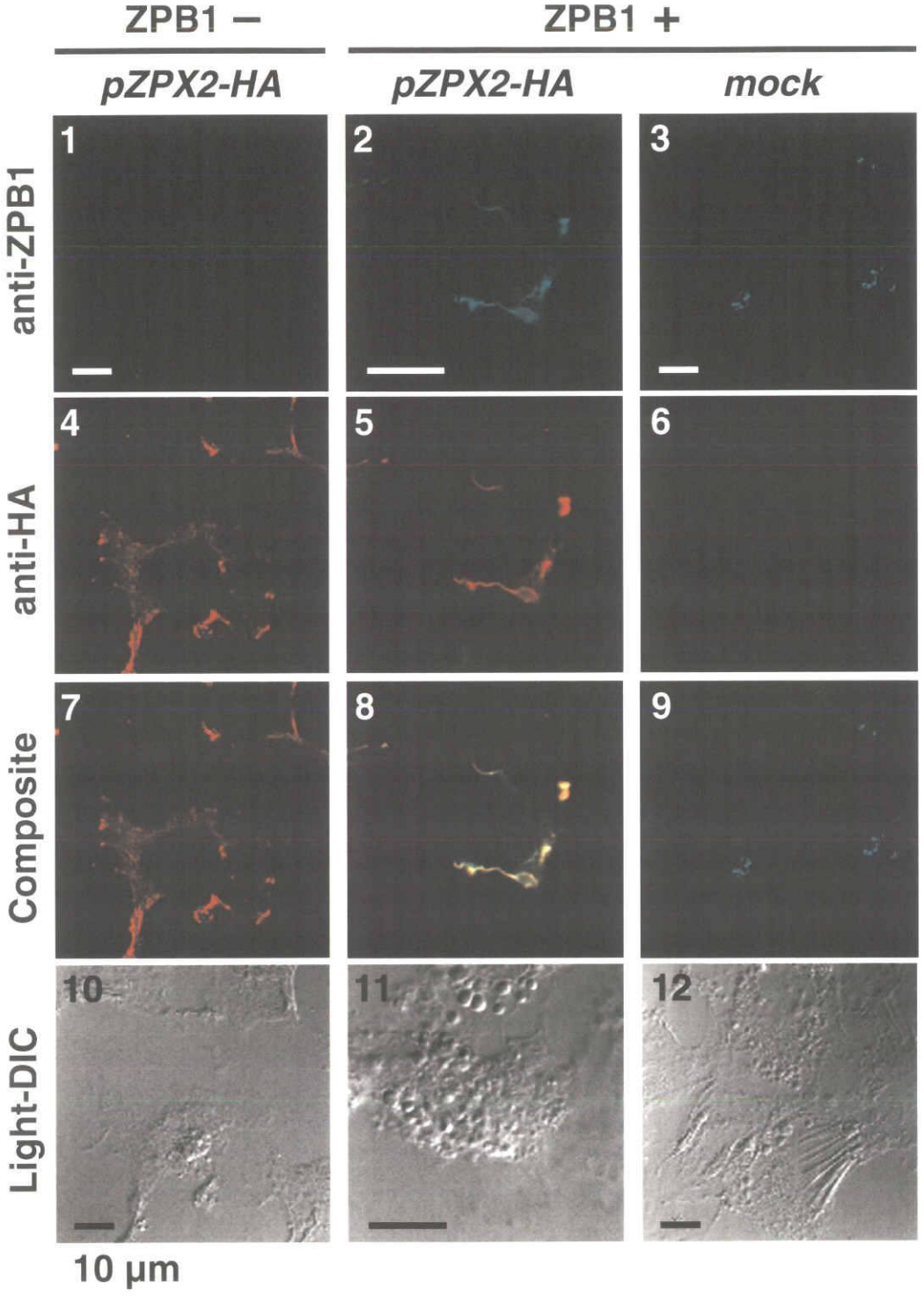

Fig. 2-16. Co-localized deposition of ZPB1 with ZPX2 around the ZPX2-transfected COS-7 cells cultured in the presence of ZPB1

Fig. 2-16. Co-localized deposition of ZPB1 with ZPX2 around the ZPX2-transfected COS-7 cells cultured in the presence of ZPB1. COS-7 cells transfected with an expression plasmid for ZPX2-HA (*pZPX2-HA*; *panels 1*, *2*, *4*, *5*, *7*, *8*, *10* and *11*) or a control plasmid (*mock*; *panels 3*, *6*, *9* and *12*) were cultured in the presence (*ZPB1+*) or absence (*ZPB1–*) of ZPB1. The cells were fixed with paraformaldehyde (without the permeabilization treatment), treated with a combination of anti-ZPB1 (*green*; Alexa Fluor® 488) and anti-HA (*red*; Alexa Fluor® 568), and then observed under a laser-scanning confocal microscope equipped with an excitation filter of 488 nm (*panels 1*, *2* and *3*) or 543 nm (*panels 4*, *5* and *6*). Superimposed images constructed from the two color images are shown (*Composite*; *panels 7*, *8* and *9*). Light images of differential interference contrast microscopy (*Light-DIC*) of the cells are also shown (*panels 10*, *11* and *12*). *Bar*: 10 μm.

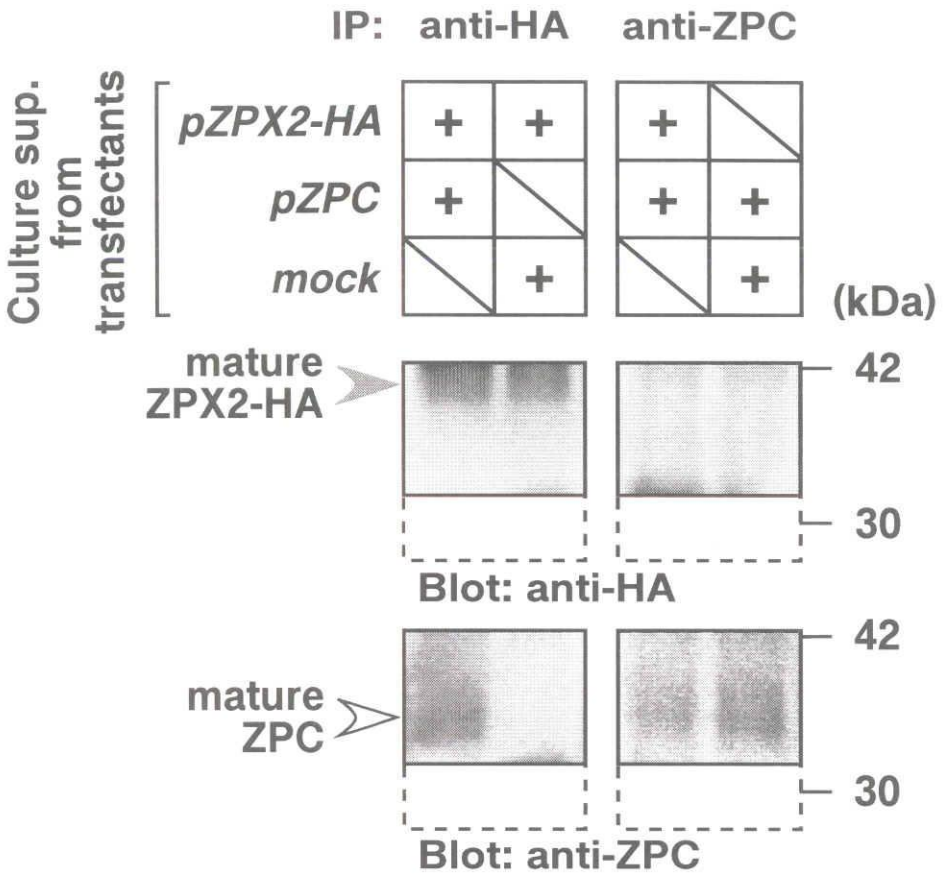

Fig. 2-17. Immunoprecipitation of ZPX2-ZPC heterocomplexes from the culture supernatant mixture from the ZPX2-expressing COS-7 cell and the ZPC-expressing one. COS-7 cells transfected with an expression plasmid for ZPX2-HA (*pZPX2-HA*) or ZPC (*pZPC*), or a control plasmid (*mock*) was cultured in the absence of ZPB1. The culture supernatants were collected, and two of them were mixed and incubated at 37 °C for 1 h followed by further incubation at 4 °C for 24 h. The incubated mixtures were subjected to the immunoprecipitation (IP) using anti-HA (*left panels*) or anti-ZPC (*right panels*) antibodies. The immunoprecipitates (1/2 of the precipitates) were subjected to SDS-PAGE under non-reducing conditions followed by immunoblotting with anti-HA (*upper panels*) and anti-ZPC (*lower panels*) antibodies. The migration positions of the protein markers are shown on the right. Protein bands corresponding to mature ZPX2-HA (*closed gray arrowhead*) and mature ZPC (*open arrowhead*) are indicated on the left.

CHAPTER 3

Identification of the Avian Egg-Envelope Components Involved in the Induction of Sperm Acrosome Reaction

Summary

Fertilization begins with interaction between the sperm and the egg. The surface of the vertebrate oocyte is covered with the egg envelope, which is composed of zona pellucida (ZP) glycoproteins. I have elucidated the matrix architecture of avian egg envelope and proposed a mechanism for its formation in the Chapter 2. Through the egg-sperm interaction, the egg-envelope component(s) trigger the sperm to release its acrosomal contents (acrosome reaction). The acrosomal contents degradate the egg-envelope matrix and enable the sperm to penetrate the hard matrix prior to fuse with the egg cell. Indeed, *in vitro* degradation of the egg envelope was observed through incubation with artificially ejaculated sperm. The *in vitro* incubation of chicken sperm with a calcium ionophore A23187 induced sperm activation, resulting in the fragmentation and release of a 41-kDa peanut agglutinin (PNA)-positive glycoprotein and the decrease or loss of sperm PNA-stainability. The incubation with ZPX2 and dimeric ZPB1, but not ZPC and monomeric ZPB1, also induced the decrease or loss of sperm PNA-stainability, suggesting the *in vitro* sperm activation by these ZP components. Collectively, ZPX2 and dimeric ZPB1 might play a key role in the avian sperm-egg interaction.

Introduction

The fertilization process in mammals consists of numerous events; capacitation of sperm, meiotic maturation of eggs, binding of acrosome-intact sperm to the egg envelope, the sperm acrosome reaction, fusion of acrosome-reacted sperm with egg plasma membrane, and the egg cortical and zona reactions [Yanagimachi, 1994; Hardy, 2002; Wassarman, 2003]. The latter participate in the establishment of a block to polyspermic fertilization. Compared with the mammalian fertilization process, the avian (chicken) sperm do not require a period of capacitation within the female reproductive tract [Howarth, 1970], and polyspermy in the chicken egg-sperm interaction is generally considered to be physiological in nature, although an additional tertiary investment, referred to as the outer perivitelline layer, prevents excessive penetration of the egg envelope [Bakst and Howarth, 1977]. Accordingly, inducing the sperm acrosome reaction is the most remarkable physiological role of the egg envelope through chicken fertilization process.

It is suggested in mammals (especially in mouse) that the *O*-linked sugar chains on ZPC are involved in the binding of sperm to the egg envelope, and the binding to ZPC induces sperm to undergo the acrosome reaction [Primakoff and Myles, 2002; Wassarman, 1988]. On the other hand, the *N*-linked sugar chains on the chicken egg-envelope component(s) induced acrosome reaction although the carrier of *N*-glycans was not identified [Robertson *et al.*, 2000].

In this study, I constructed an immunohistochemical assay for *in vitro* acrosome reaction based on the reactivity of the intact sperm with peanut agglutinin (PNA). This assay using the ZPB1, ZPC and ZPX2 prepared from chicken egg envelope in the Chapter 2 revealed that ZPX2 and dimeric ZPB1 strongly induced acrosome reaction.

Materials and Methods

Chicken sperm preparation— Semen was collected from White leghorn cocks after ejaculation induced by lumber massage. The sperm concentration was calculated by using a haemocytometer (NITIRIN, Tokyo, Japan) under a phase contrast microscope (IMT-2; OLYMPUS, Tokyo, Japan).

Induction of sperm acrosome reaction by whole egg envelope or calcium ionophore— **(I)** Semen (200 μl) including approximately 1.0 x 10^9 spermatozoa was centrifuged at 250 x g for 10 min. The precipitate (sperm) was washed twice with cold PBS, centrifuged at 250 x g for 10 min, and finally re-suspended in 1000 μl of cold PBS. Each 20 μl of 20 μM calcium ionophore (A23187; Wako Pure Chemical Industries, Osaka, Japan) or the egg envelope suspension (prepared in Chapter 2) was added to 40 μl of the sperm suspension. This sperm suspension containing A23187 or homogenized egg envelope was incubated at 39 °C for 0-60 min to induce sperm acrosome reaction [Bleil and Wassarman, 1983] and centrifuged at 13,000 x g for 5 min. The precipitates and supernatants were immediately subjected to SDS-PAGE and the measurement of trypsin-like activity, respectively.

(II) Semen (200 μl) including 9.7 x 10^8 spermatozoa was centrifuged as above, and the supernatant was collected as seminal plasma. The precipitate (sperm) was washed, centrifuged as above, and finally re-suspended in 500 μl of cold PBS. Half of this sperm suspension was centrifuged, and the precipitate (4.9 x 10^8 spermatozoa) was used as the intact sperm. Another half of the sperm suspension was centrifuged, and the precipitated sperm was suspended in cold PBS containing 20 μM A23187. This sperm suspension containing A23187 was incubated at 39°C for 30 min to induce sperm acrosome reaction [Bleil and Wassarman, 1983] and centrifuged at 13,000 x g for 5 min. The precipitate was used as the A23187-treated sperm.

Gel electrophoresis, immunoblotting, and lectin blotting— Sodium dodecyl

sulfate-polyacrylamide gel electrophoresis (SDS-PAGE) and immunoblotting were described in Chapter 2. For lectin blotting analysis, electroblotting and blocking were performed as described in Chapter 2. The membrane was incubated with peanut (*Arachis hypogaea*) agglutinin (PNA; Seikagaku Cooperation, Tokyo, Japan), with rabbit anti-PNA IgG (ICN Biomedicals), and finally with peroxidase-labeled anti-rabbit IgG antibody. Detection was performed using the ECL reagents (Amersham Biosciences).

Measurement of trypsin-like activity— Twenty microliter of sample was incubated with 150 μl of 2 mg/ml α-*N*-benzoyl-L-arginine-4-nitroanilidehydrochloride (BAPA) dissolved in PBS at 37 °C. The time course of 405-nm absorption-values was measured for 30 min by using a microplate reader (SpectraMax® 250; Global Medical Instrumentation, MN).

Induction of sperm acrosome reaction by ZP components and peanut agglutinin (PNA) staining— Sperm washed with PBS was prepared as described above. The sperm suspension (1 x 10^6 spermatozoa in 10 μl PBS) was mixed with an equal volume of each ZP preparation and incubated at 39 °C for 30 min. As the positive and negative controls, the sperm suspensions were incubated with 10 μl of PBS containing 40 μM A23187 and PBS, respectively. Ten microliter of the sperm solution were then smeared onto a poly-L-lysine coated glass slides and kept for 10 min at room temperature. The spermatozoa on slides were washed with PBS and incubated with PBS in the presence or absence of 10 μg/ml PNA for 60 min at room temperature. After wash with PBS, the spermatozoa on slides were fixed with 2% paraformaldehyde in PBS for 15 min at room temperature and then washed with PBS. The fixed spermatozoa on slides were incubated with 3 μg/ml anti-PNA rabbit IgG antibody overnight at 4 °C, washed with PBS, and finally incubated with 2 μg/ml Alexa Fluor® 488 goat anti-rabbit IgG (Molecular Probes) overnight at 4 °C in a dark place. After wash with PBS, the spermatozoa on slides were examined under a fluorescence microscope (BX-60; OLYMPUS). The number of spermatozoa whose heads were labeled with Alexa Fluor® 488 (= PNA-positive) was counted for each field. The total number of spermatozoa

(43-185 per field) was also counted under phase contrast.

Circular dichroism (CD) measurement— Each protein sample was dissolved in PBS at a concentration of 280 and 171 μg/ml for fractions I and II, respectively, and transferred to a quartz cell with a 1-mm path length. The CD spectra were recorded on a Jasco J-720 spectropolarimeter with Jasco J-700 Spectra Manager version 1.35 software (Tokyo, Japan). The CD spectrum of each sample was measured three times in accumulation mode at room temperature in the wavelength range of 200-240 nm, corrected by subtraction of the background solvent spectrum obtained under identical experimental conditions, and smoothed for clarity of display. All the data were converted to give molar ellipticity values ($[\theta]$, deg cm^2 $decimole^{-1}$) based upon the concentrations of the samples.

Results

Degradation of the egg envelope incubated with the sperm in vitro— To confirm the egg-envelope degradation being essential for that the sperm penetrate the egg envelope, the homogenized egg envelope was incubated with the artificially ejaculated sperm *in vitro* (Fig. 3-1). Whole egg envelope was homogenized by an ultrasonication treatment (Chapter 2) and incubated with the chicken sperm at 39 °C for 20-60 min and fractionated by centrifugation. SDS-PAGE of the precipitates and the supernatants showed that the limited proteolysis of the egg envelope produced some soluble peptides being resistant to such proteolysis. The fragments under 20 kDa and between 30 and 20 kDa in the supernatants were gradually disappeared through the incubation, indicating that the egg envelope was degradated through the incubation with the sperm in a time-dependent manner.

Secretion of sperm acrosomal contents through the egg-envelope-sperm incubation in vitro— To confirm the secretion of the acrosomal contents, especially the proteolytic enzymes, from the sperm through the incubation with the egg envelope or a calcium ionophore, A23187, the trypsin-like activities in the supernatants from the incubated sperm were measured (Fig. 3-2). The sperm was incubated with the homogenized egg envelope described above or the A23187 at 39 °C for 0-60 min and centrifuged. The trypsin-like activity in the supernatant was measured by using an artificial substrate, α-*N*-benzoyl-L-arginine-4-nitroanilidehydrochloride (BAPA), as the rate of rise in the absorbance at 405 nm. The trypsin-like activity in the supernatant of the sperm incubated either with the egg envelope or A23187 was increased through the incubation in a time-dependent manner. These results supported that sperm acrosome reaction was induced by *in-vitro* incubation of the sperm with the egg envelope in addition to calcium ionophore [Bleil and Wassarman, 1983].

ZPX2 and dimeric ZPB1 are key components of sperm egg-envelope interaction—

Because all major ZP glycoproteins in chicken egg envelope were identified (Chapter 2), I started to examine which of the envelope glycoproteins was involved in sperm egg-envelope interaction. For this purpose, I constructed a quantitative assay for sperm activation or sperm acrosome reaction utilizing the reactivity of PNA to the sperm [Robertson and Wishart, 1996], which shows high affinity to the disaccharide structure, Gal(β1-3)GalNAc- [Lotan *et al.*, 1975]. First, biochemical changes in PNA-positive sperm glycoprotein(s) were examined by the lectin blotting analysis before and after activation with calcium ionophore, A23187, which was reported to be a chemical inducer of acrosome reaction [Bleil and Wassarman, 1983] (Fig. 3-3*A*). By the PNA-staining a 41-kDa band was detected from the lysates of the intact sperm, but became undetectable after incubation with A23187 for 30 min, (*lanes 2* and *3*). This 41-kDa band was not detected from the seminal plasma of untreated sperm samples (*lane 1*), excluding the possibility that the 41-kDa glycoprotein was a contaminated seminal plasma protein. Furthermore, two PNA-positive bands of about 24 kDa were detected in the supernatant of the A23187-treated sperm (*lane 4*), indicating that the 41-kDa glycoprotein was degraded and released from sperm during sperm activation. These data suggested that the 41-kDa glycoprotein recognized by PNA could be used as a marker to discriminate the intact sperm from the sperm activated by interaction with egg envelope.

Next, a histochemical method was adopted for *in situ* detection of the binding of PNA to the sperm. Namely, spermatozoa were fixed on glass slides and treated sequentially with PNA, rabbit anti-PNA antibody, and Alexa Fluor® 488 goat anti-rabbit IgG. PNA-bound spermatozoa were visualized under a fluorescence microscope. Figure 3-3*B* shows typical microscopic views in control experiments. Fluorescence was strongly detected from the head of intact sperm, especially the tip portion (*panels 9*, *10*, *11* and *12*). Such PNA-stainability was diminished from the activated sperm, which had been treated with A23187. These suggest the preferential binding of PNA to the intact sperm through the 41-kDa glycoprotein described above. The PNA-stainability of sperm was lost by the A23187 treatment, probably due to the induction of morphological and/or biochemical

changes in the sperm so as to degrade and release the 41-kDa glycoprotein (Fig. 3-3*A*). The quantitative data of these control experiments are summarized in Figure 3-3*C*. The number of PNA-positive sperm obviously decreased in sperm samples treated with A23187, as compared to PBS-treated sperm samples. Taken together, it was concluded that sperm activation by a calcium ionophore A23187 resulted in release of a PNA-positive glycoprotein from sperm surface.

The ZP glycoproteins were purified from the egg envelope as described in Chapter 2 (see Fig. 2-3). The reactivity of the purified ZP glycoproteins with the sperm was finally analyzed by the PNA-staining assay (Fig. 3-4). Incubation of sperm with dimeric ZPB1 and ZPX2, but not by monomeric ZPB1 or ZPC induced the loss of PNA-stainability from sperm. The fraction I contained the dimeric ZPB1 as the major constituent and the monomeric ZPB1 as the minor one. Interestingly, no induction was observed for monomeric ZPB1 (fraction II), suggesting that dimeric ZPB1 or the mixture of dimeric and monomeric ZPB1s was the active components in fraction I. Together with dose-dependent induction by dimeric/monomeric ZPB1 and ZPX2, the result suggests that this induction by dimeric ZPB1 and ZPX2 is direct. Because small amounts of dimeric/monomeric ZPB1 (3.6 μg) and ZPX2 (1.6 μg) triggered the sperm activation or sperm acrosome reaction as crude egg envelope (400 μg, wet weight) and A23187 did, dimeric ZPB1 and ZPX2 are considered to be true inducers of sperm acrosome reaction on sperm egg-envelope interaction.

Figure 3-4 suggests that ZPB1 induces the sperm activation when it refolds after removal of urea by dialysis. To analyze the structural feature of ZPB1, I measured the far-ultra violet CD spectra of the isolated dimeric and monomeric ZPB1s (Fig. 3-5). Because the far-ultra violet CD spectra provide information about the polypeptide backbone and its conformation, CD analysis can be a sensitive assay of changes in protein conformation [Adler *et al.*, 1973]. The CD spectrum of ZPB1 in fraction I showed a negative peak around 205 nm (*solid line*). No such peak or other apparent peak was observed in the spectrum of ZPB1 in fraction II (*broken line*), suggesting that monomeric ZPB1 is rich in unordered structure. Thus, the dimeric or polymeric ZPB1 was estimated to

have ordered secondary structure more than the monomeric one. Although, due to the limitation of the purified materials, nuclear magnetic resonance or other high-resolution analysis for three-dimensional protein structure was not applicable, difference in CD spectrum suggests that conformational change is accompanied by ZPB1 dimerization or polymerization, in addition to covalent disulfide bond formation between monomers [Takeuchi *et al.*, 2001], which may contribute to the biological activity of dimeric and polymeric ZPB1.

Discussion

The interaction between sperm and egg envelope is an essential event to start the fertilization process successfully, and is conserved among vertebrates. However, the papers on the initial sperm-egg interaction in vertebrates have suggested that there is no paradigm regarding the ZP glycoprotein that interact with and induce the sperm acrosome reaction. In mice, ZPC is an absolute player for the induction of acrosome reaction [Wassarman, 1988]. Pig ZPC has the sperm binding activity only when it forms hetero-oligomers with ZPB (ZPB2) [Yurewicz *et al.*, 1998]. In *Xenopus*, gp69/64 (ZPA) works as a sperm receptor [Tian *et al.*, 1999].

I have here provided the evidence that ZPX2 as well as dimeric or polymeric ZPB1 stimulates sperm activation (Fig. 3-4), though mechanisms of such stimulation by two different components remain to be investigated. It is unclear that these different interactions may contribute to species specificity. For the activation assay using the PNA-positive glycoprotein as an indicator, ZP proteins were prepared here from the egg envelope by classical biochemical methods (Fig. 2-3 in Chapter 2). Another possible approach for preparation was the use of recombinant ZP proteins since ZPB1, ZPC, and ZPX2 were cloned (see Chapter 2). However, sugar chains of ZP glycoproteins have been indicated to be important for the sperm-egg interaction in mammals [Primakoff and Myles, 2002; Wassarman, 1988] and the frog (*Xenopus*) [Tian *et al.*, 1999]. The involvement of envelope *N*-glycans in sperm-egg interaction has been reported also in the chicken although the carrier of *N*-glycans was not identified [Robertson *et al.*, 2000]. In the present study, ZPX2 and ZPB1, which had four and three potential *N*-glycosylation sites in their sequences, were shown to stimulate sperm activation. Glycosylation of chicken ZP proteins is indicated also by molecular heterogeneity revealed by isoelectric focusing [Okumura *et al.*, 2004]. Therefore, it is skeptical that the results obtained by use of chicken ZP proteins produced in bacteria would be conclusive. Interestingly, whereas *N*-glycans are suggested to be involved in the chicken [Robertson *et al.*, 2000], *O*-glycans have been reported to be involved in the sperm-egg interaction in mice [Wassarman, 1988] and the frog [Tian *et al.*, 1999]. Therefore, diversity

in sperm receptor ZP glycoproteins appears quite complex, including structural differences in sugar chains and their carrier polypeptides. This complexity may be related to the current unconvincing knowledge on the sperm proteins that interact with the egg envelope. In mammals, more than ten sperm proteins have been published as the candidate. However, the biological importance of these proteins is still controversial [Primakoff and Myles, 2002; Howes and Jones, 2002]. Microgram-order amounts of the isolated ZP glycoproteins will directly be utilized for further molecular explanation on the sperm-egg interaction, such as the identification of receptors for dimeric ZPB1 and ZPX2 on the sperm surface.

More recently, it has been proposed that the supramolecular structure of the egg-envelope matrix including the three-dimensional structure of the ZP glycoproteins and sugar chains on them are involved in the sperm-egg interaction [Hoodbhoy and Dean, 2004]. However, the possibility that the egg-sperm interaction is dependent on a particular glycan has not been excluded [Wassarman, 2005]. The results that dimeric ZPB1 but not monomeric one induced the sperm acrosome reaction (Fig. 3-4) and the ZPB1-dimerization was accompanied by certain conformational changes in ZPB1 molecules (Fig. 3-5) supported the former 'supramolecular model'. However, the results that *N*-glycan isolated from the egg envelope [Robertson *et al.*, 2000] and ZPX2 (Fig. 3-4) induced sperm acrosome reaction agreed with the latter 'single-glycan model'. I thought that the *N*-glycans on chicken ZP glycoproteins possess the activity to induce sperm acrosome reaction, and the activity was regulated by matrix architecture of the egg envelope.

In eukaryotes, besides the egg-envelope components, several extracellular proteins sharing the ZP domain (ZP-domain proteins) have been reported [Jovine *et al.*, 2005] as described in General Introduction (Chapter 1). These proteins are detected as components of the non-collagenous extracellular matrices in several tissues and organs, and would play important roles in intercellular signal transduction pathways. Studies on egg-envelope functions in the egg-sperm interaction would give better understanding of the molecular mechanism(s) for the extracellular matrix-mediated intercellular signaling including the induction of sperm acrosome reaction by the egg-envelope ZP glycoproteins.

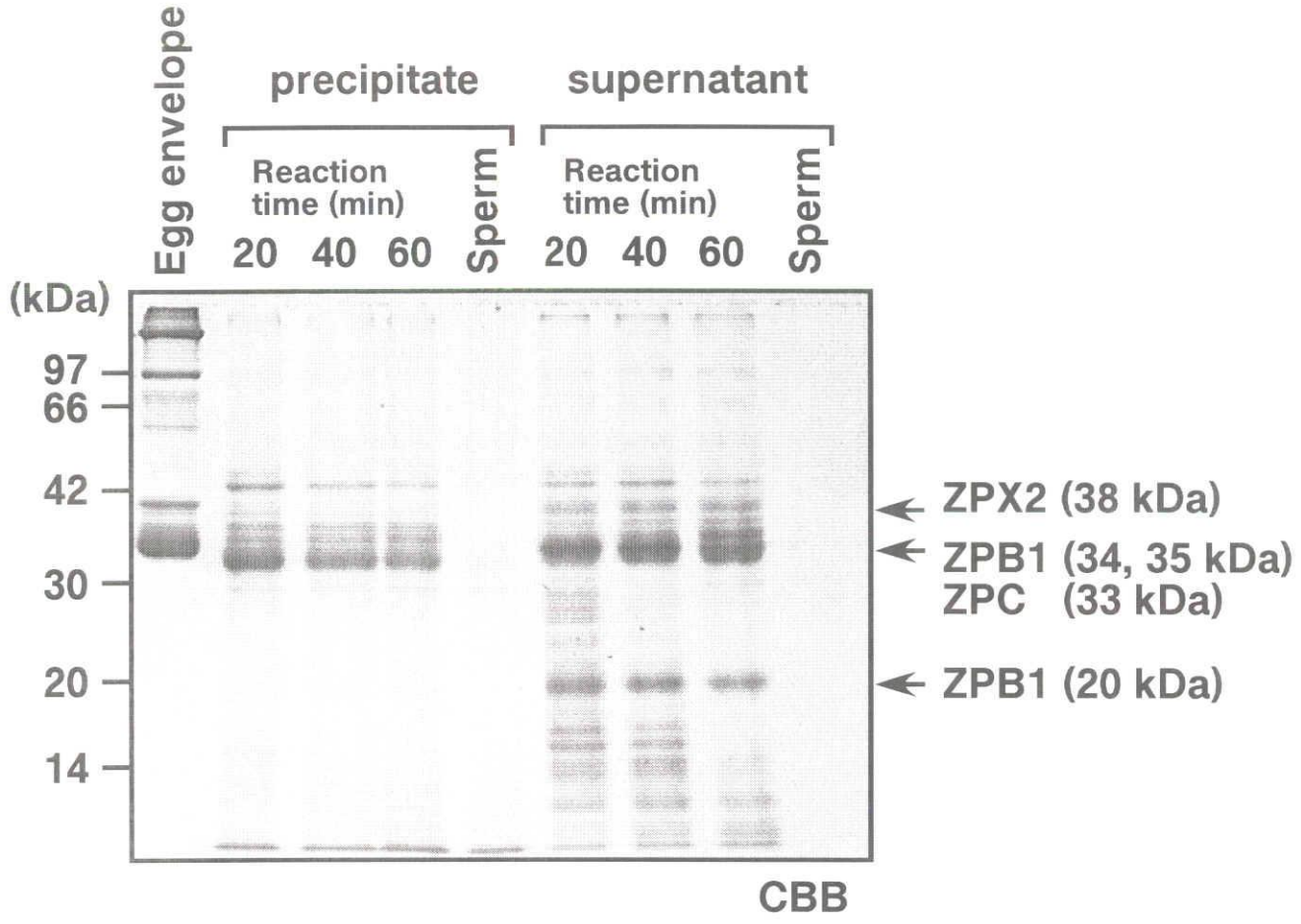

Fig. 3-1. Degradation of the egg envelope incubated with the sperm. The egg-envelope suspension (0.41 mg by wet weight) was incubated with approximately 4.0 x 10^7 sperm at 39 °C for 20-60 min, and subjected to SDS-PAGE under non-reducing conditions followed by centrifugation at 13,000 xg. The migration positions of the protein markers are shown on the right of *panels*. Bands of peptides derived from ZPB1, ZPC and ZPX2 in the supernatants (*arrows*) were identified by [Iwata *et al.* (2002)].

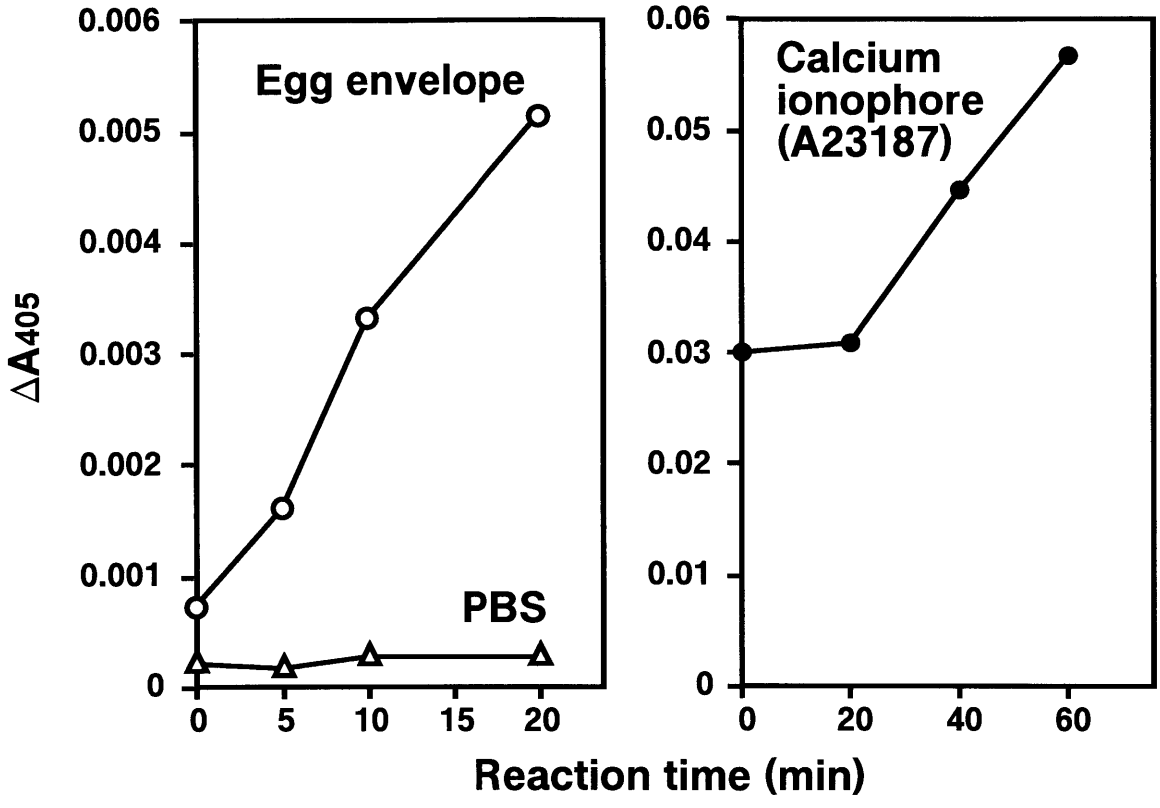

Fig. 3-2. Secretion of the proteolytic enzyme from the sperm incubated with the egg envelope or a calcium ionophore. The sperm suspension containing approximately 4.0 x 10^7 sperm was incubated with the egg-envelope suspension (0.41 mg by wet weight; *open circles*), a calcium ionophore, A23187 (*closed circles*), or PBS (*open triangles*) at 39 °C for 0-60 min, and centrifuged at 13,000 xg. The trypsin-like activity in the supernatant was measured by using an artificial substrate, α-*N*-benzoyl-L-arginine-4-nitroanilidehydrochloride (BAPA), as the rate of rise in the absorbance at 405 nm (ΔA_{405}).

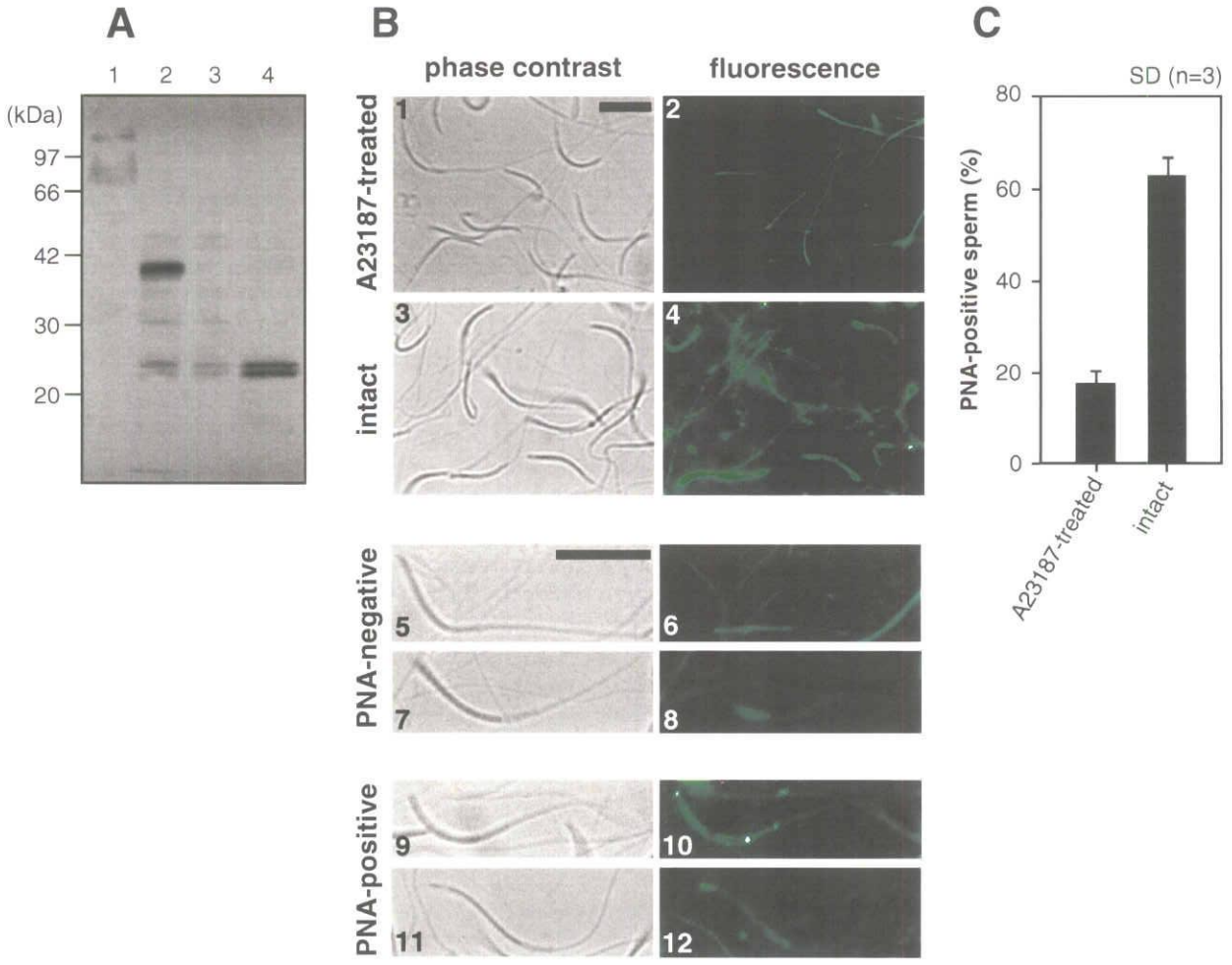

Fig. 3-3. Establishment of a sperm activation assay.

Fig. 3-3. Establishment of a sperm activation assay. *A*, Lectin blotting. Proteins from seminal plasma (*lane 1*), intact sperm (*lane 2*), sperm incubated in the presence of A23187 (*lane 3*), and the supernatant of the A23187 treated sperm (*lane 4*) were subjected to SDS-PAGE (12% acrylamide gel), electroblotted onto PVDF membrane and stained with PNA. The migration positions of the protein markers are shown on the left of the panel. *B*, Typical observation by fluorescence microscopy. Detailed assay conditions are described in Materials and Methods. Sperm samples treated with A23187 (*panels 1* and *2*), and intact sperm samples (*panels 3* and *4*) were visualized by phase contrast (*panels 1* and *3*) and staining with PNA and immunofluorescence (*panels 2* and *4*). Typical staining patterns of PNA-negative (*panels 5*, *6*, *7* and *8*) and positive (*panels 9*, *10*, *11* and *12*) sperm were shown. Bar, 12 μm. The ratio of the number of PNA-positive cells to total cell number is summarized by solid bars in *C*. The data represent the means and standard deviation for five fields. Another independent experiment was performed with similar results.

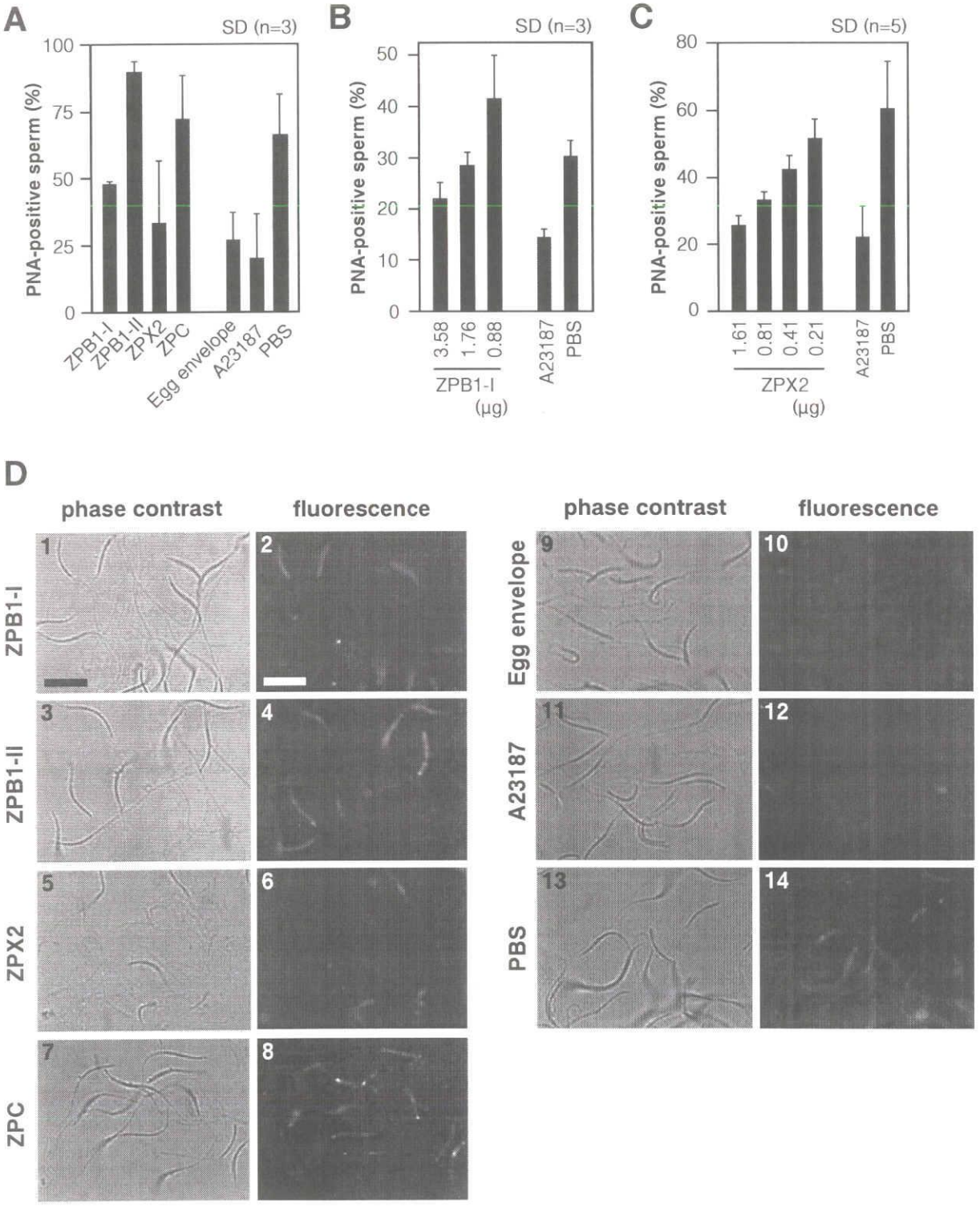

Fig. 3-4. Sperm activation assay for the ZP glycoprotein preparations.

Fig. 3-4. Sperm activation assay for the ZP glycoprotein preparations. *A*, Sperm activation induced by the four ZP protein preparations. Dimeric/monomeric ZPB1 (*ZPB1-I*, 3.58 μg), monomeric ZPB1 (*ZPB1-II*, 2.19 μg), ZPC (1.56 μg), ZPX2 (1.61 μg), and the egg envelope suspended by ultrasonication (400 μg by wet weight) were used for every measurement. *B* and *C*, Dose-dependent induction by dimeric/monomeric ZPB1 and ZPX2. The amounts of these proteins used for the assay are indicated. The calcium ionophore A23187 and PBS were used instead of the ZP proteins as positive and negative controls, respectively. The data represent the means and standard deviation for three (*A* and *B*) or five (*C*) fields. Another independent experiment was performed with similar results. *D*, Typical observation by fluorescence microscopy for *A*. Detailed assay conditions are described in Materials and Methods. Sperm samples treated with dimeric/monomeric ZPB1 (*ZPB1-I*, *panels 1* and *2*), monomeric ZPB1 (*ZPB1-II*, *panels 3* and *4*), ZPX2 (*panels 5* and *6*), ZPC (*panels 7* and *8*), egg-envelope suspension (*Egg envelope*, *panels 9* and *10*) and A23187 (*panels 11* and *12*), and intact sperm samples (*PBS*, *panels 13* and *14*) were visualized by phase contrast (*odd-numbered panels*) and staining with PNA and immunofluorescence (*even-numbered panels*). Bar, 12 μm.

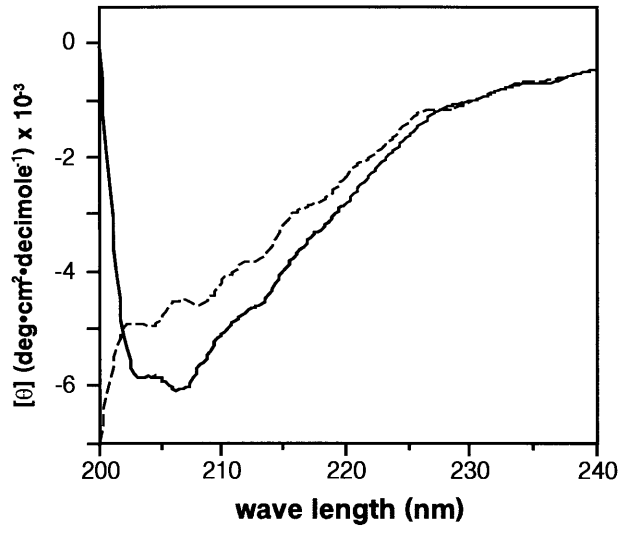

Fig. 3-5. CD spectra of ZPB1 in fractions I (*solid line*) and II (*broken line*). The dimeric/monomeric ZPB1 in fraction I and the monomeric one in fraction II were dissolved in PBS, and subjected to CD spectrum measurement. Detailed conditions for CD analysis are described in Materials and Methods.

REFERENCES

Adler, A. J., Greenfield, N. J., and Fasman, G. D. (1973). Circular dichroism and optical rotatory dispersion of proteins and polypeptides. *Methods Enzymol.* **27,** 675-735.

Aoki, N., and Matsuda, T. (2000). A cytosolic protein-tyrosine phosphatase PTP1B specifically dephosphorylates and deactivates prolactin-activated STAT5a and STAT5b. *J. Biol. Chem.* **275,** 39718-39726.

Bakst, M. R., and Howarth, B., Jr. (1977). Hydrolysis of the hen's perivitelline layer by cock sperm in vitro. *Biol. Reprod.* **17,** 370-379.

Bausek, N., Waclawek, M., Schneider, W. J., and Wohlrab, F. (2000). The major chicken egg envelope protein ZP1 is different from ZPB and is synthesized in the liver. *J. Biol. Chem.* **275,** 28866-28872.

Bausek, N., Ruckenbauer, H. H., Pfeier, S., Schneider, W. J., and Wohlrab, F. (2004). Interaction of sperm with purified native chicken ZP1 and ZPC proteins. *Biol. Reprod.* **71,** 684-690.

Bleil, J. D., and Wassarman, P. M. (1980). Structure and function of the zona pellucida: identification and characterization of the proteins of the mouse oocyte's zona pellucida. *Dev. Biol.* **76,** 185-202.

Bleil, J. D., and Wassarman, P. M. (1983). Sperm-egg interactions in the mouse: sequence of events and induction of the acrosome reaction by a zona pellucida glycoprotein. *Dev. Biol.* **95,** 317-324.

Blobe, G. C., Schiemann, W. P., Pepin, M.-C., Beauchemin, M., Moustakas, A., Lodish, H. F., and O'Connor-McCourt, M. D. (2001). Functional roles for the cytoplasmic domain of the type III transforming growth factor beta receptor in regulating transforming growth factor beta signaling. *J. Biol. Chem.* **276,** 24627-24637.

Boja, E. S., Hoodbhoy, T., Fales, H. M., and Dean, J. (2003). Structural characterization of native mouse zona pellucida proteins using mass spectrometry. *J. Biol. Chem.* **278,** 34189-34202.

Bork, P., and Sander, C. (1992). A large domain common to sperm receptors (Zp2 and Zp3) and TGF-beta type III receptor. *FEBS Lett.* **300,** 237-240.

Brune, D. C. (1992). Alkylation of cysteine with acrylamide for protein sequence analysis. *Anal. Biochem.* **207,** 285-290.

Chen, C., and Okayama, H. (1987). High-efficiency transformation of mammalian cells by plasmid DNA. *Mol. Cell. Biol.* **7,** 2745-2752.

Darie, C. C., Biniossek, M. L., Jovine, L., Litscher, E. S., and Wassarman, P. M. (2004). Structural characterization of fish egg vitelline envelope proteins by mass spectrometry. *Biochemistry* **43,** 7459-7478.

Darie, C. C., Biniossek, M. L., Gawinowicz, M. A., Milgrom, Y., Thumfart, J. O., Jovine, L., Litscher, E., and Wassarman, P. M. (2005). Mass spectrometric evidence that proteolytic processing of rainbow trout egg vitelline envelope proteins takes place on the egg. *The Journal of Biological Chemistry* **280,** 37585-37598.

Dean, J. (2004). Reassessing the molecular biology of sperm-egg recognition with mouse genetics. *Bioessays* **26,** 29-38.

Epifano, O., Liang, L.-F., Familari, M., Moos, M. C., Jr., and Dean, J. (1995). Coordinate expression of the three zona pellucida genes during mouse oogenesis. *Development* **121,** 1947-1956.

Galanopoulou, A. S., Kent, G., Rabbani, S. N., Seidah, N. G., and Patel, Y. C. (1993). Heterologous processing of prosomatostatin in constitutive and regulated secretory pathways. Putative role of the endoproteases furin, PC1, and PC2. *J. Biol. Chem.* **268,** 6041-6049.

Goodyear, R. J., and Richardson, G. P. (2002). Extracellular matrices associated with the apical surfaces of sensory epithelia in the inner ear: molecular and structural diversity. *J. Neurobiol.* **53,** 212-227.

Greve, J. M., and Wassarman, P. M. (1985). Mouse egg extracellular coat is a matrix of interconnected filaments possessing a structural repeat. *J. Mol. Biol.* **181,** 253-264.

Hardy, D. M., editor. (2002). Fertilization. San Diego: Academic Press 427p

Hayashi, N., Kayo, T., Sugano, K., and Takeuchi, T. (1994). Production of bioactive gastrin from the non-endocrine cell lines CHO and COS-7. *FEBS Lett.* **337,** 27-32.

Harris, J. D., Hibler, D. W., Fontenot, G. K., Hsu, K. T., Yurewicz, E. C., and Sacco, A. G. (1994). Cloning and characterization of zona pellucida genes and cDNAs from a variety of mammalian species: the ZPA, ZPB and ZPC gene families. *DNA Seq.* **4,** 361-393.

Ho, S. N., Hunt, H. D., Horton, R. M., Pullen, J. K., and Pease, L. R. (1989). Site-directed mutagenesis by overlap extension using the polymerase chain reaction. *Gene* **77,** 51-59.

Hoodbhoy, T., Joshi, S., Boja, E. S., Williams, S. A., Stanley, P., and Dean, J. (2005). Human sperm do not bind to rat zonae pellucidae despite the presence of four homologous glycoproteins. *J. Biol. Chem.* **280,** 12721-12731.

Howarth, B. Jr. (1970). An examination for sperm capacitation in the fowl. *Biol. Reprod.* **3,** 338-341.

Howes, L., and Jones, R. (2002). Interactions between zona pellucida glycoproteins and sperm proacrosin/acrosin during fertilization. *J. Reprod. Immunol.* **53,** 181-192.

Iwata, Y. (2002). Thesis for master degree; Graduate School of Bioagricultural Sciences, Nagoya University, Nagoya, Japan.

Jovine, L., Qi, H., Williams, Z., Litscher, E. S., and Wassarman, P. M. (2002). The ZP domain is a conserved module for polymerization of extracellular proteins. *Nat. Cell Biol.* **4,** 457-461.

Jovine, L., Qi, H., Williams, Z., Litscher, E. S., and Wassarman, P. M. (2004). A duplicated motif controls assembly of zona pellucida domain proteins. *Proc. Natl. Acad. Sci. U. S. A.* **101,** 5922-5927.

Jovine, L., Darie, C. C., Litscher, E. S., and Wassarman, P. M. (2005). Zona pellucida domain proteins. *Annu. Rev. Biochem.* **74,** 83-114.

Kohno, Y. (2000). Thesis for master degree; Graduate School of Bioagricultural Sciences, Nagoya University, Nagoya, Japan.

Laemmli, U. K. (1970). Cleavage of structural proteins during the assembly of the head of bacteriophage T4. *Nature* **227,** 680-685.

Lee, V. H., and Dunbar, B. S. (1993). Developmental expression of the rabbit 55-kDa zona pellucida protein and messenger RNA in ovarian follicles. *Dev. Biol.* **155,** 371-382.

Lefie`vre, L., Conner, S. J., Salpekar, A., Olufowobi, O., Ashton, P., Pavlovic, B., Lenton, W., Afnan, M., Brewis, I. A., Monk, M., Hughes, D. C., and Barratt, C. L. (2004). Four zona pellucida glycoproteins are expressed in the human. *Hum. Reprod.* **19,** 1580-1586.

Liang, L.-F., Chamow, S. M., and Dean, J. (1990). Oocyte-specific expression of mouse Zp-2: developmental regulation of the zona pellucida genes. *Mol. Cell. Biol.* **10,** 1507-1515.

Lindsay, L. L., Wallace, M. A., and Hedrick, J. L. (2001). A hatching enzyme substrate in the Xenopus laevis egg envelope is a high molecular weight ZPA homolog. *Dev. Growth Differ.* **43,** 305-313.

Lindsay, L. L., Yang, J. C., and Hedrick, J. L. (2002). Identification and characterization of a unique Xenopus laevis egg envelope component, ZPD. *Dev. Growth Differ.* **44,** 205-212.

Lotan, R., Skutelsky, E., Danon, D., and Sharon, N. (1975). The purification, composition, and specificity of the anti-T lectin from peanut (Arachis hypogaea). *J. Biol. Chem.* **250,** 8518-8523.

Mollenhauer, J., Herbertz, S., Helmke, B., Kollender, G., Krebs, I., Madsen, J., Holmskov, U., Sorger, K., Schmitt, L., Wiemann, S., Otto, H. F., Grone, H.-J., and Poustka, A. (2001). Deleted in Malignant Brain Tumors 1 is a versatile mucin-like molecule likely to play a differential role in digestive tract cancer. *Cancer Res.* **61,** 8880-8886.

Ohtsuki, M., Hanafy, A. M., Mori, M., and Sasanami, T. (2004). Involvement of interaction of ZP1 and ZPC in the formation of quail perivitelline membrane. *Cell Tissue Res.* **318,** 565-570.

Okumura, H., Kohno, Y., Iwata, Y., Mori, H., Aoki, N., Sato, C., Kitajima, K., Nadano, D.,

and Matsuda, T. (2004). A newly identified zona pellucida glycoprotein, ZPD, and dimeric ZP1 of chicken egg envelope are involved in sperm activation on sperm-egg interaction. *Biochem. J.* **384,** 191-199.

Primakoff, P., and Myles, D. G. (2002). Penetration, adhesion, and fusion in mammalian sperm-egg interaction. *Science* **296,** 2183-2185.

Rankin, T., Familari, M., Lee, E., Ginsberg, A. M., Dwyer, N., Blanchette-Mackie, J., Drago, J., Westphal, H., and Dean, J. (1996). Mice homozygous for an insertional mutation in the Zp3 gene lack a zona pellucida and are infertile. *Development* **122,** 2903-2910.

Rankin, T., Talbot, P., Lee, E., and Dean, J. (1999). Abnormal zonae pellucidae in mice lacking ZP1 result in early embryonic loss. *Development* **126,** 3847-3855.

Rankin, T., and Dean, J. (2000). The zona pellucida: using molecular genetics to study the mammalian egg coat. *Rev. Reprod.* **5,** 114-21.

Rankin, T. L., O'Brien, M., Lee, E., Wigglesworth, K., Eppig, J., and Dean, J. (2001). Defective zonae pellucidae in Zp2-null mice disrupt folliculogenesis, fertility and development. *Development* **128,** 1119-1126.

Ringuette, M. J., Sobieski, D. A., Chamow, S. M., and Dean, J. (1986). Oocyte-specific gene expression: molecular characterization of a cDNA coding for ZP-3, the sperm receptor of the mouse zona pellucida. *Proc. Natl. Acad. Sci. U. S. A.* **83,** 4341-4345.

Robertson, L., and Wishart, G. J. (1996). Detection on the acrosome reaction of chicken sperm. *J. Reprod. Fertil. Abs. Ser.* **17,** 41.

Robertson, L., Wishart, G. J., and Horrocks, A. J. (2000). Identification of perivitelline N-linked glycans as mediators of sperm-egg interaction in chickens. *J. reprod. Fertil.* **120,** 397-403.

Säemann, M. D., Weichhart, T., Horl, W. H., and Zlabinger, G. J. (2005). Tamm-Horsfall protein: a multilayered defence molecule against urinary tract infection. *Eur. J. Clin. Invest.* **35,** 227-235.

Sasanami, T., Atsumi, E., Toriyama, M., and Mori, M. (2003a). Asparagine-linked oligosaccharide-independent secretion of egg envelope glycoprotein ZPC of the

Japanese quail (Coturnix japonica). *Comp. Biochem. Physiol. A. Mol. Integr. Physiol.* **134,** 631-638.

Sasanami, T., Hanafy, A. M., Toriyama, M., and Mori, M. (2003b). Variant of perivitelline membrane glycoprotein ZPC of Japanese quail (Coturnix japonica) lacking its cytoplasmic tail exhibits the retention in the endoplasmic reticulum of Chinese hamster ovary (CHO-K1) cells. *Biol. Reprod.* **69,** 1401-1407.

Sasanami, T., Toriyama, M., and Mori, M. (2003c). Carboxy-terminal proteolytic processing at a consensus furin cleavage site is a prerequisite event for quail ZPC secretion. *Biol. Reprod.* **68,** 1613-1619.

Schägger, H., and Von Jagow, G. (1987). Tricine-sodium dodecyl sulfate-polyacrylamide gel electrophoresis for the separation of proteins in the range from 1 to 100 kDa. *Analytical Biochemistry* **166,** 368-379.

Spargo, S. C., and Hope, R. M. (2003). Evolution and nomenclature of the zona pellucida gene family. *Biol. Reprod.* **68,** 358-362.

Sugiyama, H., Yasumasu, S., Murata, K., Iuchi, I., and Yamagami, K. (1998). The third egg envelope subunit in fish: cDNA cloning and analysis, and gene expression. *Dev. Growth Differ.* **40,** 35-45.

Takeuchi, Y., Nishimura, K., Aoki, N., Adachi, T., Sato, C., Kitajima, K., and Matsuda, T. (1999). A 42-kDa glycoprotein from chicken egg-envelope, an avian homolog of the ZPC family glycoproteins in mammalian Zona pellucida. Its first identification, cDNA cloning and granulosa cell-specific expression. *Eur. J. Biochem.* **260,** 736-742.

Takeuchi, Y., Cho, R., Iwata, Y., Nishimura, K., Kato, T., Aoki, N., Kitajima, K., and Matsuda, T. (2001). Morphological and biochemical changes of isolated chicken egg-envelope during sperm penetration: degradation of the 97-kilodalton glycoprotein is involved in sperm-driven hole formation on the egg-envelope. *Biol. Reprod.* **64,** 822-830.

Thompson, J. D., Higgins, D. G., and Gibson, T. J. (1994). CLUSTAL W: improving the sensitivity of progressive multiple sequence alignment through sequence weighting,

position-specific gap penalties and weight matrix choice. *Nucleic Acids Res.* **22,** 4673-4680.

Tian, J., Gong, H., and Lennarz, W. J. (1999). Xenopus laevis sperm receptor gp69/64 glycoprotein is a homolog of the mammalian sperm receptor ZP2. *Proc. Natl. Acad. Sci. U. S. A.* **96,** 829-834.

Tsuda, T. (1999). Thesis for master degree; Graduate School of Bioagricultural Sciences, Nagoya University, Nagoya, Japan.

Wang, H., and Gong, Z. (1999). Characterization of two zebrafish cDNA clones encoding egg envelope proteins ZP2 and ZP3. *Biochim Biophys Acta.* **1446**.

Warren, T. G., and Shields, D. (1984). Expression of preprosomatostatin in heterologous cells: biosynthesis, posttranslational processing, and secretion of mature somatostatin. *Cell* **39,** 547-555.

Wassarman, P. M. (1988). Zona pellucida glycoproteins. *Annu. Rev. Biochem.* **57,** 415-420.

Wassarman, P. M. (2003). Fertilization. ChemTracts-Biochem Mol Biol 16:117-204.

Wassarman, P. M. (2005). Contribution of mouse egg zona pellucida glycoproteins to gamete recognition during fertilization. *J. Cell. Physiol.* **204,** 388-391.

Wyburn, G. M., Aitken, R. N. C., and Johnston, H. S. (1965). The ultrastructure of the zona radiata of the ovarian follicle of the domestic fowl. *J. Anat.* **99,** 469-484.

Yanagimachi, R. (1994). Mammalian fertilization. In: The physiology of reproduction Knobil, E., Neill, J. D., editors. New York: Raven Press. pp 189-317.

Yanagita, M., Nakayama, K., and Takeuchi, T. (1992). Processing of mutated proinsulin with tetrabasic cleavage sites to bioactive insulin in the non-endocrine cell line, COS-7. *FEBS Lett.* **311,** 55-59.

Yamamura, J.-i., Adachi, T., Aoki, N., Nakajima, H., Nakamura, R., and Matsuda, T. (1995). Precursor-product relationship between chicken vitellogenin and the yolk proteins: the 40 kDa yolk plasma glycoprotein is derived from the C-terminal cysteine-rich domain of vitellogenin II. *Biochim. Biophys. Acta* **1244,** 384-394.

Yurewicz, E. C., Sacco, A. G., Gupta, S. K., Xu, N., and Gage, D. A. (1998).

Hetero-oligomerization-dependent binding of pig oocyte zona pellucida glycoproteins ZPB and ZPC to boar sperm membrane vesicles. *J. Biol. Chem.* **273,** 7488-7494.

Zhao, M., Boja, E. S., Hoodbhoy, T., Nawrocki, J., Kaufman, J. B., Kresge, N., Ghirlando, R., Shiloach, J., Pannell, L., Levine, R. L., Fales, H. M., and Dean, J. (2004). Mass spectrometry analysis of recombinant human ZP3 expressed in glycosylation-deficient CHO cells. *Biochemistry* **43,** 12090-12104.

ACKNOWLEDGEMENTS

The author would like to express sincere gratitude to Dr. Tsukasa Matsuda, Professor of Nagoya University for kind advice, warm encouragement, valuable discussion and critical reading of this thesis.

The author greatly appreciates to Dr. Naohito Aoki, Associate professor of Mie University and Dr. Daita Nadano, Associate professor of Nagoya University for their direction, useful discussion, their critical reading of the manuscript, and great encouragement in carrying out this study.

The author wishes to Dr. Chihiro Sato, Associate professor of Nagoya University and Dr. Ken Kitajima, Professor of Nagoya University for their continuous interest and kind encouragement. The author is also grateful to Yuki Iwata and Mami Sasaki as representatives of many colleagues from Laboratory of Molecular Bioregulation and Organogenesis for their kindness and helpful discussion.

Finally, the author express thankfulness to my friends in our wind orchestra who were shared our joys and sorrows with and to parents for providing with their mentally and physically excessive support.

奥村裕紀

Hiroki Okumura

List of Publications:

Publications Concerning This Dissertation

Okumura, H., Kohno, Y., Iwata, Y., Mori, H., Aoki, N., Sato, C., Kitajima, K., Nadano, D., and Matsuda, T. (2004). A newly identified zona pellucida glycoprotein, ZPD, and dimeric ZP1 of chicken egg envelope are involved in sperm activation on sperm-egg interaction. *Biochem. J.* **384,** 191-199.

Okumura, H., Aoki, N., Sato, C., Nadano, D., and Matsuda, T. Heterocomplex formation and cell-surface accumulation of hen's serum ZPB1 with ZPC expressed by COS-7 cells: a possible initiation step of egg-envelope matrix construction. Submitted for Publication

Okumura, H., Aoki, N., Sato, C., Nadano, D., and Matsuda, T. ZPD/ZPX2, a novel ZP glycoprotein found in chicken egg envelope, weakly associates with both of ZPB1 and ZPC. In Preparation